Oxidative depolymerization of technical lignins into value added chemicals

Thesis submitted in partial fulfilment of the requirements for the degree of

Master of Science (Polymer Science)

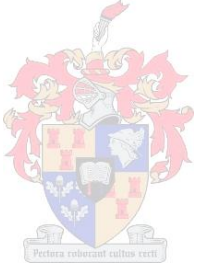

by

Ndumiso Sibanda

at the

University of Stellenbosch

Supervisors:

Prof H Pasch

Dr H Pfukwa

April 2019

Declaration

IBy submitting this thesis electronically, I declare that the entirety of the work contained therein is my own, original work, that I am the sole author thereof (save to the extent explicitly otherwise stated), that reproduction and publication thereof by Stellenbosch University will not infringe any third party rights and that I have not previously in its entirety or in part submitted it for obtaining any qualification.

Ndumiso Sibanda March 2019

Abstract

Most functional polymeric materials are being derived from non-renewable feedstocks e.g. petroleum and coal. The growing concerns regarding the depletion of non-renewable feedstocks have challenged researchers to investigate renewable and comparably cleaner alternatives to liquid fuels and chemicals. There has been a staggering interest in recent years in the use of lignin as a source of high value chemicals. Lignin has been used mainly as an energy source in combustion processes with only a small fraction (<5%) being used for other purposes. However, due to lignin's notably high functionalization and aromatic nature, it has great potential for the direct production of aromatic speciality and fine chemicals, and subsequent functionalization to desired platform chemicals.

A novel DMSO/HBr oxidative depolymerization approach was developed in order to depolymerize technical lignins, Kraft lignin and SAPPI lignosulfonate, into low molar mass compounds. A mechanism for this depolymerization process which is in agreement with the structure of the compounds formed is proposed. Since there is not much information in published literature focusing on the oxidative depolymerization of lignin using DMSO as the oxidant, other well established oxidative depolymerization methods were carried out in this work for comparison. The methods investigated included oxidative depolymerization using nitrobenzene and oxidative depolymerization in ionic liquid (1-ethyl-3-methylimidazolium trifluoromethanesulfonate) and water using oxygen as an oxidant.

Lignin depolymerization products were analyzed by a molar mass determination technique (SEC). LC-MS and GC-MS were used to deconvulate the monomeric and oligomeric compounds according to chemical functionality. Structural elucidation was carried out using ESI-MS, NMR spectroscopy and FTIR spectroscopy. Results obtained using the aforementioned techniques confirmed the successful depolymerization of lignin by DMSO/HBr, as a plethora of carbonyl functionalized compounds were identified. Vanillin (29.5%) and syringaldehyde (28.8%) had the highest amounts of the total quantifiable monomeric compounds. Phloroglucinol, not widely reported as a product of oxidative depolymerization of lignin, was also identified and quantified at approximately 5.4%.

Finally, a novel fully bio-based monomer for radical polymerization was successfully synthesized by the reaction of itaconic anhydride and guaiacol (one of the lignin monomeric compounds of lignin depolymerization) via an esterification reaction.

Opsomming

Die meeste funksionele polimeriese materiale word afgelei van nie-herwinbare toevoerstowwe (bv. petroleum en steenkool). Die toenemende kommer oor die uitputting van nie-herwinbare voedingsbronne daag navorsers egter uit om herwinbare en relatief skoner alternatiewe te ondersoek. Daar is 'n groot belangstelling in lignien as ‘n bron van hoë toegevoegde waarde chemikalieë. Lignien word hoofsaaklik as energiebron in verbrandingsprosesse gebruik, met slegs klein hoeveelhede (<5%) wat vir ander doeleindes gebruik word. As gevolg van lignin se hoë funksionaliteit en aromatiese aard, het dit groot potensiaal vir gebruik in die direkte produksie van aromatiese spesialiteit chemikalieë en die daaropvolgende funksionalisering na gewenste chemikalieë.

'n Nuwe DMSO / HBr oksidatiewe-depolymerisasie benadering word gebruik om tegniese ligniene – Kraft lignin en SAPPI lignosulfonate – in lae molêre massa verbindings te depolymeriseer. Die meganisme van hierdie benadering word voorgestel. Aangesien daar nie veel inligting in gepubliseerde literatuur is wat fokus op hierdie oksidatiewe depolymerisasie van lignien met DMSO as die oksidant nie, is ander goed gevestigde oksidatiewe depolymerisasiemetodes in hierdie werk vir vergelyking uitgevoer. Die metodes wat ondersoek is sluit in oksidatiewe-depolymerisasie met behulp van nitrobenzeen en oksidatiewe-depolymerisasie in ioniese vloeistof (1-etiel-3-methylimidazolium trifluormetansulfonaat) en water, deur suurstof as oksidant te gebruik.

Lignien depolymerisasie produkte was geanaliseer met behulp van 'n molekulêremassa bepalingstegniek (SEC). LC-MS en GC-MS word as skeidingstegnieke gebruik om die monomeer- en oligomere volgens chemiese funksionaliteit te dekonvulueer. Strukturele verduideliking is met behulp van ESI-MS, NMR spektroskopie, en FTIR-spektroskopie uitgevoer. Die resultate dui die suksesvolle depolymerisasie van lignien deur DMSO / HBr aan, deur 'n groot hoeveelheid karboniel verbindings te identifiseer. Vanillien (29%) en syringaldehied (28.8%) het die hoogste hoeveelhede van die totale kwantifiseerbare monomere. Floroglucinol, wat nie wyd gerapporteer word as 'n produk van die oksidatiewe depolymerisasie van lignien nie, is ook geïdentifiseer en gekwantifiseer teen ongeveer 5.4%.

Tenslotte word 'n nuwe volledig bio-gebaseerde monomeer vir radikale polimerisasie gesintetiseer deur die veresteringsreaksie van itakonanhidried en guaiacol (een van die lignienmonomeriese verbindings van lignien-depolymerisasie).

Acknowledgements

Firstly I want to thank God Almighty for His guidance throughout this study, for without Him, I would not have come this far. My utmost gratitude goes to my supervisors **Prof. Harald Pasch** and **Dr. Helen Pfukwa** for their guidance, patience and encouragement throughout the course of this study. The discussions we had were certainly very educative and enlightening. **Prof. Harald Pasch** gave me the opportunity to be part of his research group and also supported me with financial assistance, and for that I am greatly honoured.

I would also like to thank the following people and organizations for their contributions to this project:

Dr. Jaco Brand and **Mrs Elsa Malherbe** for the solution NMR analyses, **Mr. L. Mokwena** for GC-MS analysis, **Dr. M Stander** for ESI-MS analysis.

All the staff at the Department of Chemistry and Polymer Science, **Mrs Aneli Fourie**, **Mrs Erinda Cooper, Mr. Deon Koen, Mr. Jim Motshweni and Mr. Calvin Maart.**

Dr. R. Pfukwa for being a mentor and **Anthony** for being of assistance in every way and for being a teacher.

All members of the Pasch's group past and present: **Mawande, Douglas, Lucky, Josh, Nonkululeko, Clement, Zanelle, Guilaume, Paul**

Family and friends

Thembelihle, my love and pillar of strength, for standing by my side throughout my studies.

May God bless you all!.

Table of contents

List of figures

List of schemes

List of tables

List of symbols

α	Selectivity factor
R_s	Resolution
K_i	Retention factor
N	Number of theoretical plates
Đ	Molar mass dispersity
M_n	Number average molar mass
M_w	Weight average molar mass
M_p	Peak molar mass
δ	Chemical shift

List of abbreviations

^{13}C NMR	Carbon-13 nuclear magnetic resonance
^{1}H NMR	Proton nuclear magnetic resonance
AA	Acetic acid
COSY	Correlation spectroscopy
DMAC	Dimethylacetamide
DMF	Dimethylformamide
DMSO	Dimethyl-sulfoxide
EI	Electron impact
ESI-MS	Electrospray ionization mass spectroscopy
FTIR	Fourier transform infrared
FRP	Free radical polymerization
GC	Gas chromatography
GC-MS	Gas chromatography - mass spectrometry
HBr	Hydrogen bromide
HPLC	High performance liquid chromatography
HSQC	Heteronuclear single-quantum correlation spectroscopy
IL	Ionic liquid
KL	Kraft lignin
KFTA	Potassium trifluoro acetic acid
LAC	Liquid adsorption chromatography
LC-MS	Liquid chromatography - mass spectrometry
MALDI-MS	Matrix-assisted laser desorption/ionization mass spectrometry
MALLS	Multiangle laser light scattering
MeOH	Methanol
MS	Mass spectrometry

NP-LC	Normal phase liquid chromatography
NMR	Nuclear magnetic resonance
POFs	Polymeric organic frameworks
PLA	Poly(lactic acid)
RAFT	Reversible addition-fragmentation chain transfer
RDRP	Reversible deactivation radical polymerization
RI	Refractive index
RP-LC	Reversed phase liquid chromatography
SEC	Size exclusion chromatography
SIM	Single ion monitoring
SRM	Single reaction monitoring
TFA	Trifluoro acetic acid
TIC	Total ion count
TMS	Tetramethylsilane
UPLC	Ultrahigh pressure liquid chromatography
V_e	Elution volume
[EMIM][CF_3SO_3]	1-ethyl-3-methylimidazolium trifluoromethanesulfonate

Chapter 1

Introduction and objectives

1.1 Introduction

For a number of years, chemistry has been evolving with regard to new technologies, its relevance to industry and to the welfare of the society. In light of the worldwide economic and environmental pollution issues there has been increasing research interest in the value of bio-sourced lignocellulosic biomass.[1–2] Lignocellulosic biomass has been viewed as a key to unlock the future of bioenergy and the production of high value added chemicals. Lignocellulosic biomass is considered an inexpensive, renewable, abundant feedstock that can be exploited to supply direct replacements for existing non-renewable petrochemical feedstocks, and for the synthesis of new building blocks for chemical and materials production.[3–5]

Lignocellulosic biomass is composed of carbohydrate polymers (cellulose and hemicellulose) and the aromatic biopolymer lignin. Cellulose has been regarded as a major resource of the bio-based economy as it yields sustainable aliphatic monomers for the production of biopolymers.[6] There has been staggering interest in recent years in the use of lignin as a source of high value chemicals. Lignin has been used mainly as an energy source in combustion processes, with only a small fraction (<5%) being used for other purposes. However, due to lignin's notably high functionalization and aromatic nature, it has great potential for the direct production of aromatic speciality and fine platform chemicals.[7]

These platform aromatic chemicals, i.e. vanillin (4-hydroxy-3-methoxybenzaldehyde), eugenol (2-methoxy-4-prop-2-enylphenol) and syringaldehyde (4-hydroxy-3,5-dimethoxy benzaldehyde), have been used in polymeric and biomaterials synthesis for applications in medicinal technology, organic catalysts synthesis, coatings, and electronics.[8–11] As a result, efforts have been channeled to devising different methods of selectively breaking down this aromatic polymer into valuable low molar mass compounds, i.e. by depolymerization. Methods include pyrolysis, hydrogenolysis, enzymatic hydrolysis, acid/base hydrolysis and oxidative depolymerization.[12–15]

Oxidative depolymerization has been viewed as the preferred method of lignin depolymerization because compared to other methods, it has high selectivity towards targeting the arylglycerol-β-aryl ether (β-O-4), which accounts for 40–60% of inter-unit linkages.[15] Other methods of depolymerization employ extremely harsh conditions that break up the aromatic ring, whereas oxidative depolymerization preserves the aromatic character of the fragments and gives highly functionalized compounds.[16] Hence, oxidative depolymerization of lignin is the main focus in this work.

The analytical approach used in this work for investigating lignin depolymerization comprises molar mass determination using size exclusion chromatography (SEC) and structural elucidation using nuclear magnetic resonance spectroscopy (NMR), electrospray ionization-mass spectrometry (ESI-MS) and Fourier transform infrared spectroscopy (FTIR). It also involves the use of separation techniques coupled to concentration sensitive and spectrometric detection, i.e. high performance liquid chromatography with UV and mass spectrometric detection (HPLC-UV and HPLC-MS, respectively) as well as gas chromatography coupled to mass spectrometry (GC-MS), to deconvolute and qualitatively and quantitatively analyze the formed monomeric compounds.[17]

1.2 Problem Statement

The depletion of non-renewable feedstocks and the emission of greenhouse gases and pollutants versus the increasing availability of renewable feedstocks contribute effectively to the background of this study. The expectations of this study are to develop and optimize procedures for the oxidative depolymerization of lignin and to develop analytical techniques for characterizing depolymerized products regarding functionality, molar mass and chemical composition. In the oxidative depolymerization of lignin, reported methods focus mainly on vanillin or syringaldehyde, which are often obtained in yields less than 20%. The question is, what is the remaining 80% and what can be done with it, because quantitative separation and isolation techniques are potentially a challenge.

1.3 Objectives

The main objectives of this work were to:

i. Develop and optimize a method for oxidatively depolymerizing lignins into low molar mass compounds using mild oxidizing agents. Here the aims were to:

- Investigate the use of dimethyl sulfoxide (DMSO) as a mild oxidizing agent and solvent in the depolymerization of lignin.
- Investigate and compare the newly developed depolymerization procedure with well established procedures such as (i) depolymerization using nitrobenzene and (ii) depolymerization using oxygen.

ii. To develop analytical techniques for characterizing the depolymerized products regarding:
   - Molar mass, and
   - Functionality.

iii. To compare the different chemical structures of the compounds obtained from different sources (Kraft lignin and industrial lignosulfonate) under different reaction conditions.

iv. To modify the lignin monomeric compounds with radically polymerizable groups. Here the aims were to:
   - Modify lignin monomeric compounds with itaconic anhydride, and
   - Polymerize the modified monomeric compounds via radical polymerization.

1.4 Layout of thesis

Chapter 1

A brief introduction to the topic of this study and the objectives of the study are given in Chapter 1.

Chapter 2

An overview of the historical and theoretical background to this work is presented in Chapter 2. This includes a review of different renewable feedstocks including lignin as a bio-based resource for value added chemicals. Chapter 2 also outlines the chemistry and the different methods of lignin depolymerization. The merits and flaws of each depolymerization technique are outlined and explained. The analytical approach for investigating lignin depolymerization is reviewed in detail in this chapter. Applications of the functionalized monomeric compounds of lignin depolymerization are briefly outlined and the methods of monomer modification for polymerization with regard to lignin chemistry are described.

Chapter 3

The oxidative depolymerization of technical lignins i.e. Kraft lignin and industrial lignosulfonate, is investigated by SEC in Chapter 3. The development and optimization of a method of depolymerizing lignin by oxidation using DMSO (dual role of oxidant and solvent) is outlined and a mechanism for the reaction is proposed. Other well established oxidative lignin depolymerization procedures are also investigated by SEC in order to highlight merits and limitations of each method.

Chapter 4

Chapter 4 outlines the analytical techniques used to determine the chemical functionality, molar mass and the chemical structures of the bulk reaction products obtained from the oxidative depolymerization of technical lignins under different reaction conditions. The structures of the compounds within the bulk product mixtures are elucidated using electrospray ionization-mass spectrometry (ESI-MS), proton nuclear magnetic resonance (^{1}H NMR) spectroscopy and Fourier transform infrared (FTIR) spectroscopy. A high performance liquid chromatography (HPLC) method using both ultraviolet (UV) and MS detection is developed and optimized for selectively separating the depolymerized compounds according to chemical composition. Gas chromatography coupled to MS (GC-MS) is also used to determine the nature of the volatile compounds present in the product mixture.

Chapter 5

This chapter outlines the fractionation of the bulk, complex depolymerized product mixture by vacuum distillation into less complex fractions. These fractions are characterized extensively and the structures elucidated with the aid of HPLC-UV, LC-MS and the following spectroscopic techniques: ^{13}C NMR, ^{1}H NMR and FTIR. The amounts of selected compounds in the product mixtures are then determined using MS in the SIM mode, and an external calibration.

Chapter 6

Chapter 6 outlines preliminary work on modification of lignin monomeric compounds for radical polymerization. Itaconic anhydride, a bio-based monomer, was successfully used in modifying guaiacol (lignin monomeric compound) by attaching radically polymerizable

groups via an esterification reaction. Polymerization of this novel fully bio-based monomer is carried out by radical polymerization.

Chapter 7

The final chapter presents the conclusions, brief mention of the challenges encountered during the study, and suggestions for future research.

1.5 References

1. Anwar, Z.; Gulfraz, M.; Irshad, M., *Journal of Radiation Research and Applied Sciences* **2014,** *7* (2), 163–173.

2. Menon, V.; Rao, M., *Progress in Energy and Combustion Science* **2012,** *38* (4), 522–550.

3. Lucia, L. A., *BioResources* **2008,** *3* (4), 981–982.

4. Zhang, Y.-H. P., *Journal of Industrial Microbiology and Biotechnology* **2008,** *35* (5), 367–375.

5. Saini, J. K.; Saini, R.; Tewari, L., *3 Biotech* **2015,** *5* (4), 337–353.

6. Klemm, D.; Heublein, B.; Fink, H. P.; Bohn, A., *Angewandte Chemie International Edition* **2005,** *44* (22), 3358–3393.

7. Rinaldi, R.; Jastrzebski, R.; Clough, M. T.; Ralph, J.; Kennema, M.; Bruijnincx, P. C.; Weckhuysen, B. M., *Angewandte Chemie International Edition* **2016,** *55* (29), 8164–8215.

8. Kralik, M.; Biffis, A., *Journal of Molecular Catalysis A: Chemical* **2001,** *177* (1), 113–138.

9. Neffe, A. T.; Grijpma, D. W.; Lendlein, A., *Macromolecular Bioscience* **2016,** *16* (12), 1743–1744.

10. Kiriy, A.; Pötzsch, R.; Wei, Q.; Voit, B., *Polymer Degradation and Stability* **2017,** *145*, 150–156.

11. Weil, T.; Barz, M., *Macromolecular Bioscience* **2017,** *17* (10), 1–4.

12. Xu, C.; Arancon, R. A. D.; Labidi, J.; Luque, R., *Chemical Society Reviews* **2014,** *43* (22), 7485–7500.

13. Carlson, T. R.; Vispute, T. P.; Huber, G. W., *ChemSusChem* **2008,** *1* (5), 397–400.

14. Toledano, A.; Serrano, L.; Pineda, A.; Romero, A. A.; Luque, R.; Labidi, J., *Applied Catalysis B: Environmental* **2014,** *145*, 43–55.

15. Zhang, C.; Li, H.; Lu, J.; Zhang, X.; MacArthur, K. E.; Heggen, M.; Wang, F., *ACS Catalysis* **2017,** *7* (5), 3419–3429.

16. Wang, Q.; Guan, S.; Shen, D., *International Journal of Molecular Sciences* **2017,** *18* (10), 1-10.

17. Dier, T. K.; Rauber, D.; Durneata, D.; Hempelmann, R.; Volmer, D. A., *Scientific Reports* **2017,** *7* (1), 1–12.

Chapter 2

Historical and theoretical background

2.1 Renewable feedstocks for polymer production

Functional polymers are macromolecules that have unique properties or applications. A functional polymer possesses the combination of the physical properties of the polymer backbone and the chemical properties (reactivity) of the attached functional groups. The polymer backbone can be either organic or inorganic and the attachment of the functional group can be done either by physical interaction or through chemical bonds. The presence of functional groups induces specified physical, chemical and biological properties depending on the attached chemical groups.[1–2] Most functional polymers are based on simple linear backbones, however, there has been a marked interest in functional polymers with special topologies or architectures (dendrimers, stars and hyper-branched polymers).[1, 3] Functional polymers have found a wide range of applications in medicinal technology, as organic catalysts, coatings, electronics and in biomaterial synthesis (bio-medical engineering).[4–7]

Most functional polymeric materials are being derived from non-renewable feedstocks such as petroleum and coal. However, the growing concerns over the excessive emission of greenhouse gases and the depletion of non-renewable feedstocks have challenged researchers to investigate renewable and comparably cleaner alternatives to liquid fuels and chemicals.[8] Therefore, there is an urgent need to develop new synthetic routes to functional polymeric materials using renewable resources. Renewable and non-renewable feedstocks begin as complex multicomponent mixtures which are processed into more easily managed building blocks before conversion to final useful polymeric products.[9–10] Biomass is a renewable and sustainable feedstock of polymeric (cellulose, starch, lignin, hemicellulose and protein) and monomeric (sugars, oils, amino acids) components.[10] In recent years, efforts have been made to replace existing petrochemical raw materials with biomass so as to synthesize new building blocks for chemical production with new properties and applications.[10–12] Polymers derived from renewable resources are attractive as they provide an incentive from a feedstock point of view and also from a waste disposal perspective, as most products derived from renewable resources can be rendered biodegradable under appropriate conditions.[13]

Two different working principles can be defined when synthesizing polymers from renewable feedstocks. The first approach is the chemical or physical modification of natural polymers with the intent of improving their pristine properties, e.g. carboxylation of cellulose, and the second approach involves the synthesis of polymers from monomers derived from renewable feedstocks, e.g. the synthesis of formaldehyde free resins from lignin derived monomers.[14] These polymers are intended to replicate the performance of existing polymers derived from non-renewable feedstocks.

The following subsections of this chapter shall briefly discuss the various components of biomass.

2.1.1 Cellulose

Cellulose is a fascinating and versatile biopolymer that consists of linear, covalently linked chains of D-glucose units and it is a major component of the lignocellulosic biomass (20–55%).[15] Cellulose is considered as an almost inexhaustible source of raw materials for the increasing demand of biocompatible products (see Scheme 2.1 for the applications of cellulose).[16–17] It is regarded as a major resource of the bio-based economy as it yields sustainable monomers for the production of aliphatic biopolymers.

Glucose is a well-established sugar degradation product of cellulose. It is used in the production of bio-ethanol via the fermentation process. The manufacture of bio-ethylene from bio-ethanol is achieved by the dehydration reaction. Ethylene is a major building block in the polyolefin chemistry. Therefore, the bio-based ethylene production is an attractive alternative to the fossil-based ethylene production and decreases the environmental consequences involved in the manufacture of this chemical commodity from fossil fuels.[18–19]

Cellulose conversion can yield another platform known chemically as levulinic acid, which has been used as a renewable source for novel polymers that can be used as ingredients in drug delivery systems and other industrial applications. Levulinic acid has been widely used as monomer due to the presence of two reactive functional groups (ketone and carboxylic acid), which has enhanced levulinic acid as a valuable bio-based multi-purpose building block.[20–21] Besides being a source of monomers, cellulose has been used as a polymer in a variety of applications. Microcrystalline cellulose (refined wood pulp cellulose) and carboxylated methyl

cellulose have been used mainly as binders or diluents in drug formulations and as film-coating agent for drugs and ointment. Cellulose acetate fibres have been used in wound dressings.[22–24]

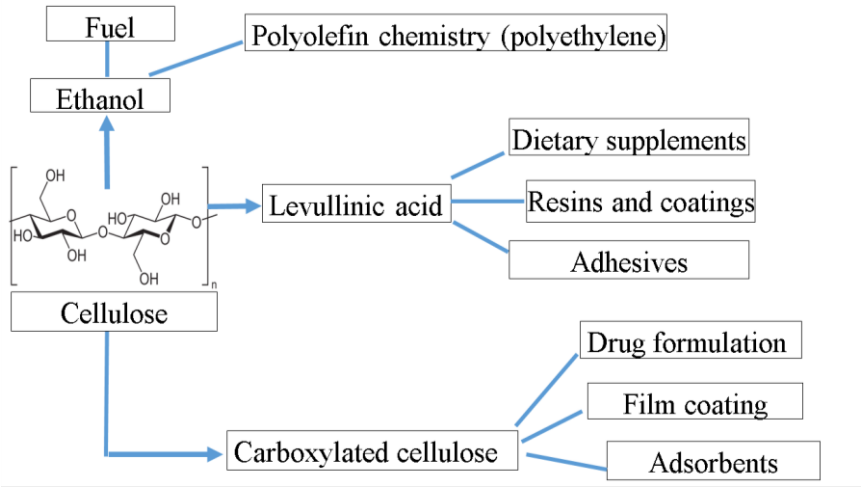

Scheme 2.1: Applications of high value added chemicals of cellulose

2.1.2 Tannins

Tannins have received great attention as a source of high value chemicals as they are polyphenolic biomacromolecules. Tannins are classified into two major groups, namely, condensed and hydrolyzable tannins (see Fig. 2.1). Condensed tannins are flavonoid-based tannins which possess flavonoid units that undergo condensation and polymerization reactions to form oligomers with varying degrees of polymerization.[25–26] Hydrolyzable tannins are tannins characterized by the presence of a polyhydric alcohol at their core, the hydroxyl groups of which are partially, or fully, esterified with either gallic or hexahydroxydiphenic acid.[27–28] Tannins are mainly extracted from food products (strawberries, apples and nuts), sumac leaves, Chinese gall and Tara wood.

Tannin-derived compounds such as gallic acid, flavone and phloroglucinol have been used in the synthesis of novel polymers. Poly(gallic acid) is used in the drug delivery system when used as a coating on magnetite nanoparticles.[29] Phloroglucinol has been combined with di- or trialdehydes in a condensation reaction to produce microporous polymeric organic frameworks (POFs) which exhibit semi-conductor optical properties.[30] The aforementioned applications of tannin-derived compounds highlight the relevance of tannins in both medicinal and electronic applications.

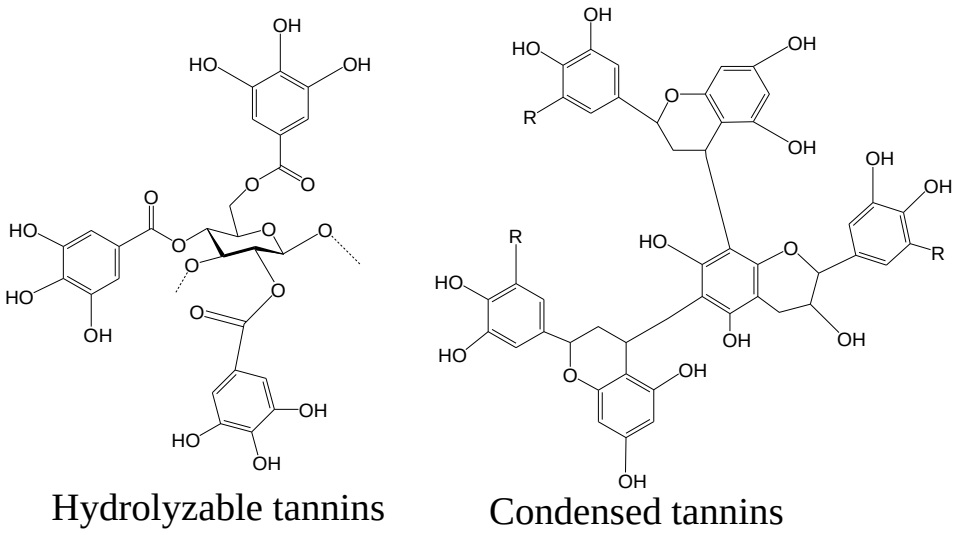

Fig. 2.1: Structure of tannins (hydrolyzable tannins and condensed tannins)

2.1.3 Starch

The exploitation of starch, as a precursor to macromolecular materials, like other renewable feedstocks such as cellulose and lignin, can follow two strategies. Starch can be exploited as a raw material for the production of chemicals used in the synthesis of other polymers, or can be directly used as a high molecular weight polymer by keeping its molecular structure as unchanged as possible e.g in the production of thermoplastic starch.[31] The main advantage of starch over cellulose is that the conversion into small molecules is easier for starch, making it an economic option in the production of hydroxyl-functionalized compounds, which can be exploited as monomers in the production of bio-based polymers.

Starch is mainly extracted from food products (cereals, potatoes, corn and some vegetables). Poly(lactic acid) is a well-known, established and extensively studied polymer that is prepared from starch or sugars which are processed to yield dextrose glucose, which is then fermented to produce lactic acid.[12, 32] Some researchers report that PLA has properties related to polyolefins and polystyrene and can be functionalized into various building blocks mainly exploited in packaging and fibre applications.[12, 33] Therefore, it has been successfully employed as an alternative for a variety of applications that have classically been dominated by petroleum-based polymers. Starch has also been exploited as a raw material in the production of polyhydroxyalkanoates which find applications in the biomedical sector and plastics.[34–35]

There are critical concerns regarding the sustainability of compounds which depend on starch and sugar crops. This is because the limited supply of such crops can lead to competition with food production. Therefore, to avoid competition with societal needs, lignin, a waste product that accumulates in the form of black liquor in the pulp and paper making process, and is incinerated in industry as a source of energy, has attracted profound interest as a renewable source of chemicals. The relevant historical background and literature concerning lignin as a renewable resource shall be discussed in the subsequent sections.

2.2 Background of lignin

Due to its composition (wide-range of functional groups which include methoxy, phenolic hydroxyl, aldehyde and other carbonyl moieties) lignin is regarded as the major resource of the bio-based economy.[36] Several efforts have been channelled towards understanding the structure and composition of lignin in order to find suitable routes to breakdown the bio-polymer into useful, high value monomeric (or oligomeric) compounds which can be used in the synthesis of functional polymers (valorization of lignin). It is the second most abundant natural polymer in the plant world making up to 10–25% of lignocellulosic biomass.[37] Lignin is the main non-carbohydrate component of wood, where its roles include binding cellulose and hemicellulose fibers, and hardening the plant cell walls to provide mechanical support.[38] It is a very complex, irregular and randomly cross-linked polymer that is also found in jute, hemp and cotton.

Lignin is composed of the following monomers: p-coumaryl alcohol (4-[(E)-3-hydroxyprop-1-enyl]phenol), coniferyl alcohol (4-[(E)-3-hydroxyprop-1-enyl]-2-methoxyphenol) and sinapyl alcohol (4-[(E)-3-hydroxyprop-1-enyl]-2,6-dimethoxyphenol), see Fig. 2.2. Lignin consists of seven inter-unit linkages which include: aryl-glycerol-β-aryl ether (β-O-4), non-cyclic benzyl aryl ether, biphenyl (5-5), side chain linkage (β-β), diaryl ether (4-O-5), phenylcoumaran (β-5) and 1,2-diaryl ether (β-1), see Fig. 2.3. It is essential to emphasize that this proposed model does not depict the actual structure of lignin; it, therefore, serves as a tool to visualize the linkages and functional groups in lignin. The β-O-4 linkage accounts for 40–60% of inter-unit linkages.

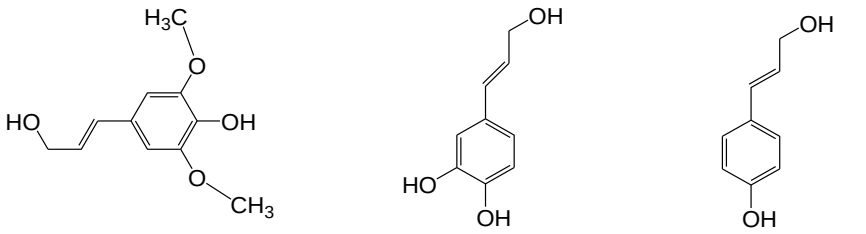

sinapyl alcohol coniferyl alcohol p-coumaryl alcohol

Fig. 2.2: Monomers of lignin (sinapyl alcohol, coniferyl alcohol and p-coumaryl alcohol)

Studies on various lignin extracts show that the actual structure and functional groups present in lignin depend on three major factors that include: method of isolation, nature or type of species (hardwood or softwood) and location of species.[39]

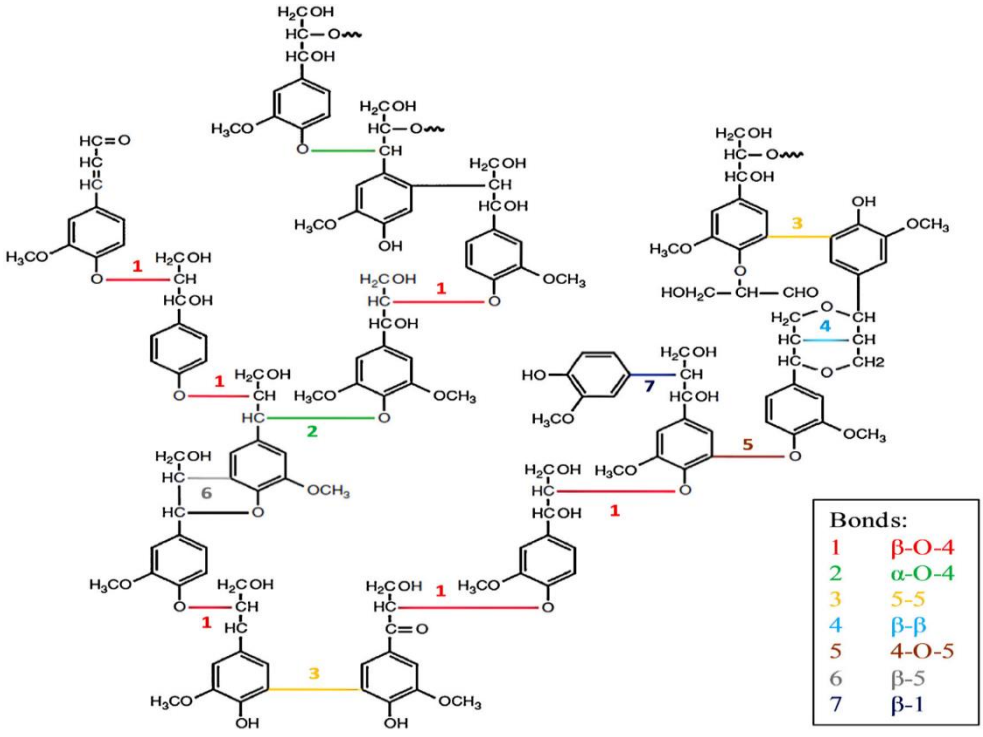

Fig. 2.3: Model structure of lignin[40]

Lignins are classified into two major groups, namely natural lignins and technical lignins. Natural lignins also referred to as native lignins are derived directly from the lignocellulosic component in plants.[41] Technical lignins are by-products of lignin processing (industrial lignins) and they differ dramatically in properties from the native lignins in plants.[42] An overview of technical lignins will be given in the following section.

Technical lignins

Although lignin is the second most abundant organic substance, it is the most underutilised fraction of lignocellulosic biomass. Therefore, different techniques of recovering lignin (delignification) from lignocellulosic biomass during the pulp and paper process have been explored, in order to fully realize the potential of this biopolymer. Technical lignins are different types of lignins that possess highly variable structures that depend on the species (softwood or hardwood), its seasonal and geographical location, the delignification method employed and the extent or intensity of delignification process. There are different examples of technical lignins and these include: lignosulfonates, Kraft lignin, and organosolv (sulphite-free lignins).[42] It is important to note that technical lignins have significant variability in terms of constituent aromatic units, inter unit linkages, molar mass and molar mass distributions and contain impurities that are dependent on the processing method.[42]

Lignosulfonates

In sulphite pulping, lignin is removed from wood pulp as lignosulfonates. Chemically, lignosulfonates are sodium salts of lignosulfonic acids possessing an admixture of reducing and mineral substances.[43] Lignosulfonates are water-soluble sulfonated derivatives of lignin. Lignosulfonates are used as dispersants in cement applications, water treatment formulations and textile dyes. Lignosulfonates are also used as environmentally sustainable dust-suppression agents for roads.

Kraft lignin

Kraft lignin macromolecules are considered as being polyelectrolytes in black liquor and are separated from black liquor by precipitation. During Kraft pulping, the native lignin undergoes chemical and structural changes due to severe conditions (temperatures greater than 150 °C and high pH). Kraft lignin contains several characteristic features distinguishing it from the other technical lignins. These include (1) an increased number of phenolic groups due to the cleavage of β-aryl bonds during cooking, (2) some biphenyl and other condensed structures that are formed under severe cooking conditions and (3) an increased number of carbonyl groups as well as quinine and catechol structures that are formed under oxidative conditions during the delignification process.[44–46]

Organosolv lignin

Organosolv lignin is obtained from the organosolv pulping technique that uses an organic solvent to solubilize lignin and hemicellulose. The commonly used organic solvents are acetic acid, formic acid and ethanol. This type of technique has been considered to be an environmentally benign alternative to Kraft pulping.[47] Organosolv lignin is an example of sulphite-free lignin. The homogeneity of organosolv lignin is higher than that of lignosulfonates and Kraft lignin.[48]

2.3 Depolymerization of lignin

Lignin depolymerization is the process of breaking down lignin into low molar mass compounds. Depolymerization of lignin is an attractive process as lignin is a renewable bio-based material rich in aromaticity (functionalized aromatic compounds) when selectively broken down. However, the natural structural complexity and high stability of lignin bonds makes lignin depolymerization a highly challenging task.[49] In recent years, many methods of depolymerization have been developed and explored and these include: pyrolysis, hydrogenolysis, enzymatic hydrolysis, acid/base hydrolysis and oxidative depolymerization.[50–53]

During depolymerization of lignin, it is important to have high selectivity towards targeting aryl glycerol–β–aryl ether (β-O-4) bonds of lignin that account for 40–60% of all the linkages found in lignin, shown in Fig. 2.3. It is also important to have efficient control over the depolymerization process. Simultaneously achieving the efficient cleavage of the ether bonds and restraining the condensation of the formed fragments represents a challenge thus far, especially when using extreme conditions of high temperatures ≥300 °C and high pressures>1500 kPa.[54] In the sections that follow, different methods of lignin depolymerization will be reviewed.

2.3.1 Pyrolysis

Pyrolysis of lignin is the thermal treatment of lignin in the absence of oxygen. It can be carried out in the presence or absence of solvents, with or without any catalysts or additives at high temperatures greater than 400 °C.[51, 55] There are two main factors that govern the nature of the products formed, and these are feedstock type and reaction temperature. The main drawback

of pyrolysis is that reaction control is difficult and selectivity is compromised, since very high temperatures ranging between 400 and 600 °C and high pressures are employed. [53] Another drawback of pyrolysis is that this method produces lots of solid char. The mechanism of the reaction involves the homolytic and heterolytic cleavage of the C–O, C–C bonds, and the cleavage of the aryl ether linkages (β-O-4 and α-O-4).[56] The main products of depolymerization are gaseous hydrocarbons, carbon monoxide and carbon dioxide, phenols and simple aromatic compounds, see examples in Fig. 2.4.

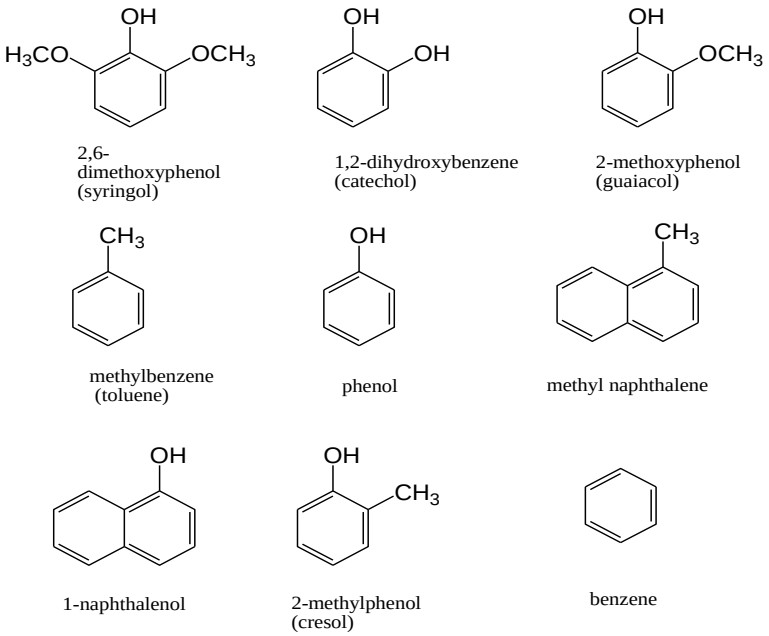

Fig. 2.4: Aromatic products of depolymerization of lignin by pyrolysis

2.3.2 Hydrogenolysis

Hydrogenolysis is a pyrolysis method of depolymerizing lignin in the presence of hydrogen. Hydrogenolysis is a reductive depolymerization technique that depolymerizes lignin into smaller fragments, oligomers and monomers through the cleavage of bonds. Compared to conventional pyrolysis, hydrogenolysis produces less solid char as lower temperatures are employed (<400 °C). There is better control of the depolymerization process as compared to conventional pyrolysis, hence better selectivity and higher yields. There are two ways in which hydrogenolysis can be achieved, (1) by treating the lignin with gaseous hydrogen or (2) by reacting lignin with a hydrogen-donating solvent.[57–58] The main products of hydrogenolysis are shown in Fig. 2.5 [57–58]

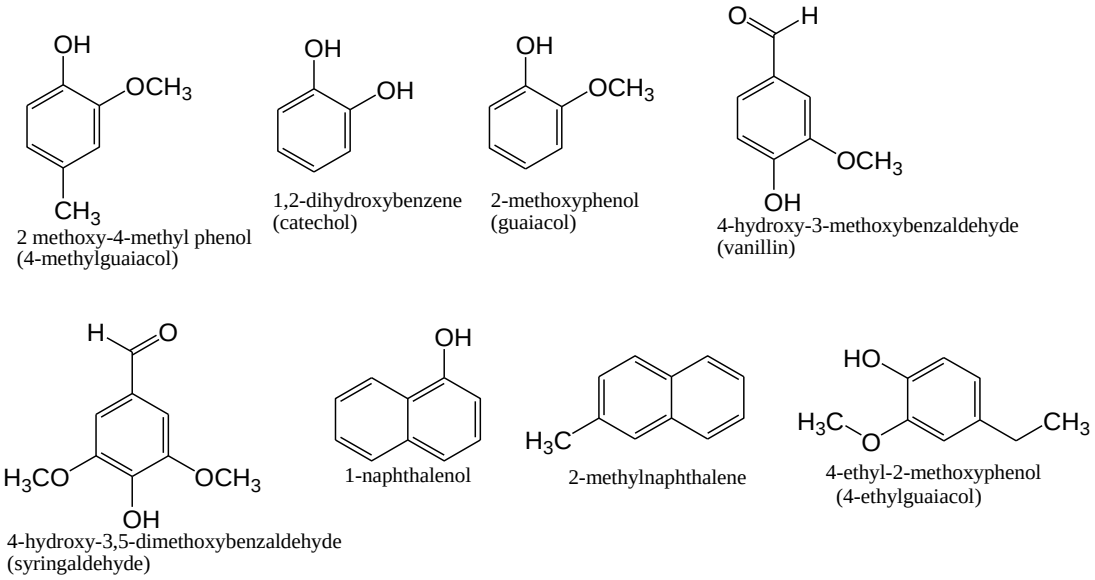

Fig. 2.5: Products of depolymerization of lignin by hydrogenolysis

2.3.3 Enzymatic hydrolysis

In nature, lignin is depolymerized using enzymes.[59–60] Enzymes are biological catalysts that speed up chemical reactions. The two main sources of enzymes for lignin depolymerization are fungi and bacteria. White roti fungi secrete several types of oxidoreductases which act indirectly in a cascading manner, hence results in an oxidative cleavage of aryl ether bonds in lignin.[61] Some fungi produce a hydroxyl radical via Fenton oxidation, which oxidizes compounds obtained by depolymerization, therefore forming a significant amount of acid functionalized monomers, which are shown in Fig. 2.6.[61] The drawbacks of enzymatic depolymerization of lignin is that it is time consuming, for example, a sludge-derived bacterial consortium is able to degrade 60% of the lignin at 30 °C in 15 days.[50]

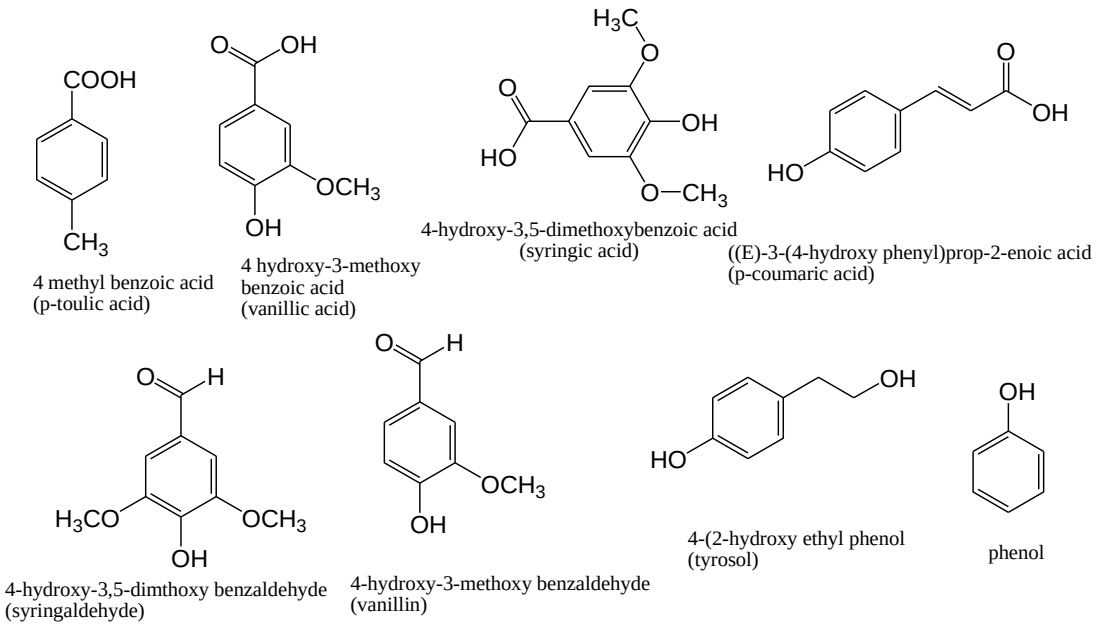

Fig. 2.6: Products of depolymerization of lignin by enzyme catalysed hydrolysis

2.3.4 Chemical depolymerization

Compared to hydrogenolysis and pyrolysis, chemical treatment has its advantages in that, it has better reaction control and high selectivity. Chemical treatment also employs low temperatures compared to pyrolysis and hydrogenolysis. Compared to biological treatment, chemical treatment is also not time consuming. Factoring all the advantages, chemical treatment provides great potential in lignin conversion for renewable fuels and chemical production. Chemical treatment can be categorized into three main classes and these are: acid/base hydrolysis, oxidative depolymerization and ionic liquid depolymerization.

2.3.4.1 Acid/base hydrolysis

Acid/base hydrolysis has been widely used to carry out the fragmentation of lignin to high value monomeric compounds tracing back to Hewson and Hibbert's work in the 1940s.[62] Acid/base hydrolysis is mostly conducted at temperatures ranging between 300 and 330 °C.[53, 63] Compared to other forms of chemical treatment used in lignin depolymerization, acid/base hydrolysis uses higher temperatures to achieve depolymerization which, therefore, compromises selectivity. The mechanism for acid/base hydrolysis involves the cleavage of the aryl-alkyl linkages (β-O-4, α-O-4) but the base-catalyzed depolymerization reaction cleaves not only the susceptible lignin linkages but also other functional groups attached to the aromatic

rings for example methoxy groups.[50] Therefore, taking into account the aforementioned limitations, Wang et al. proposed, the use of co-catalysts in acid-base catalyzed reactions so as to increase selectivity towards achieving highly functionalized aromatics.[53]

The employment of high pressures (greater than 8000 kPa) and the use of very strong acids/bases, increases the cost of reaction equipment (as specialized equipment is needed to withstand the harsh reaction conditions) and post handling. [53] 4-Ethenylphenol, 4-ethyl-2-methoxyphenol (4-ethyl-guaiacol), 4-ethenyl-2-methoxyphenol (vinyl guaiacol), 4-hydroxy-3-methoxybenzaldehyde (vanillin), 4-hydroxy-3,5-dimethoxybenzaldehyde (syringaldehyde), benzene-1,2-diol (catechol) and other monophenols are the compounds mainly formed from acid/base hydrolysis of lignin (see Fig. 2.7).

2.3.4.2 Ionic liquid depolymerization

The use of ionic liquids in lignin depolymerization has recently attracted significant attention. Ionic liquids are regarded as green solvents because they are non-flammable, non-volatile, chemically and thermally stable and they have the ability to dissolve a wide range of compounds. The volatile aromatic products can be removed by distillation and the by-products of lignin depolymerization can be precipitated with water and separated by membrane technologies.[6, 64–65] In addition to the previously mentioned properties and advantages, ionic liquids can act as both an acidic catalyst and a solvent in lignin depolymerization.[50] Xu et al. proposed the use of ionic liquid (1-H-3-methylimidazolium chloride) to enhance the acidolytic cleavage of β-O-4 linkage over a mild temperature range of 110–150 °C.[50]

Ionic liquids can be co-utilized with transition metal catalysts to enhance depolymerization via oxidation.[66] The major drawbacks of lignin depolymerization in ionic liquids include: the cost of ionic liquids, recyclability challenges and difficulties in separation of the ionic liquid with lignin-derived molecules due to the π- π interactions between the aromatic moieties and the ionic liquid.[67] The main compounds in ionic liquid depolymerization of lignin include: 1-(4-hydroxy-3-methoxyphenyl)ethanone (acetovanillone), 1-(4-hydroxy-3,5-dimethoxyphenyl) ethanone (acetosyringone), 2-(4-hydroxy-3-methoxyphenyl)acetic acid (homovanillic acid) and 4-hydroxy-3-methoxybenzaldehyde (vanillin).

2.3.4.3 Oxidative depolymerization

The key issues for lignin deconstruction lie in the development of highly selective and active catalysts and the employment of mild reaction conditions (low temperatures ≤150 °C and low pressures) that effectively cleave the ubiquitous ether bonds leaving the aromatic benzene ring intact.[53] Oxidative depolymerization techniques have several advantages over other methods of depolymerization which include higher selectivity towards the β-O-4 linkages and preserving the aromatic character of the fragments formed during the depolymerization reaction, yielding highly functionalized compounds such as vanillin (4-hydroxy-3-methoxybenzaldehyde), syringaldehyde (4-hydroxy-3,5-dimethoxybenzaldehyde) and acid derivatives of these two (homo-vanillic acid (4-hydroxy-3-methoxybenzoic acid) and syringic acid (4-hydroxy-3,5-dimethoxybenzoic acid)), see Fig. 2.7.

It is important to avoid using extremely severe oxidizing conditions at elevated temperatures as they can disrupt the aromaticity and also promote the repolymerization or recombination of fragments, resulting in a decrease in product yield. Nitrobenzene, oxygen and metal oxides, widely referred to as mild oxidizing agents because they preserve the lignin aromatic ring and produce aldehyde-functionalized aromatic compounds, are often used in oxidative depolymerization reactions.[68–69] Nitrobenzene is an effective oxidant, however, a large portion of the reaction mixture is made up of toxic nitrobenzene derivatives such as azobenzene, 4-(phenylazo)-phenol and azoxybenzene, many of which are volatile and nitrobenzene is also a proven carcinogen.[69–72]

Oxygen is a fairly inexpensive oxidant that is used in the conversion of lignin to aldehydes. The major advantage of using oxygen as an oxidant is that it does not involve the use of added toxic chemicals to the reaction. The major setback is low yield, hence the use of elevated temperatures and pressure. Use of oxygen without a catalyst frequently causes over-oxidation, less selectivity and features a significantly reduced level of conversion to desired products.[73] Oxidative depolymerization can also be done in ionic liquids. Stark et al. oxidatively cleaved lignin in ionic liquid (1-ethyl-3-methylimidazolium trifluoromethane sulfonate, [EMIM][CF_3SO_3]) in the presence of a transition metal catalyst manganese (II) nitrate ($Mn(NO_3)_2$) to give phenols, unsaturated propylaromatics and aromatic aldehydes.[74] Heterogeneous catalysts, mainly metal oxides and metallic transition metals, are also common oxidants in oxidative depolymerization. With relative ease of catalyst recovery, heterogeneous

catalysts are usually preferred industrially and have proven to be advantageous in lignin oxidation.[75]

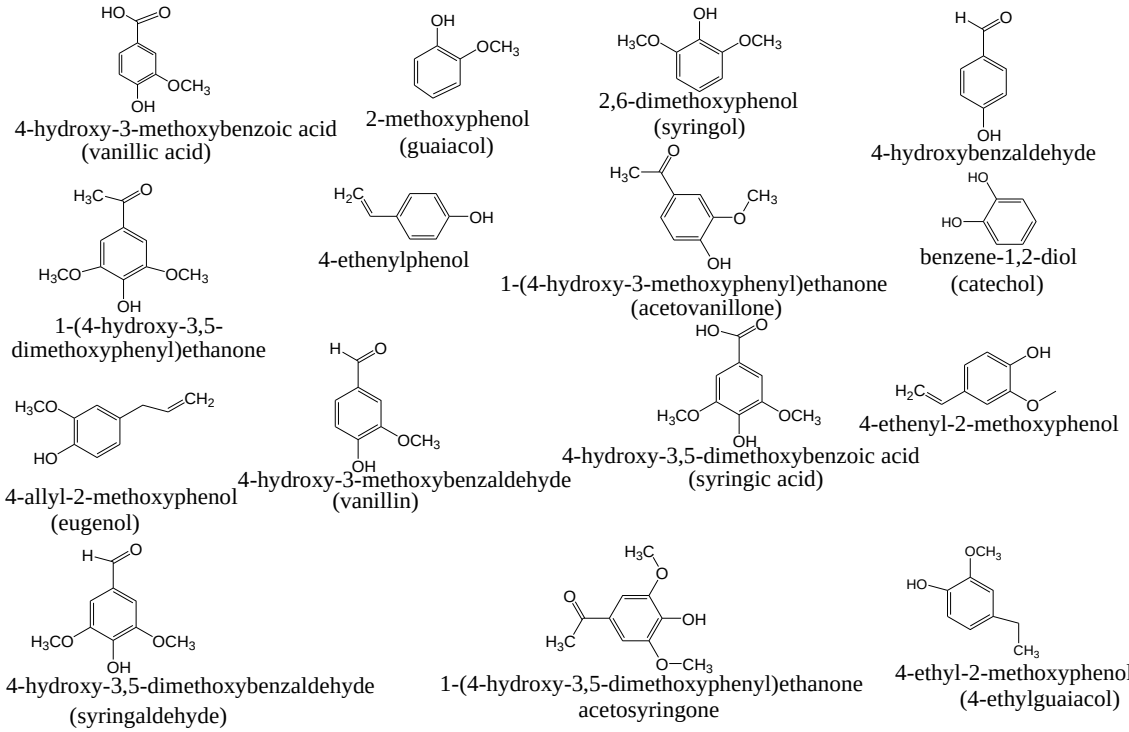

Fig. 2.7: Products of depolymerization of lignin by chemical hydrolysis

2.3.5 Challenges in lignin depolymerization

The natural structural complexity and high stability of lignin bonds makes lignin depolymerization a highly challenging task. Due to its complex composition and structure, the depolymerization of lignin is strongly influenced by its nature, the reaction temperature and deconstruction atmosphere (reaction conditions), which consequently affect conversion and product yields.[76] The nature or character of lignin is determined by delignification conditions, as different conditions including temperatures, pressures, solvents and pH ranges alter the chemical structure and linkages of the lignin.[77]

Simultaneously achieving the efficient cleavage of the ether bonds and restraining the condensation of the formed fragments represents a challenge thus far, especially when using extreme conditions.[54] This is because the cleavage of the arylglycerol-β-aryl ether (β-O-4) and non-cyclic benzyl aryl ether (α-O-4) results in the formation of highly unstable free radicals that may react by electron abstraction or radical-radical interactions to form products with

increased stability.[76] Low monomer yields and low selectivity pose a significant disadvantage in process economics when technical lignins are used as feedstocks. The use of individual compounds from a depolymerized mixture is a challenge from a separation technology point of view. A potential way forward is to make use of the entire depolymerized mixture in a process towards targeted end-products.

2.3.6 Uses of Lignin monomeric compounds

Lignin monomers have a potential to become key-intermediates for the synthesis of bio-based polymers, for which aromatic monomers are needed to reach good thermo-mechanical properties.[78] Vanillin is the most available pure mono-aromatic phenol that is being produced and exploited at an industrial scale from lignin.[79] The application of vanillin has been demonstrated in epoxy polymers as a major substitute for bisphenol A. It is also used in the synthesis of polyesters, acrylate and methacrylate polymers.[80] Van and co-workers used vanillin to synthesize a polybenzoxazine resin for use in electronics, aerospace and composite pipes. The reaction also produces an unused pendant aldehyde group from vanillin which is used to form a reactive monomeric surfactant.[81]

Eugenol is one of the monomers or compounds produced from lignin depolymerization that has also attracted the attention of researchers. Polymers with eugenol moieties covalently bonded to macromolecular chains have been synthesized for the potential application in orthopaedic and dental cements.[82] Eugenol polymer modified titanium electrode is used for the electrochemical determination of cysteine which plays a major role in several biological processes.[83]

Syringaldehyde has been used for the synthesis of poly(ethylene) terephthalate (PET) mimic polymers and for designing a wide range of polymers such as polyacetals, polyanhydrides and polyacrylates.[84] In general, it is important to note that the presence of methoxy substituents on the aromatic ring due to the inherent structure of lignin makes polymers derived from lignin monomers have improved thermal and mechanical properties.[84] Stanzione et al. reported the use of lignin model monomers (vanillin, guaiacol and eugenol) as non-volatile reactive diluents in vinyl ester resins that produced resin viscosities higher than that of ester styrene blends with good cured-resin thermal performance.[85]

2.4 Analytical techniques

Modern analytical techniques are useful to researchers, product development specialists, and quality control experts in polymer synthesis and manufacturing. Because the chemical structure and composition of lignin varies depending on source, type of lignin and isolation method, characterization is important.[86] The depolymerized products of lignin and their respective resultant polymers can be studied using a variety of spectroscopic and chromatographic techniques and these are: size exclusion chromatography (SEC), liquid adsorption chromatography (LAC), gas chromatography (GC), nuclear magnetic resonance (NMR) spectroscopy, mass spectrometry (MS) and Fourier transform infrared (FTIR) spectroscopy.

In recent years, hyphenated techniques have attracted a plethora of research work in pursuit of solving complex analytical problems. Hyphenated techniques synergize chromatographic and spectral methods to exploit the advantages of both e.g liquid chromatography-mass spectrometry (LC-MS) and gas chromatography-mass spectrometry (GC-MS).[87] These techniques are briefly described in the forthcoming section.

2.4.1 Chromatographic techniques

2.4.1.1 Size exclusion chromatography (SEC)

Spectrometric techniques belong to the routine methods for molar mass determination of technical lignins. These methods include matrix-assisted laser desorption/ionization mass spectrometry (MALDI-MS) and electrospray ionization mass spectrometry (ESI-MS). The major disadvantage of MALDI-MS is that it is only applicable to narrow fractions of lignin with low molar mass dispersity.[88–89] When using ESI-MS in molar mass determination, the major shortcoming is that the lignin sample cannot be ionized uniformly due to the heterogeneous chemical nature hence only smaller fragments are detected, larger molecules are suppressed and also the correct assignment of the detected fraction is still a challenge without complementary methods.[90] Therefore, to circumvent some of the challenges associated with spectrometric methods in molar mass determination of lignin, SEC has been widely used.

SEC also known as gel permeation chromatography is an important analytical technique in lignin characterization. The reactivity and physiochemical properties of lignins are partly governed by their molar mass distributions.[91–92] Therefore the determination of molar mass distributions is fundamental in lignin studies. SEC can also be used as a tool for monitoring

and elucidating delignification and depolymerization processes.[91] In principle, separation in SEC is according to the hydrodynamic size of molecules when exposed to a swollen, highly cross-linked organic stationary phase.[93–94] The separation in SEC is governed by entropic effects as compared to liquid adsorption chromatography where enthalpic interactions are predominant.[93] SEC mainly separates polymers according to their molecular dimensions, regardless of their functionality. The general characterization of polymers by SEC involves the determination of the number-average molar mass (M_n), weight-average molar mass (M_w), peak maximum molar mass (M_p) and molar mass dispersity (Đ). Đ is calculated according to Equation 2.1:

$$Đ = \frac{Mw}{Mn} \qquad 2.1$$

where *Đ* is the molar mass dispersity, M_w is the weight-average molar mass, M_n is the number-average molar mass.

The choice of mobile phase composition is very critical in SEC, therefore, it is essential to conduct solubility studies to establish the right mobile phase composition, depending on the nature of the sample and the nature of the stationary phase. A thermodynamically good solvent is one that does not induce any other interactions between the sample and the stationary phase and must be able to dissolve the sample. For most technical lignins, prior to their analysis by SEC, derivatization is typically accomplished through methylation, acetylation or silylation in order to enhance solubility in commonly used organic solvents for SEC such as THF.

The major drawback of derivatization is that it requires sensitive and attentive sample handling as most methods are moisture sensitive and sample derivatization is often a last resort in analysis and method development because of sample modification. Underivatized lignin samples, e.g. lignosulfonates, are relatively well soluble in polar organic solvents such as DMSO, DMAc and DMF.[95] Mobile phase modifiers, e.g. lithium bromide and lithium chloride, are usually added to these organic solvents in order to suppress non-covalent polymer–polymer or polymer–stationary phase interactions.

Lignin has an unusual molecular structure in solution which compromises data accuracy when conventional, single detector, calibration-based SEC is applied. This is because there is an absence of calibration standards of similar molecular structure. Polystyrene standards have

been used as calibration standards but the hydrodynamic volumes of lignin and polystyrene differ, making the analysis to be relative.[95] Therefore, routes of determining absolute molar masses for lignin samples have been explored. SEC coupled to multiangle laser light scattering (MALLS) detection has been used to avoid calibration problems. SEC-MALLS directly measures molar mass without any requirement of calibration. However, lignin has a tendency to fluoresce in solution and, therefore, corrections for fluorescence, light absorption and polarization complicated the analysis. The other concern of using MALLS with reference to lignin analysis involves poor signal-to-noise ratios in scattered light intensities from compounds possessing molar masses below 10 000 g/mol.[96] Zinovyev and co-workers developed a SEC-MALLS method in pursuit of overcoming the limitations posed by lignin analysis using SEC-MALLS by applying fluorescence filters to eliminate the effects of lignin fluorescence. Any residual fluorescence was corrected by extrapolation of the molar mass data from the high molar mass range towards the medium and low molar mass range. The light absorption problem was eliminated by referencing with the laser forward monitor of the detector.[97]

2.4.1.2 Liquid adsorption chromatography

Liquid adsorption chromatography (LAC) is directed by adsorptive (enthalpic) interactions between the molecules and the stationary phase, as compared to SEC which is governed mainly by entropic effects.[93–94] Reversed phase liquid chromatography (RP-LC) and normal phase liquid chromatography (NP-LC) have been employed for the separation and quantification of the main degradation products of lignin.[98–99] RP-LC employs a non-polar stationary phase and a more polar mobile phase. The hydrophobic stationary phase has a stronger affinity for hydrophobic or less polar compounds, as they tend to adsorb to the hydrophobic stationary phase whereas hydrophilic molecules in the mobile phase elute first. NP-LC employs a polar stationary phase and non-polar mobile phase. In NP-LC, the least polar compounds elute first and the most polar are retained to elute later.[100]

HPLC analysis can either be isocratic or gradient elution. Isocratic analysis is when the composition of the mobile phase does not change during the analysis whereas in gradient elution, the composition of the mobile phase is altered over the course of the analysis. Jiang et al. used RP-LC for the separation and quantification of the main degradation products of lignin (vanillin, syringaldehyde, syringic acid and vanillic acid) on a C_{18} column with acetonitrile-

water as the mobile phase at 30 ^{o}C at a flowrate of 0.8 mL/min, using UV as the detector (at wavelengths of 254 and 280 nm).[98] Co-elution is a challenge with regard to the depolymerized product mixtures of lignin due to the similarities in properties (polarity, chemical composition and or size) of the compounds in the product mixture. A mass spectrometer (MS) has been used as an additional detector to the concentration detectors (ultraviolet (UV) and refractive index (RI)) in HPLC. The hyphenation of chromatographic techniques with mass spectrometry will be reviewed in section 2.4.1.4.

2.4.1.3 Gas chromatography

Gas chromatography has been used for the qualitative and quantitative analysis of lignin depolymerized products.[63, 101] The principle of separation is that the sample is injected into the GC inlet where it is volatilized and carried onto the column by the mobile phase (carrier gas that is helium or nitrogen or hydrogen).[102]

The sample constituents are separated by differential partitioning in the stationary (polar or nonpolar) and gaseous mobile phases. Separation on polar columns is based on specific interactions between analytes and the stationary phase (as well as volatility), including hydrogen bonding and dipole-dipole interactions. Thus, the compounds are separated due to differences in their activity coefficients. On nonpolar columns, interactions are non-specific dispersion interactions (van der Waals forces). Therefore, compound retention is largely determined by the amount present in the vapour phase, hence compounds are commonly eluted from the column in order of increasing boiling point. The separated sample components elute from the column into the detector, e.g a flame ionization detector or an electron capture detector. Mass spectrometry is an extremely versatile detection system for GC that has been widely used to characterize degradation products of lignin.[101, 103] The hyphenation of GC or LC with mass spectrometry (MS) will be discussed in the following section.

2.4.1.4 Hyphenation of chromatographic techniques with mass spectrometry

The hyphenation of chromatographic separations with MS provide powerful analytical tools that combine the resolving power of chromatography with the detection specificity of MS. MS is an analytical technique that is used to determine the molar mass of molecules or fragments and for the identification of compounds within a sample in order to elucidate the structure and chemical properties of different molecules. MS involves the ionization of a chemical species

and sorts the ions based on their mass-to-charge ratio (m/z). The common ionization modes that have been used for the analysis of lignin and its monomeric compounds in LC-MS and GC-MS are electrospray ionization (ESI) and electron impact ionization (EI), respectively.

ESI is a soft ionization technique, where the analyte is ionized by forcing a solution (commonly in an organic solvent) of the sample through a small heated capillary into an electric field to produce a very fine mist of charged droplets. The respective ions are then sorted by their mass to charge ratio (m/z) and relative abundance in the mass analyzer. Compared to EI, ESI is more suitable for analyzing non-volatile and thermally labile biomacromolecules hence its hyphenation with HPLC. In lignin analysis, the advantages for using ESI are that it accounts for oligomeric species and high molar mass species that cannot be analyzed by GC-MS. ESI-MS has been used as a useful tool in an attempt to identify compounds that are formed by the depolymerization of lignin. [104] However, due to the high complexity of the large number of products formed during depolymerization, it is not practical to determine all the monomeric compounds after depolymerization.[105]

On the other hand, ionization in EI involves thermal vaporization, and the bombardment of the analyte with a high energy beam of electrons to produce positive ions and fragmented ion species. The resulting fragmentation pattern provides useful structural information. Compared to ESI, EI provides mass spectral libraries for easy and convenient structural elucidation. EI's shortcomings are that the samples must be volatile and stable. In addition, due to the use of high energies, EI induces analyte fragmentation, hence the parent ion might be absent.

In LC-MS and GC-MS, mass spectrometers can be operated in two modes, scan mode or selected ion/reaction monitoring mode (SIM/SRM). In scan mode, the mass spectrometer detects signals over a mass range (e.g. 50–2000 g/mol) in a short period of time hence sensitivity is compromised for a complex sample matrix. This mode of operation is typically used for qualitative analysis. In SIM/SRM mode, the mass spectrometer is set to only monitor a few m/z values, hence the mass analyzer (typically quadrupole mass analyzer) is able to spend significantly more time sampling each of the m/z values and, therefore, increased sensitivity is obtained. The term SRM is used for a triple quadrupole mass analyzer, and SIM for a single quadrupole mass analyzer.[106]

2.4.2 Spectroscopic techniques

Lignin is a complex, hyperbranched, heterogeneous polymer and, therefore, many techniques have been employed to determine its chemical structure. Because the chemical structure of lignin varies based on source, type, and even isolation technique, a significant number of techniques are used to identify these differences.[86] Depending on its mode of modification for various industrial uses, technical lignins might have differences in structure, therefore, a comprehensive chemical structural analysis is necessary. Technical lignins have a modified structure and contain impurities reliant or dependent on the processing method.[42] Spectroscopic techniques can be used to provide qualitative and quantitative information on functional groups and linkages in lignin as well as the depolymerized products.

2.4.2.1 Fourier transform infrared (FTIR) spectroscopy

FTIR spectroscopy is widely used for the qualitative and quantitative analysis of polymers and organic compounds. The principle of this spectroscopic technique relies on the fact that different functional groups in a molecule have different dipole moments, hence, the energy that is required to cause the bonds to vibrate is different for each type of functional group.[11] Energy is quantified as either absorbance or transmittance. This technique has been widely used for the analysis of lignin and its derivatives (including the depolymerized products of lignin). FTIR spectroscopy has been used to trace the progress or extent of depolymerization as the spectra of the native technical lignin and of the depolymerized lignin can be compared.[107–109]

2.4.2.2 Nuclear magnetic resonance (NMR) spectroscopy

Nuclear Magnetic Resonance (NMR) is a well-established universal technique that has been extensively employed in the domain of wood chemistry due to its sensitivity and reliability in structural elucidation of unknown compounds.[86, 110] Polymers like lignin, historically, posed a challenge for NMR studies. This was because the higher the molecular weight, the higher the viscosity. Therefore, this would lead to low mobility which in turn leads to short relaxation times, broadening of signals and, therefore, limiting a detailed characterization of the polymeric components.[86]

Recent advances in nuclear magnetic resonance (NMR) spectroscopy undoubtedly have made NMR to become the most widely used technique in structural characterization of lignin due to its versatility in illustrating structural features and structural transformations of lignin and its

degradation products.[111] However, because of the polymeric nature of lignin, diversity of protons from various structures, and irregularity of linkages between building units in lignin, the ^{1}H NMR spectrum of lignin is somewhat overlapped and difficult to accurately interpret. ^{13}C NMR has been extensively used in lignin characterization in order to elucidate a large amount of lignin structural information including the presence of aryl ethers, as well as condensed and uncondensed aromatic and aliphatic carbons. However, ^{13}C NMR analysis is less sensitive and, therefore, long acquisitions times and very high sample concentration are required to promote sensitivity (signal-to-noise ratio).[112]

NMR can be used to confirm the successful depolymerization of lignin. Deepa and Dhepe, established by NMR that the few functional groups and aromaticity present in lignin are retained in the products (a good depolymerization technique is one that preserves the aromatic character of the fragments and gives functionalized compounds). [101]

With advances in NMR technology, 2D NMR has been used for the characterization of the structure of lignin and the products of lignin depolymerization (qualitatively and quantitatively). Due to the complexity of this biopolymer and complex depolymerized product mixtures, 1D NMR experiments cannot fully elucidate the structural features of lignin, hence the use of 2D NMR.[113–114] 2D NMR is a set of NMR methods which outline data plotted in space defined by two axes highlighting more than 1 variable depending on the experimental conditions (usually displayed as contour plots) e.g HSQC (heteronuclear single-quantum correlation spectroscopy) and COSY (correlation spectroscopy).

The following section briefly discusses the potential fate of lignin-derived monomers, with the attention being on bio-based polymers.

2.5 Polymerization of lignin derived monomers

The synthesis of new polymers with novel properties may use two different strategies which include: the synthesis of new monomers or the development of new polymerization methods.[115] Due to a wide range of functional groups in the depolymerized products of lignin, different avenues of modification of these aromatic monomeric compounds can be explored for different types of polymerization techniques which include polycondensation, conventional radical polymerization and reversible deactivation radical polymerization (RDRP).

The synthesis of renewable homopolymers and block copolymers via functionalization and subsequent controlled reversible addition fragmentation chain transfer polymerization has been reported.[85, 116–119] Controlled synthesis such as RAFT unlock possibilities for the lignin monomeric compounds to be incorporated into block copolymers for applications such as thermoplastic elastomers, pressure-sensitive adhesives and composite binders.[117] Separating complex mixtures of depolymerized products of lignin into single or two-component streams has been reported to be a challenge thus far. It has, therefore, prompted researchers to exploit the molecular diversity of the complex mixtures to synthesize multicomponent polymers, and heteropolymers.[78, 120]

Depolymerization of lignin produces a wide array of functionalized aromatic compounds (vanillin, guaiacol and syringaldehyde) that mimic common monomers which include bisphenol A and styrene essential for polymer applications. Depending on the polymerization technique employed, functionalization of lignin monomeric compounds for polymerization is diverse.[117] In radical polymerization the principle of polymerization is based on the presence of a vinyl group. Since the compounds produced by the depolymerization of lignin are not often vinyl-functionalized, it is important that a polymerizable vinyl group be introduced to these compounds but still maintaining their functionalized state. Stanzione et al. introduced a vinyl group to the lignin monomeric compounds by the esterification reaction with methacrylic anhydride in the presence of a catalytic amount of 4-dimethylaminopyridine, see Scheme 2.2.[85]

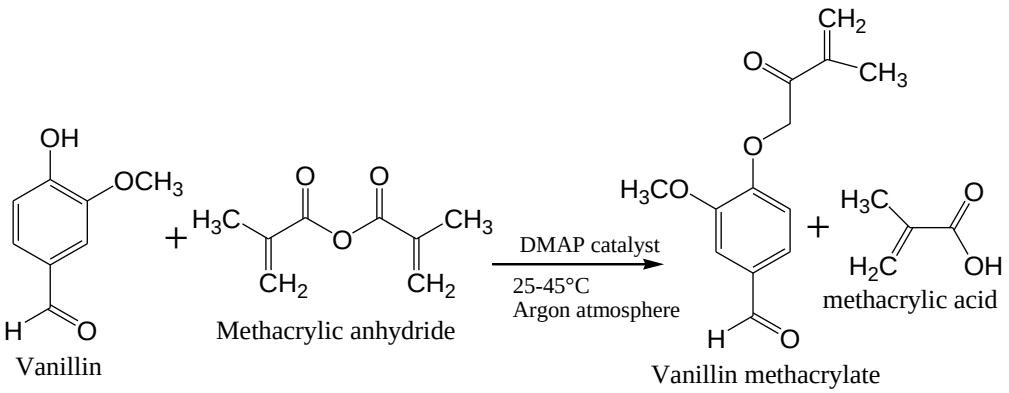

Scheme 2.2: Reaction of vanillin with methacrylic anhydride

Polycondensation reactions can also be initiated by the modification of lignin monomeric compounds (for example vanillin) with an external compound such as acetic anhydride for the

polymerization of acetyldihydroferulic acid, see Scheme 2.3. Poly(dihydroferulic acid) is a sustainable polymer that exhibits properties similar to polyethylene terephthalate.[119]

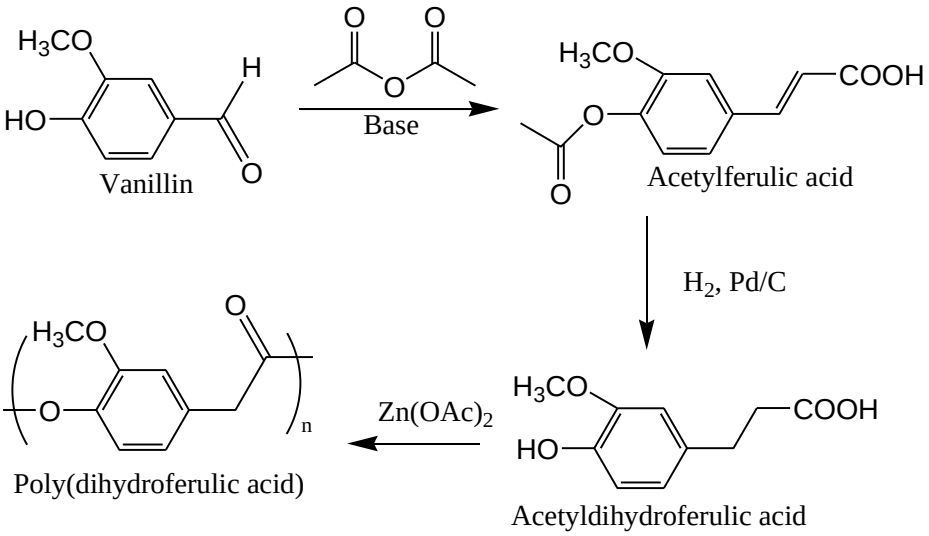

Scheme 2.3: Synthesis of Poly(dihydroferulic acid) via polycondensation reaction

In this work guaiacol (a product derived from lignin depolymerisation) was modified using itaconic anhydride to give a radically polymerizable fully bio-based monomer. The details of this reaction are presented in Chapter 6.

2.6 References

1. Schulz, D.; Patil, A. O., Functional Polymers: An Overview. In *Functional Polymers*, 1st ed.; Patil, A. O., Schulz, D.N., Novak, M.N, Ed. American Chemical Society Washington, D.C., United States, 1998; Vol. 704, pp 1–14.

2. Wegner, G., *Acta Materialia* **2000,** *48* (1), 253–262.

3. Frechet, J. M., *Science* **1994,** *263* (5154), 1710–1715.

4. Kralik, M.; Biffis, A., *Journal of Molecular Catalysis A: Chemical* **2001,** *177* (1), 113–138.

5. Neffe, A. T.; Grijpma, D. W.; Lendlein, A., *Macromolecular Bioscience* **2016,** *16* (12), 1743–1744.

6. Kiriy, A.; Pötzsch, R.; Wei, Q.; Voit, B., *Polymer Degradation and Stability* **2017,** *145*, 150–156.

7. Weil, T.; Barz, M., *Macromolecular Bioscience* **2017,** *17* (10), 1–4.

8. Yang, B.; Willies, D. M.; Wyman, C. E., *Biotechnology and Bioengineering* **2006,** *94* (6), 1122–1128.

9. Vijjamarri, S.; Streed, S.; Serum, E. M.; Sibi, M. P.; Du, G., *ACS Sustainable Chemistry and Engineering* **2018,** *6* (2), 2491–2497.

10. Bozell, J. J.; Moens, L.; Elliott, D.; Wang, Y.; Neuenscwander, G.; Fitzpatrick, S.; Bilski, R.; Jarnefeld, J., *Resources, Conservation and Recycling* **2000,** *28* (3–4), 227–239.

11. Diop, A.; Jradi, K.; Daneault, C.; Montplaisir, D., *BioResources* **2015,** *10* (3), 4933–4946.

12. Williams, C. K.; Hillmyer, M. A., *Polymer Reviews* **2008,** *48* (1), 1–10.

13. Nakajima, H.; Dijkstra, P.; Loos, K., *Polymers* **2017,** *9* (10), 1–26.

14. Hollabaugh, C.; Burt, L. H.; Walsh, A. P., *Industrial and Engineering Chemistry* **1945,** *37* (10), 943–947.

15. Rose, M.; Palkovits, R., *Macromolecular Rapid Communications* **2011,** *32* (17), 1299–1311.

16. Klemm, D.; Heublein, B.; Fink, H. P.; Bohn, A., *Angewandte Chemie International Edition* **2005,** *44* (22), 3358–3393.

17. Wang, J.; Zhou, X.; Xiao, H., *Carbohydrate Polymers* **2013,** *94* (2), 749–754.

18. Mohsenzadeh, A.; Zamani, A.; Taherzadeh, M. J., *ChemBioEng Reviews* **2017,** *4* (2), 75–91.

19. Clark, J. H.; Farmer, T. J.; Hunt, A. J.; Sherwood, J., *International Journal of Molecular Sciences* **2015,** *16* (8), 17101–17159.

20. Chalid, M. Levulinic acid as a renewable source for novel polymers. PhD, University of Groningen, The Netherlands, 2012.

21. Werpy, T.; Petersen, G.; Aden, A.; Bozell, J.; Holladay, J.; White, J.; Manheim, A.; Eliot, D.; Lasure, L.; Jones, S. *Top value added chemicals from biomass. Volume 1-Results of screening for potential candidates from sugars and synthesis gas*; Department of Energy Washington DC: 2004.

22. Liakos, I. L.; Holban, A. M.; Carzino, R.; Lauciello, S.; Grumezescu, A. M., *Nanomaterials* **2017,** *7* (4), 1–10.

23. Reier, G. E.; Shangraw, R. F., *Journal of Pharmaceutical Sciences* **1966,** *55* (5), 510–514.

24. Xiao, C.; Xia, C.; Ma, Y.; He, X., *Journal of Applied Polymer Science* **2013,** *127* (6), 4750–4755.

25. Schofield, P.; Mbugua, D.; Pell, A., *Animal Feed Science and Technology* **2001,** *91* (1–2), 21–40.

26. Reed, J. D.; McDowell, R. T.; Van Soest, P. J.; Horvath, P. R., *Journal of the Science of Food and Agriculture* **1982,** *33* (3), 213–220.

27. Pasch, H.; Pizzi, A., *Journal of Applied Polymer Science* **2002,** *85* (2), 429–437.

28. Pizzi, A.; Pasch, H.; Rode, K.; Giovando, S., *Journal of Applied Polymer Science* **2009,** *113* (6), 3847–3859.

29. Szekeres, M.; Illés, E.; Janko, C.; Farkas, K.; Tóth, I. Y.; Nesztor, D.; Zupkó, I.; Földesi, I.; Alexiou, C.; Tombácz, E., *Journal of Nanomedicine and Nanotechnology* **2015,** *6* (1), 1–7.

30. Katsoulidis, A. P.; Kanatzidis, M. G., *Chemistry of Materials* **2011,** *23* (7), 1818–1824.

31. Curvelo, A.; De Carvalho, A.; Agnelli, J., *Carbohydrate Polymers* **2001,** *45* (2), 183–188.

32. Okuda, T.; Ishimoto, K.; Ohara, H.; Kobayashi, S., *Macromolecules* **2012,** *45* (10), 4166–4174.

33. Auras, R.; Harte, B.; Selke, S., *Macromolecular Bioscience* **2004,** *4* (9), 835–864.

34. Carvalho, A. J., Starch: major sources, properties and applications as thermoplastic materials. In *Monomers, Polymers and Composites from Renewable Resources*, Elsevier: 2008; pp 321–342.

35. Raza, Z. A.; Abid, S.; Banat, I. M., *International Biodeterioration and Biodegradation* **2018,** *126*, 45–56.

36. Boeriu, C. G.; Bravo, D.; Gosselink, R. J.; van Dam, J. E., *Industrial Crops and Products* **2004,** *20* (2), 205–218.

37. Lora, J. H.; Glasser, W. G., *Journal of Polymers and the Environment* **2002,** *10* (1–2), 39–48.

38. Lu, F.; Ralph, J., *Journal of Agricultural and Food Chemistry* **1997,** *45* (7), 2590–2592.

39. Guerra, A.; Filpponen, I.; Lucia, L. A.; Argyropoulos, D. S., *Journal of Agricultural and Food Chemistry* **2006,** *54* (26), 9696–9705.

40. Laurichesse, S.; Avérous, L., *Progress in Polymer Science* **2014,** *39* (7), 1266–1290.

41. Del Rio, J. C.; Rencoret, J.; Marques, G.; Gutiérrez, A.; Ibarra, D.; Santos, J. I.; Jiménez-Barbero, J. s.; Zhang, L.; Martínez, A. n. T., *Journal of Agricultural and Food Chemistry* **2008,** *56* (20), 9525–9534.

42. Crestini, C.; Lange, H.; Sette, M.; Argyropoulos, D. S., *Green Chemistry* **2017,** *19* (17), 4104–4121.

43. Matsushita, Y.; Yasuda, S., *Bioresource Technology* **2005,** *96* (4), 465–470.

44. Vishtal, A. G.; Kraslawski, A., *BioResources* **2011,** *6* (3), 3547–3568.

45. Hu, J.; Zhang, Q.; Lee, D.-J., *Bioresource Technology* **2018,** *247*, 1181–1183.

46. Chakar, F. S.; Ragauskas, A. J., *Industrial Crops and Products* **2004,** *20* (2), 131–141.

47. Toledano, A.; Serrano, L.; Labidi, J., *Journal of Chemical Technology and Biotechnology* **2012,** *87* (11), 1593–1599.

48. de la Torre, M. J.; Moral, A.; Hernández, M. D.; Cabeza, E.; Tijero, A., *Industrial Crops and Products* **2013,** *45*, 58–63.

49. Amen-Chen, C.; Pakdel, H.; Roy, C., *Bioresource Technology* **2001,** *79* (3), 277–299.

50. Xu, C.; Arancon, R. A. D.; Labidi, J.; Luque, R., *Chemical Society Reviews* **2014,** *43* (22), 7485–7500.

51. Carlson, T. R.; Vispute, T. P.; Huber, G. W., *ChemSusChem* **2008,** *1* (5), 397–400.

52. Toledano, A.; Serrano, L.; Pineda, A.; Romero, A. A.; Luque, R.; Labidi, J., *Applied Catalysis B: Environmental* **2014,** *145*, 43–55.

53. Wang, H.; Tucker, M.; Ji, Y., *Journal of Applied Chemistry* **2013**, Article ID 838645 (http://dx.doi.org/10.1155/2013/838645).

54. Zhang, C.; Li, H.; Lu, J.; Zhang, X.; MacArthur, K. E.; Heggen, M.; Wang, F., *ACS Catalysis* **2017,** *7* (5), 3419–3429.

55. Akash, B., *Procedia Computer Science* **2015,** *52*, 827–834.

56. Kawamoto, H., *Journal of Wood Science* **2017,** *63* (2), 117–132.

57. Das, L.; Li, M.; Stevens, J. C.; Li, W.; Pu, Y.; Ragauskas, A. J.; Shi, J., *ACS Sustainable Chemistry and Engineering* **2018,** *6* (8), 10408–10420.

58. Gillet, S.; Aguedo, M.; Petitjean, L.; Morais, A.; da Costa Lopes, A.; Łukasik, R.; Anastas, P., *Green Chemistry* **2017,** *19* (18), 4200–4233.

59. de Gonzalo, G.; Colpa, D. I.; Habib, M. H.; Fraaije, M. W., *Journal of Biotechnology* **2016,** *236*, 110–119.

60. Salvachúa, D.; Katahira, R.; Cleveland, N. S.; Khanna, P.; Resch, M. G.; Black, B. A.; Purvine, S. O.; Zink, E. M.; Prieto, A.; Martínez, M. J., *Green Chemistry* **2016,** *18* (22), 6046–6062.

61. Bugg, T. D.; Ahmad, M.; Hardiman, E. M.; Singh, R., *Current Opinion in Biotechnology* **2011,** *22* (3), 394–400.

62. Hewson, W. B.; Hibbert, H., *Journal of the American Chemical Society* **1943,** *65* (6), 1173–1176.

63. Lavoie, J.-M.; Baré, W.; Bilodeau, M., *Bioresource Technology* **2011,** *102* (7), 4917–4920.

64. Zhang, Z. C., *Advances in Catalysis* **2006,** *49*, 153–237.

65. Diop, A.; Bouazza, A. H.; Daneault, C.; Montplaisir, D., *BioResources* **2013,** *8* (3), 4270–4282.

66. Crestini, C.; Crucianelli, M.; Orlandi, M.; Saladino, R., *Catalysis Today* **2010,** *156* (1–2), 8–22.

67. Zakzeski, J.; Bruijnincx, P. C.; Jongerius, A. L.; Weckhuysen, B. M., *Chemical Reviews* **2010,** *110* (6), 3552–3599.

68. F. De Gregorio, G.; Prado, R.; Vriamont, C.; Erdocia, X.; Labidi, J.; Hallett, J. P.; Welton, T., *ACS Sustainable Chemistry and Engineering* **2016,** *4* (11), 6031–6036.

69. Pandey, M. P.; Kim, C. S., *Chemical Engineering and Technology* **2011,** *34* (1), 29–41.

70. Villar, J. C.; Caperos, A.; García-Ochoa, F., *Journal of Wood Chemistry and Technology* **1997,** *17* (3), 259–285.

71. Pew, J. C., *Journal of the American Chemical Society* **1955,** *77* (10), 2831–2833.

72. Jablonsky, M.; Haz, A.; Škulcova, A.; Dubinyova, L.; Šurina, I.; Kacik, F.; Kacikova, D., *Cellulose Chemistry and Technology* **2016,** *50* (7–8), 731–735.

73. Upton, B. M.; Kasko, A. M., *Chemical Reviews* **2015,** *116* (4), 2275–2306.

74. Stärk, K.; Taccardi, N.; Bösmann, A.; Wasserscheid, P., *ChemSusChem* **2010,** *3* (6), 719–723.

75. Das, L.; Kolar, P.; Sharma-Shivappa, R., *Biofuels* **2012,** *3* (2), 155–166.

76. Brebu, M.; Vasile, C., *Cellulose Chemistry and Technology* **2010,** *44* (9), 353–363.

77. Erdocia, X.; Prado, R.; Corcuera, M. A.; Labidi, J., *Biomass and Bioenergy* **2014,** *66*, 379–386.

78. Fache, M.; Boutevin, B.; Caillol, S., *Green Chemistry* **2016,** *18* (3), 712–725.

79. Holladay, J. E.; White, J. F.; Bozell, J. J.; Johnson, D. *Top value-added chemicals from biomass-Volume II—Results of screening for potential candidates from biorefinery lignin*; Pacific Northwest National Laboratory (PNNL), Richland, WA (US): 2007.

80. Fache, M.; Boutevin, B.; Caillol, S., *ACS Sustainable Chemistry and Engineering* **2015,** *4* (1), 35–46.

81. Van, A.; Chiou, K.; Ishida, H., *Polymer* **2014,** *55* (6), 1443–1451.

82. Rojo, L.; Vazquez, B.; Parra, J.; López Bravo, A.; Deb, S.; San Roman, J., *Biomacromolecules* **2006,** *7* (10), 2751–2761.

83. El Qouatli, S.; Ngono, R.; Najih, R.; Chtaini, A., *Scientific Study and Research. Chemistry and Chemical Engineering* **2012,** *13* (2), 137–143.

84. Peng, L.; Wu, C. S.; You, M.; Han, D.; Chen, Y.; Fu, T.; Ye, M.; Tan, W., *Chemical Science* **2013,** *4* (5), 1928–1938.

85. Stanzione, J. F.; Sadler, J. M.; La Scala, J. J.; Wool, R. P., *ChemSusChem* **2012,** *5* (7), 1291–1297.

86. Stark, N. M.; Yelle, D. J.; Agarwal, U. P., Techniques for characterizing lignin. In *Lignin in Polymer Composites*, Omar Faruk, M. S., Ed. Elsevier: Oxford, UK, 2016; pp 49–66.

87. Patel, K. N.; Patel, J. K.; Patel, M. P.; Rajput, G. C.; Patel, H. A., *Pharmaceutical Methods* **2010,** *1* (1), 2–13.

88. Jacobs, A.; Dahlman, O., *Biomacromolecules* **2001,** *2* (3), 894–905.

89. Rönnols, J.; Jacobs, A.; Aldaeus, F., *Holzforschung* **2017,** *71* (7–8), 563–570.

90. Mattinen, M.-L.; Suortti, T.; Gosselink, R.; Argyropoulos, D. S.; Evtuguin, D.; Suurnäkki, A.; de Jong, E.; Tamminen, T., *BioResources* **2008,** *3* (2), 549–565.

91. Baumberger, S.; Abaecherli, A.; Fasching, M.; Gellerstedt, G.; Gosselink, R.; Hortling, B.; Li, J.; Saake, B.; de Jong, E., *Holzforschung* **2007,** *61* (4), 459–468.

92. Constant, S.; Wienk, H. L.; Frissen, A. E.; de Peinder, P.; Boelens, R.; Van Es, D. S.; Grisel, R. J.; Weckhuysen, B. M.; Huijgen, W. J.; Gosselink, R. J., *Green Chemistry* **2016,** *18* (9), 2651–2665.

93. Pasch, H., Trathnigg, B, *HPLC of Polymers*. Springer-Verlag Berlin Heidelberg: Berlin Heidelberg, 1999, pp 1–16.

94. Pasch, H., Trathnigg, B, *Multidimensional HPLC of Polymers*. Springer-Verlag Berlin Heidelberg: Berlin, 2013, pp 41–80.

95. Tolbert, A.; Akinosho, H.; Khunsupat, R.; Naskar, A. K.; Ragauskas, A. J., *Biofuels, Bioproducts and Biorefining* **2014,** *8* (6), 836–856.

96. Himmel, M. E., Mlynár, J., Sarkanen, S, Size Exclusion Chromatography of Lignin Derivatives. In *Handbook of Size Exclusion Chromatography*, Chi-san Wu, Ed. Marcel Dekker, Inc.: Marcel Dekker, Inc, 270 Madison Avenue, New York, 1995; pp 353–380.

97. Zinovyev, G.; Sulaeva, I.; Podzimek, S.; Rössner, D.; Kilpeläinen, I.; Sumerskii, I.; Rosenau, T.; Potthast, A., *ChemSusChem* **2018,** *11* (18), 3259–3268

98. Jiang, Z.; Zhu, J.; Li, X.; Lian, Z.; Yu, S.; Yong, Q., *Chinese Journal of Chromatography* **2011,** *29* (1), 59–62.

99. Ingalls, A. E.; Ellis, E. E.; Santos, G. M.; McDuffee, K. E.; Truxal, L.; Keil, R. G.; Druffel, E. R., *Analytical Chemistry* **2010,** *82* (21), 8931–8938.

100. Snyder, L. R., Kirkland, J.J., Glajch, J.L, *Practical HPLC Method Development*. 2nd Edition ed.; John Wiley and Sons, Inc: Canada, 1997, pp 233–288 .

101. Deepa, A. K.; Dhepe, P. L., *ACS Catalysis* **2014,** *5* (1), 365–379.

102. Martin, A.; Synge, R. M., *Biochemical Journal* **1941,** *35* (12), 1358–1368.

103. Ouyang, T.; Wang, L.; Cheng, F.; Hu, Y.; Zhao, X., *BioResources* **2018,** *13* (2), 3880–3891.

104. Evtuguin, D.; Domingues, P.; Amado, F.; Neto, C. P.; Correia, A. F., *Holzforschung* **1999,** *53* (5), 525–528.

105. Xia, G.-G.; Chen, B.; Zhang, R.; Zhang, Z. C., *Journal of Molecular Catalysis A: Chemical* **2014,** *388*, 35–40.

106. Lange, V.; Picotti, P.; Domon, B.; Aebersold, R., *Molecular Systems Biology* **2008,** *4* (1), 1–14.

107. Mansouri, N. E. E.; Pizzi, A.; Salvado, J., *Journal of Applied Polymer Science* **2007,** *103* (3), 1690–1699.

108. Xiao, B.; Sun, X.; Sun, R., *Polymer Degradation and Stability* **2001,** *74* (2), 307–319.

109. Tejado, A.; Pena, C.; Labidi, J.; Echeverria, J.; Mondragon, I., *Bioresource Technology* **2007,** *98* (8), 1655–1663.

110. Bovey, F. A.; Mirau, P. A., 1 - Fundamentals of Nuclear Magnetic Resonance. In *NMR of Polymers*, Bovey, F. A.; Mirau, P. A., Eds. Academic Press: San Diego, 1996; pp 1–115.

111. Wen, J.-L.; Sun, S.-L.; Xue, B.-L.; Sun, R.-C., *Materials* **2013,** *6* (1), 359–91.

112. Gellerstedt, G.; Robert, D., *Acta Chemica Scandinavica. B* **1987,** *41* (7), 541–546.

113. Mattsson, C.; Andersson, S.-I.; Belkheiri, T.; Åmand, L.-E.; Olausson, L.; Vamling, L.; Theliander, H., *Biomass and Bioenergy* **2016,** *95*, 364–377.

114. Sette, M.; Lange, H.; Crestini, C., *Computational and Structural Biotechnology Journal* **2013,** *6* (7), 1–7.

115. Boyer, C.; Lacroix-Desmazes, P.; Robin, J.-J.; Boutevin, B., *Macromolecules* **2006,** *39* (12), 4044–4053.

116. Holmberg, A. L.; Reno, K. H.; Nguyen, N. A.; Wool, R. P.; Epps III, T. H., *ACS Macro letters* **2016,** *5* (5), 574–578.

117. Holmberg, A. L.; Stanzione III, J. F.; Wool, R. P.; Epps III, T. H., *ACS Sustainable Chemistry and Engineering* **2014,** *2* (4), 569–573.

118. Zhou, J.; Zhang, H.; Deng, J.; Wu, Y., *Macromolecular Chemistry and Physics* **2016,** *217* (21), 2402–2408.

119. Mialon, L.; Pemba, A. G.; Miller, S. A., *Green Chemistry* **2010,** *12* (10), 1704–1706.

120. Stanzione III, J. F.; Giangiulio, P. A.; Sadler, J. M.; La Scala, J. J.; Wool, R. P., *ACS Sustainable Chemistry and Engineering* **2013,** *1* (4), 419–426.

Chapter 3

Oxidative depolymerization of lignin

3.1 Introduction

The primary purpose of lignin depolymerization is to convert lignin into useful, high value monomeric and oligomeric compounds that can be used for further applications. The motivation and merits of using lignin as an alternative feedstock for the generation of high value platform compounds that can mimic the properties of chemicals derived from non-renewable feedstocks were highlighted in Chapter 2.

This study focuses on developing a new approach for depolymerizing lignin into valuable functionalized low molar mass compounds. In this work, dimethyl sulfoxide (DMSO) in the presence of catalytic amounts of hydrogen bromide (HBr) was used both as an oxidant and solvent to oxidatively depolymerize technical lignins into aldehyde, methoxy and vinyl functionalized phenolic monomers and oligomers.

DMSO has been used as a mild oxidant in the oxidation of primary alcohols into aldehydes, and the oxidation of secondary alcohols into ketones, via the Swern and Pfitzner-Moffat oxidation reaction.[1] However, there is not much information in published literature focusing on its use as a mild oxidizing agent in the depolymerization of technical lignins. Gao et al. recently developed a microwave-assisted catalytic Swern oxidation system using $MoO_2Cl_2(DMSO)_2$ (dioxomolybdenum (VI) complex) as the catalyst, and DMSO as the solvent and oxidant to oxidatively depolymerize lignin model compounds.[2] The products from this reaction included sinapaldehyde ((E)-3-(4-hydroxy-3,5-dimethoxyphenyl)prop-2-enal), p-coumaraldehyde ((E)-3-(4-hydroxyphenyl)prop-2-enal), coniferaldehyde ((E)-3-(4-hydroxy-3-methoxyphenyl)prop-2-enal) and vanillin (4-hydroxy-3-methoxybenzaldehyde). Mottweiler et al. used DMSO as a solvent in an iron-catalysed oxidative cleavage of lignin and β-O-4 lignin model compounds with peroxides. They attributed the cleavage of β-O-4 ether bonds to methyl radicals which are generated from H_2O_2 and DMSO. [3]

Since there is not much information in published literature focusing on the oxidative depolymerization of lignin using DMSO as the oxidant, other well established oxidative

depolymerization methods were carried out in this work for comparison. The methods investigated included oxidative depolymerization using nitrobenzene and oxidative depolymerization in ionic liquid (1-ethyl-3-methylimidazolium trifluoromethanesulfonate) and water using oxygen as an oxidant. Water was used as a solvent in lignin depolymerization because it is a greener solvent and cheap compared to other solvents used. In this chapter, SEC was subsequently used to monitor the success of the depolymerization reaction through comparing the molar masses of the various technical lignins before and after depolymerization.

3.2 Experimental

Materials

Alkaline lignin (Kraft lignin) with low sulfonate content (Sigma-Aldrich, St. Louis, USA) and lignosulfonate (kindly supplied by SAPPI, Pretoria, South Africa) were dried overnight in an oven at 105 °C to a constant mass, before depolymerization. 1-ethyl-3-methylimidazolium trifluoromethanesulfonate ([EMIM][CF_3SO_3] (≥98%, Sigma-Aldrich, St. Louis, USA), nitrobenzene (≥99%, Sigma-Aldrich, St. Louis, USA), dimethyl sulfoxide (DMSO, HPLC grade, ≥99.7%, Sigma-Aldrich, Poznan, Poland), hydrogen bromide (HBr, 48%, Sigma-Aldrich, St. Louis, USA), manganese (II) nitrate ($Mn(NO_3)_2$, ≥98%, Sigma-Aldrich, St. Louis, USA), de-ionized water from a laboratory Millipore water purification system, sodium hydroxide (NaOH, ≥98%, Science World, South Africa) and hydrochloric acid (HCl, 32%, Merck, Darmstadt, Germany) were used as received.

3.2.1 Oxidative depolymerization of technical lignins using DMSO as the oxidant

With HBr as the catalyst

Kraft lignin (0.2 g) was dissolved in DMSO (8 mL, 1.13×10^{-1} moles) in a round bottom flask, and a catalytic amount of HBr (1 mL, 1.84×10^{-2} moles) added to the reaction mixture. The reaction flask was immersed in an oil bath set at 110 °C, and the reaction mixture refluxed for 12 hrs. The reaction was then stopped by cooling to room temperature. The same procedure and experimental conditions were used for the depolymerization of SAPPI lignosulfonate.

With HCl as catalyst

Kraft Lignin (0.2 g) was dissolved in DMSO (8 mL, 1.13×10^{-1}moles) in a round bottom flask, and a catalytic amount of HCl (1 mL, 3.18×10^{-2} moles) added into the reaction mixture. The reaction flask was immersed into an oil bath thermostated at 110 °C, and the reaction mixture refluxed for 12 hrs. The reaction was then stopped by cooling to room temperature.

3.2.2 Depolymerization of Kraft lignin using nitrobenzene as an oxidant

Kraft lignin (0.2 g), 2M NaOH (14 mL) and nitrobenzene (1 mL, 9.75×10^{-3} moles) were transferred to a 250 mL round bottom flask. The reaction flask was immersed into an oil bath thermostated at 170 °C, and the reaction mixture refluxed for 2.5 hrs. The reaction was then stopped by cooling to room temperature.

3.2.3 Depolymerization of Kraft lignin using oxygen as an oxidant

Oxidative depolymerization of lignin (Kraft lignin) using oxygen as an oxidant in ionic liquid [EMIM][CF_3SO_3] was adapted from Stärk et al. [4] and another experiment using deionized water as an alternative solvent was set up since water is a cheaper and greener solvent compared to the highly expensive ionic liquid which is difficult to recover after the reaction. The reaction procedures and experimental conditions for the two reactions are outlined and detailed in the sections that follow.

3.2.3.1 Oxidative depolymerization of Kraft lignin by oxygen in ionic liquid

Kraft lignin (1 g) was dissolved in [EMIM][CF_3SO_3] (7.2 mL, 3.84×10^{-2} moles), and $Mn(NO_3)_2$ (0.2 g, 1.12×10^{-3} moles) added. The reaction vessel was inserted into an autoclave reactor, which was sealed and immersed into an oil bath preheated and thermostated at 105 °C. The reaction mixture was pressurized with compressed air to 500 kPa. The reaction was stopped after 24 hrs by cooling down to room temperature and releasing the pressure.

3.2.3.2 Oxidative depolymerization of Kraft lignin by oxygen in deionized water.

Kraft lignin (3 g) was dissolved in deionized water (30 mL, 1.875 moles) at 40 °C to aid solubility, and $Mn(NO_3)_2$ (0.6 g, 3.35×10^{-3} moles) added. The reaction vessel was inserted into an autoclave reactor, which was then sealed and immersed into an oil bath preheated and

thermostated at 95 °C. The reaction mixture was pressurized with compressed air to 500 kPa. The reaction was stopped after stirring for 24 hrs by cooling down to room temperature and releasing pressure. Residual water was removed from the product by freeze-drying.

Further experiments were carried out at the following time intervals 2, 5 and 10 hrs in order to investigate how time influences the depolymerization reaction.

3.2.4 Conversion

The extent of depolymerization under mild oxidizing conditions was determined gravimetrically using Equations 3.1 and 3.2:

$$\% \text{ of native lignin} = \frac{Weight\ of\ precipitated\ lignin}{Initial\ weight\ of\ lignin} \times 100\% \qquad (3.1)$$

$$\text{Conversion} = 100 - \% \text{ native lignin} \qquad (3.2)$$

where *Initial weight of lignin* is the mass of lignin before the depolymerization reaction and *Weight of precipitated lignin* is the native lignin, which was precipitated from water from the product mixture and isolated through centrifugation. The supernatant was decanted and residual water removed under vacuum.

3.3 Analyses

3.3.1 Size exclusion chromatography (SEC)

An Agilent 1200 HPLC instrument (Agilent Technologies, Waldbronn, Germany) comprising the following: autosampler, on-line degasser, quaternary pump unit and a thermostated column compartment set to 55 °C was used. The detector used was an Agilent ultraviolet (UV) detector at a wavelength of 277 nm. Two 10 µm PSS GRAM columns (PSS Polymer Standards Service GmbH, Mainz, Germany) (with polyester copolymer as a stationary phase) with porosities of 100 Å and 1000 Å and a 10 µm guard column were used. The sample solvent and mobile phase was DMSO/H_2O/LiBr (90:10:0.05 M respectively), and a flowrate of 0.4 mL/min was used. Calibration was carried out using narrow poly(styrene sulfonate) sodium salt (PSS Polymer Standards Service GmbH, Mainz, Germany) with peak maximum molar masses (M_p) ranging from 891 to 1 000 000 g/mol. PSS WinGPC Unichrom software (8.2) was used to acquire and process the data.

An Agilent 1100 refractive index (RI) detector was later added to the HPLC instrument because pullulan standards (PSS Polymer Standards Service GmbH, Mainz, Germany) with M_p between 342 and 1 220 000 g/mol which do not have UV chromophore were used for calibration. The pullulan standards were used because SAPPI lignosulfonate and most depolymerized products were eluting after the lowest poly(styrene sulfonate) sodium salt standard with M_p of 891 g/mol. All molar mass values are, therefore, calculated and reported as pullulan equivalents.

3.4 Results and Discussion

3.4.1 Investigation of depolymerization of lignin by SEC

SEC analysis was used to investigate the oxidative depolymerization of lignin. The following parameters that ensure optimum separation were considered: mobile phase composition, choice of stationary phase, operating temperature, and use of an electrolyte to disrupt non-covalent polymer–polymer and polymer–stationary phase interactions. Since SEC relies on measuring a physical parameter (elution volume) of a polymer in solution, the choice of mobile phase and use of appropriate additives is important.

When solubility studies were carried out, it was found that Kraft lignin (with low sulfonate content) and SAPPI lignosulfonate (with high sulfonate content) together with their respective products of depolymerization, dissolved completely in a DMSO/H_2O/LiBr (90:10% (v/v):0.05M) mobile phase, without the need for derivatization.[5] This is a significant advantage since lignin derivatization not only alters the chemistry of the lignin, but also the molar mass.[6] PSS GRAM columns were selected due to their compatibility with the mobile phase and polymer. Porosities of 100 Å and 1000 Å were selected for the columns in order to cover a wider separation range taking into account that depolymerization of lignin would result in low molar mass compounds.

The UV detector was the ideal choice of concentration detector because lignin and the polystyrene sulfonate sodium salt (PSS) standards which are typically used for lignin molar mass determination showed strong UV absorbance between 275 nm and 280 nm. All SEC measurements were carried out at a UV wavelength of 277 nm which is above the UV cut off of DMSO (268 nm). However, in this study there was a challenge in determining molar masses by conventional calibration using the UV detector because the SAPPI lignosulfonate and most

of the depolymerized product mixtures were eluting after the lowest PSS standard which had a peak molar mass (M_p) of 891 g/mol (eluting at 20.6 mL), see Fig. 3.1.

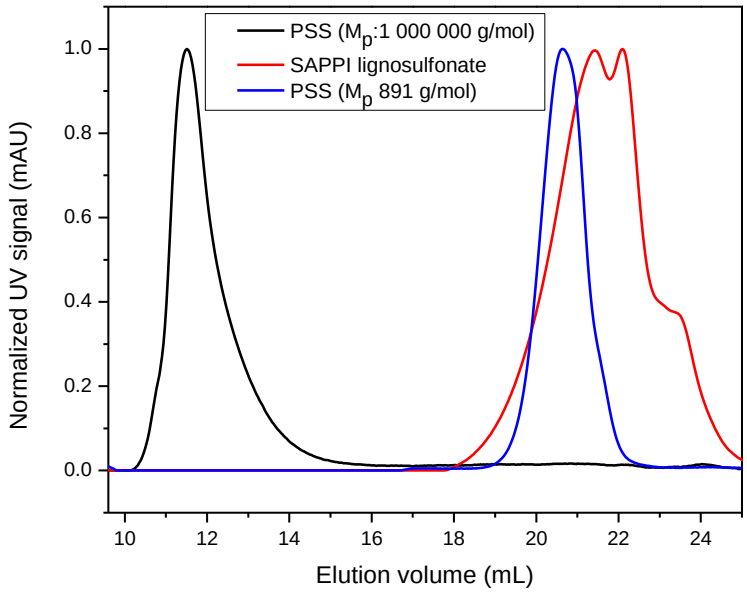

Fig. 3.1: SEC elugrams showing SAPPI lignosulfonate eluting after the lowest PSS standard with (peak molar mass) M_p of 891 g/mol

Pullulan standards were then used because the lowest calibrant had a molar mass of 342 g/mol, and the polymer was also soluble in the selected mobile phase. The problem with pullulan is that it is not UV active, therefore a UV detector could not be used for molar mass determination. A universal RI detector was thus opted for. Fig. 3.2 shows the RI detector responses of the pullulan calibration standard with the lowest and highest molar masses i.e. 342 g/mol and 1 220 000 g/mol. The elution volumes for these compounds give an indication of the total permeation (the lowest standard elutes at 23.7 mL, see Figs. 3.2 and 3.3) and exclusion limits (11.9 mL), respectively, of these columns.

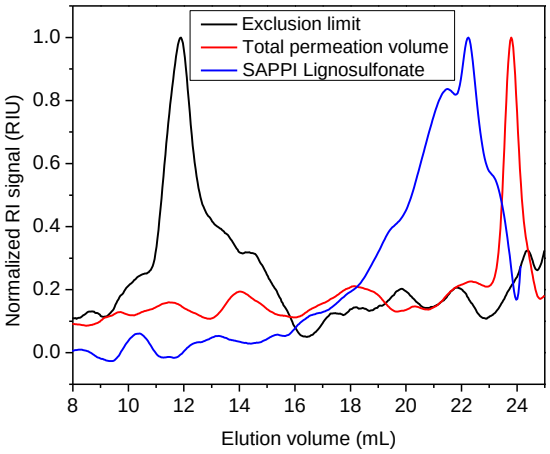

Fig. 3.2: SEC elugrams showing the total permeation and exclusion limits and SAPPI lignosulfonate using non-UV active pullulan standards

Fig 3.3 shows the calibration curves of the PSS and pullulan standards. From the calibration curves, it can be observed that using the pullulan calibration (and not the PSS calibration) will enable the molar mass determination of oligomeric species from lignin depolymerization, which have a molar mass of less than 500 g/mol. The R^2 values for the calibration plots are: 0.99979 for PSS and 0.99935 for pullulan.

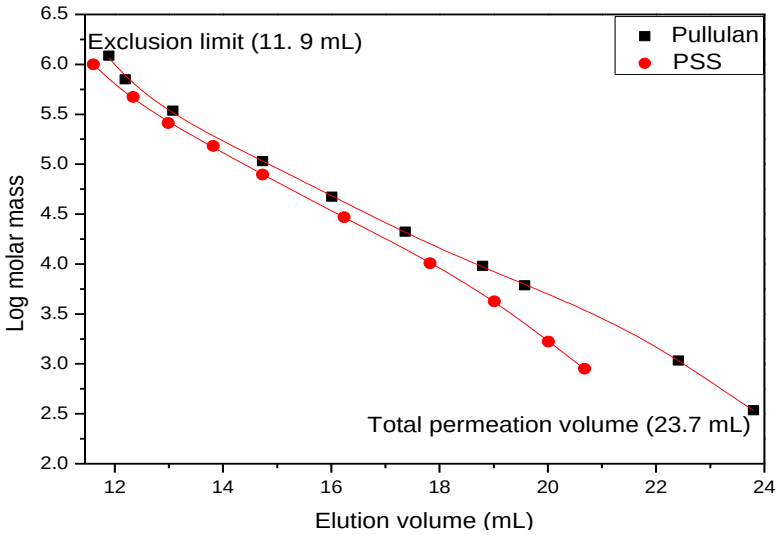

Fig. 3.3: Pullulan and PSS calibration plots

From the elution profiles in Fig. 3.2, baseline instability can be observed due to the viscosity of DMSO and possible fluctuations in ambient conditions which compromises signal-to-noise ratios due to noisy baseline. Due to the poor signal-to-noise ratio in the RI, in order to ascertain the peaks of interest for molar mass calculations, a dual detector approach was applied with the UV detector where the signal-to-noise ratio was better, see Fig. 3.4. Please note, because of this only the UV traces of the SEC elugrams will be presented.

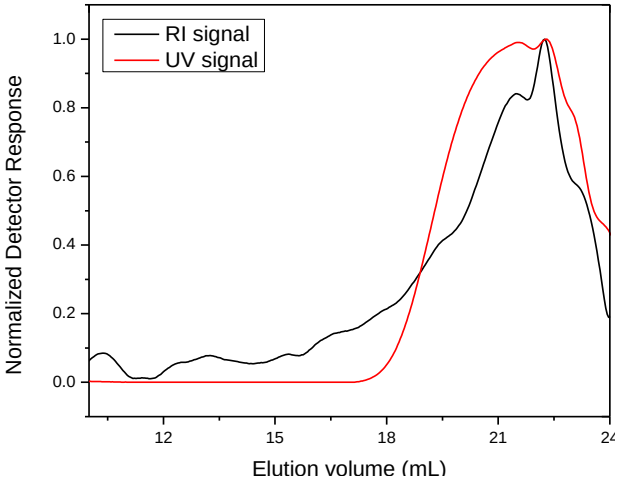

Fig. 3.4: Correlation of RI and UV signals of one of the depolymerized product mixtures of lignin (DMSO/HBr)

3.4.1.1 Oxidative depolymerization of Kraft lignin by oxygen

The first set of experiments carried out involved the depolymerization of Kraft lignin using oxygen and in two different solvents (1) ionic liquid and (2) deionized water. In order to confirm the success of the depolymerization reaction, the unpurified product mixture was dissolved in the SEC mobile phase and analyzed.

Fig. 3.5a and 3.5b show the elution profiles of the native Kraft lignin sample (KL), lignin depolymerized in ionic liquid (IL) and lignin depolymerized in deionized water (H_2O).

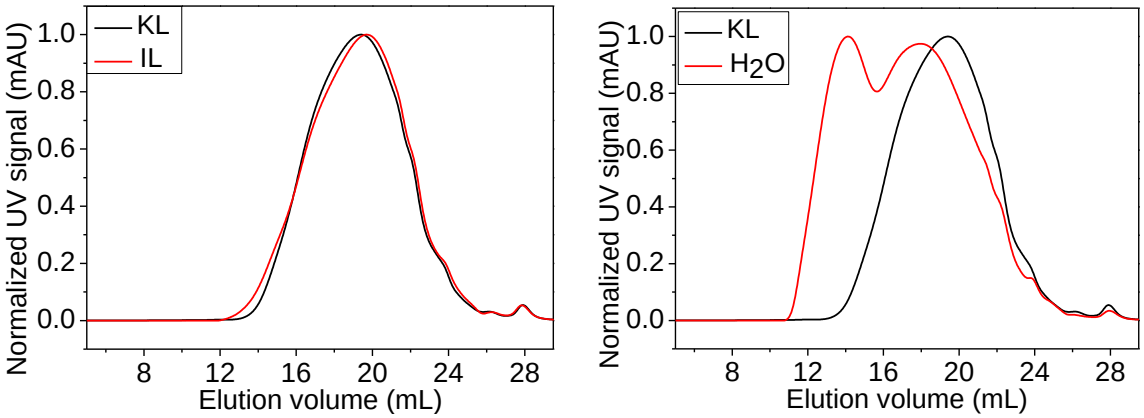

Fig. 3.5: SEC elugrams for depolymerization of Kraft lignin (KL) in ionic liquid (IL) (a) and depolymerization in H_2O (b)

A shift from lower to higher elution volume would be an indication of successful lignin depolymerization to presumably low molar mass compounds. The elugrams show that the oxidative depolymerization of Kraft lignin in the ionic liquid was not successful since there was no significant shift in elution volumes. This was corroborated by the molar mass values

calculated from pullulan calibration and tabulated in Table 3.1. The Kraft lignin before depolymerization had a weight average molar mass (M_w) of 14 680 g/mol, which did not change significantly after depolymerization.

Table 3.1: Molar mass distributions of Kraft lignin and products of depolymerization in deionized water and ionic liquid (IL)

	[a] M_n (g/mol)	[b] M_w (g/mol)	[c] M_p (g/mol)	[d] Đ
Kraft lignin	3780	14 680	9600	3.9
Depolymerization in ionic liquid	3530	13 780	8300	3.9
Depolymerization in H_2O (24hrs	8550	113 400	25 480	13.2
Depolymerization in H_2O (10hrs)	4750	25 300	7060	5.3
Depolymerization in H_2O (5hrs)	4350	21 800	6550	5.0
Depolymerization in H_2O (2hrs)	3660	16 950	5920	4.6

[a] Number average molar mass (M_n), [b] weight average molar mass (M_w), [c] peak molar mass (Mp), [d] molar mass dispersity (Đ)

It is known that oxygen has a poor solubility in ionic liquids and, therefore, adjusting the oxygen partial pressure is paramount in ensuring effective oxygen transfer into the ionic liquid.[4, 7–8] One approach is to carry out the depolymerization reaction at pressures of up to 8 000 kPa in order to effectively cleave the β-O-4 bond.[4] The challenge is that the use of such high pressures needs highly specialized equipment, which is not always available and, on the other hand, these conditions are not desirable for depolymerization since they lead to less selectivity of the process. [9]

The easiest way to increase the partial pressure of oxygen is to increase its solubility; hence, oxidative depolymerization was carried out in water. The other advantages of using water are it is cheaper and more environmentally friendly. Fig. 3.5b shows the SEC elugrams for a product depolymerized in water. There was a significant shift towards lower elution volumes (corresponding to higher molar masses, M_w of 113 400 g/mol.) and a bimodal distribution was observed.

The increase in molar mass was attributed to repolymerization reactions that are a result of over-oxidation. Since oxygen is highly soluble in water, there is less selectivity of the depolymerization process, which leads to over-oxidation and the formation of an aromatic carbocation which becomes the centre of repolymerization, see Scheme 3.1.[4, 10]

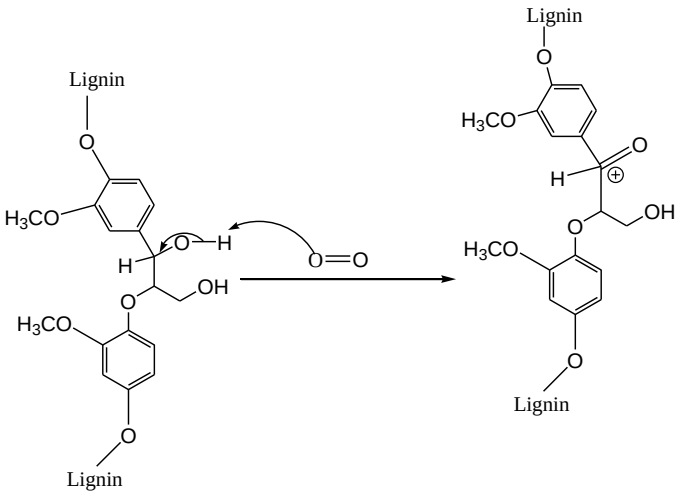

Scheme 3.1: Proposed mechanism of the formation of an aromatic carbocation causing self-condensation

Brebu and Vasile also account for repolymerization by highlighting that the cleavage of the ether bonds may also result in the formation of highly unstable free radicals that may react by electron abstraction or radical-radical interactions to form products with increased stability and of high molar mass. [11] Some researchers have reported that higher temperatures and longer reaction times decreased the monomer yield and increased the formation of solid residue due to the condensation reactions (repolymerization) of the depolymerized intermediates or products.[11-12] Therefore, in an attempt to avoid over-oxidation and to investigate the influence of reaction time on repolymerization, the depolymerization reaction in water was carried out at additional time intervals of 2, 5, 10 hrs.

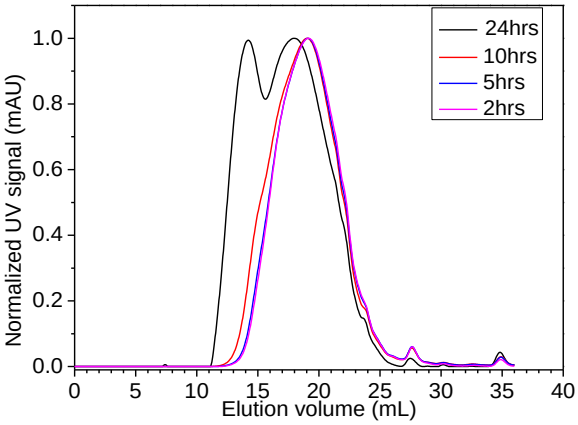

Fig. 3.6: SEC elugrams showing relationship between time and extent of repolymerization for lignin depolymerization in H_2O

The SEC results suggest that the extent of repolymerization increased with an increase in reaction time (see Fig. 3.6), highlighting that the aromatic carbocation becomes predominant under long reaction times. The molar mass dispersity (Đ) also increased with prolonged reaction time for the depolymerization reactions in deionized water, see Table 3.1

3.4.1.2 Depolymerization of lignin using (1) nitrobenzene and (2) DMSO as the oxidants

Nitrobenzene has been extensively used as a mild oxidizing agent in lignin depolymerization because it forms a wide array of functionalized aromatic compounds, and preserves the structure of the aromatic ring. Although nitrobenzene is an effective oxidant, a large portion of the reaction mixture is made up of toxic volatile and non-volatile nitrobenzene derivatives such as azobenzene, 4-(phenylazo)-phenol and azoxybenzene, which makes its use in lignin depolymerization undesirable.[13–14] However, in this study the nitrobenzene reaction was used as a template for the novel DMSO/HBr reaction which was developed in this work. The aim was to compare the two oxidative depolymerization processes with regard to the average molar mass of the depolymerized products as well as their chemical structure. HCl was also used as a catalyst for comparison with HBr.

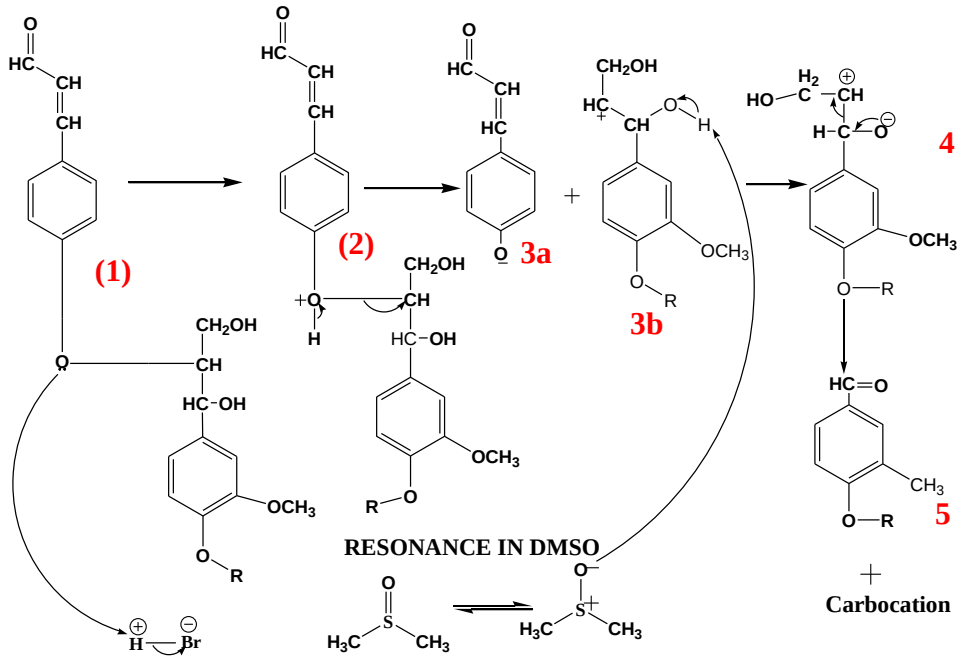

Scheme 3.2: Proposed mechanism of oxidative depolymerization of lignin by DMSO/HBr

(R: Hydrogen, alkyl, alkyloxy, phenyl groups)

In this work DMSO had the dual role of acting as both the solvent and the oxidant in depolymerizing lignin, and HBr was used as a catalyst (a Bronsted acid that has been used as a catalyst in selectively cleaving aryl methyl ethers).[15] To explain the role of DMSO as an oxidant in the presence of HBr, a reaction mechanism was proposed (see Scheme 3.2). A detailed study of the depolymerization products formed using DMSO/HBr was conducted and is further discussed in this work.

The β-O-4 oxygen atom acts as a nucleophile to abstract a proton from the HBr catalyst to form a cationic species (2). The redistribution of electrons induces the loss of a proton and the formation of a phenoxide type ion (3a) and formation of a benzylic alkyloxy cationic species (3b). Resonance in DMSO allows the oxide ion in DMSO to act as a nucleophile to abstract a proton from the benzylic alkyloxy cationic species (3b, α position). A rearrangement occurs, and an aldehyde functionalized compound (5) typical of vanillin (later discussed) is formed while releasing an aliphatic carbocation. The phenoxide type ion (3a) can also go on to abstract a proton from within the lignin to form (7a) (4-hydroxycinnamaldehyde which is typical of one of the compounds that was identified in this work, later discussed), see Scheme 3.3. The bromide ion abstracts a proton from the protonated resonance structure of DMSO (see Scheme 3.3) and the reaction continues.

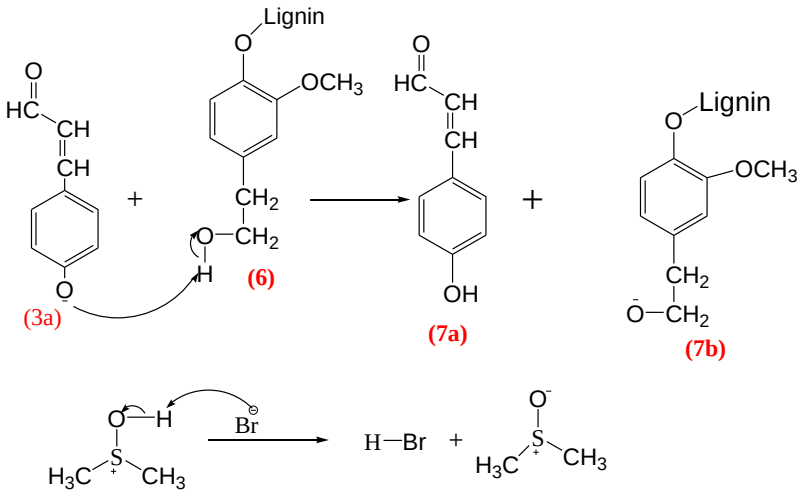

Scheme 3.3: Possible pathways of forming new compounds within the reaction mechanism

When analyzed by SEC, there was a clear shift from lower to higher elution volumes, and no evidence of repolymerization products at lower elution volumes, an indication that DMSO and nitrobenzene are effective mild lignin depolymerization agents, see Fig. 3.7. The M_w decreased from 14 650 g/mol (for native Kraft Lignin) to 1460 g/mol and 2180 g/mol for the nitrobenzene and DMSO/HBr systems, respectively. When the molar masses for the DMSO/HBr system were compared to the DMSO/HCl system, the results showed that the former system was more effective in depolymerizing lignin. The molar mass dispersity for all three systems also decreased significantly after depolymerization.

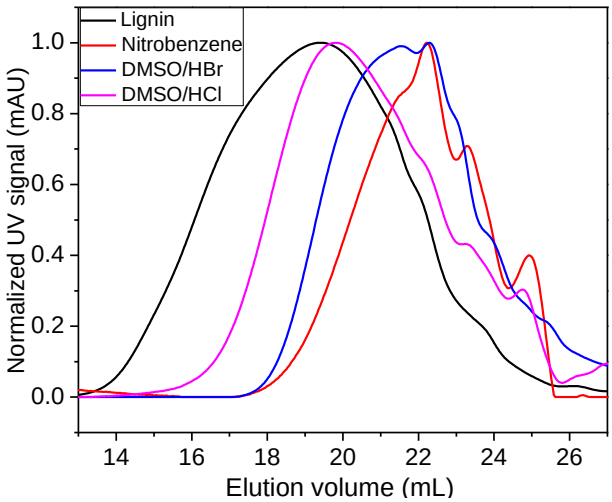

Fig. 3.7: SEC elugrams of untreated Kraft lignin and products of depolymerization by DMSO/HBr, nitrobenzene, DMSO/HCl

Table 3.2: Molar mass information of Kraft lignin and depolymerized product of oxidative depolymerization by nitrobenzene, DMSO/HBr, DMSO/HCl

	[a] M_n (g/mol)	[b] M_w (g/mol)	[c] M_p (g/mol)	[d] Đ
Kraft lignin	3750	14 650	9630	3.9
Depolymerization by nitrobenzene	1000	1460	750	1.5
Depolymerization by DMSO/HBr	1400	2180	1550	1.6
Depolymerization by DMSO/HCl	2830	6340	5230	2.2

[a] Number average molar mass (M_n), [b] weight average molar mass (M_w), [c] peak molar mass (Mp), [d] molar mass dispersity (Đ)

Oxidative depolymerization by DMSO/HBr was also carried out at a reaction time of 2.5 hrs to show the influence of time on the reaction. It was observed that a reaction time of 12 hrs showed a significant shift towards low molar mass compounds compared to the reaction carried out for 2.5 hrs (see Fig. A1.1 in Appendix A).

Scaling up and conversion

Table 3.3 tabulates the conversions obtained for the nitrobenzene and the DMSO/HBr systems. The values obtained i.e. 49% and 46%, respectively, are in agreement with conversion rates previously reported for lignin.[4, 16]

Table 3.3: Conversion of the reactions showing the highest shifts towards low molar mass compounds (nitrobenzene reaction and DMSO/HBr reaction)

Method of oxidative depolymerization	Conversion
Nitrobenzene	48.5%
DMSO/HBr	46.3%

Since one of the ultimate aims of this project is to use the lignin depolymerization products in the synthesis of functionalized aromatic polymers, the oxidative depolymerization of lignin by DMSO/HBr was scaled up from 0.2 g to 10 g, with other reagents also scaled up by the same factor. Scaling up was also carried out to validate reproducibility of the method of oxidatively depolymerizing lignin by DMSO/HBr.

Fig. 3.8 shows the SEC elugrams of the native Kraft lignin, DMSO/HBr depolymerization product (0.2 g) and DMSO/HBr depolymerization product (10 g). There was a clear shift from lower to higher elution volumes for the scaled up reaction comparable to DMSO/HBr (0.2 g). Therefore, scaling up did not limit the reaction to go to completion and the % conversion was 44.5%.

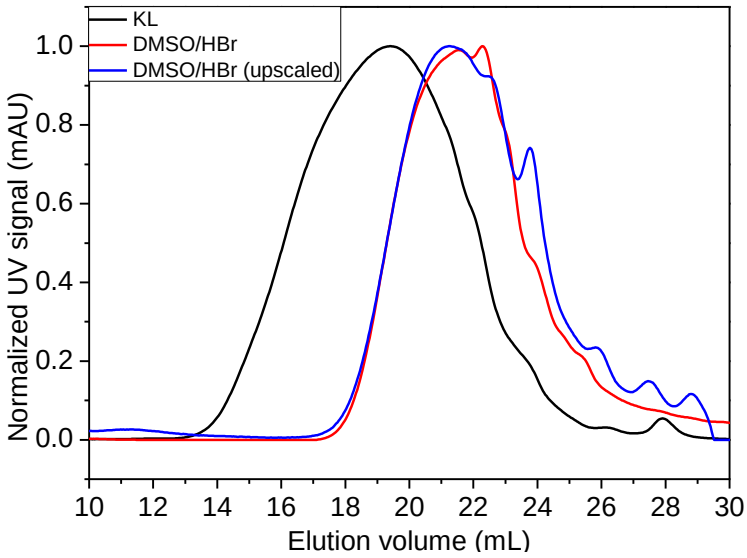

Fig. 3.8: SEC elution profile for scaled up reaction and native Kraft lignin
Native Kraft lignin (KL), DMSO/HBr (0.2 g), DMSO/HBr upscaled (10 g)

Oxidative depolymerization of SAPPI lignosulfonate by DMSO/HBr

After establishing and optimizing the oxidative depolymerization of Kraft lignin (with low sulfonate content from Sigma Aldrich) by DMSO/HBr, the same reaction conditions were applied on a less pure industrial lignosulfonate sample from a different source (SAPPI Ltd South Africa). SAPPI currently produces thousands of tonnes of lignosulfonates during the paper making process, and these lignosulfonates are used as binders, emulsifiers, and dispersing agents. Successfully depolymerizing these lignosulfonates would significantly enhance the value of these by-products.

Fig. 3.9 shows the SEC elugrams of the SAPPI lignosulfonate and the depolymerization product. There was a clear shift from lower to higher elution volumes, and a clear decrease in M_w as attested by the values in Table 3.4. The results show that the lack of calibration standards with high structural similarity to lignin impairs the quality of the molar masses (M_n, M_p and M_w) determined by conventional SEC.

Table 3.4: Molar mass information of SAPPI lignosulfonate and SAPPI DMSO/HBr

	[a] M_n (g/mol)	[b] M_w (g/mol)	[c] M_p (g/mol)	[d] Đ
SAPPI lignosulfonate	1550	4020	1220	2.6
Depolymerization by DMSO/HBr	900	1080	950	1.2

[a] Number average molar mass (M_n), [b] weight average molar mass (M_w), [c] peak molar mass (Mp), [d] molar mass dispersity (Đ)

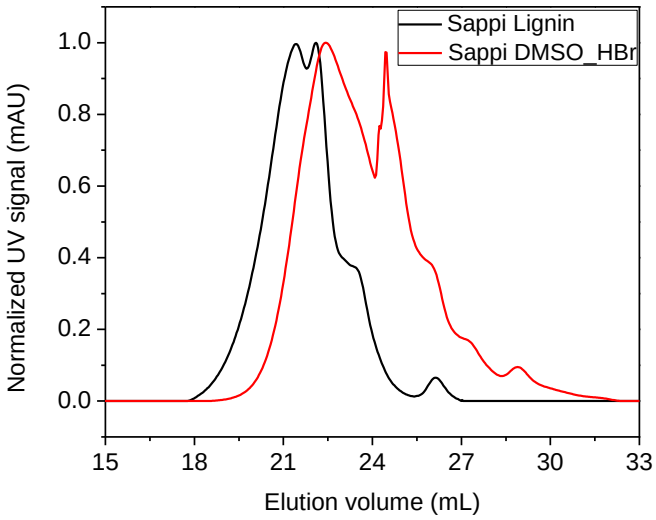

Fig. 3.9: SEC elution profile for untreated SAPPI lignosulfonate and SAPPI DMSO/HBr

3.5 Conclusions

Oxidative depolymerization by nitrobenzene and by DMSO/HBr showed the highest shifts towards low molar mass compounds by SEC compared to the other approaches conducted in this study. DMSO was successfully used as a novel approach in this study in oxidatively depolymerizing lignin into low molar mass compounds. To validate the method, an up-scaled reaction was done and also a lignin from a different source was successfully depolymerized under the same reaction conditions.

HBr showed to be more effective in its catalytic action compared to HCl as established by SEC. Oxidative depolymerization in deionized water showed evidence of self-condensation/ recombination reactions (repolymerization) due to the high solubility of oxygen in water, consequently inducing harsh oxidizing conditions. It was also noted that the extent of repolymerization was proportional to reaction time. Oxidative depolymerization in ionic liquid

did not show a significant shift towards low molar mass compounds. Therefore, adjusting the oxygen partial pressure and ensuring effective oxygen transfer into the ionic liquid was necessary because oxygen solubility in ionic liquids has been reported to be low. Hence the reaction has to be done under elevated pressures. Molar mass distributions of the samples were successfully determined by conventional calibration using pullulan standards.

3.6 References

1. Wu, X.-F.; Natte, K., *Advanced Synthesis and Catalysis* **2016,** *358* (3), 336–352.

2. Gao, R.; Li, Y.; Kim, H.; Mobley, J. K.; Ralph, J., *ChemSusChem* **2018,** *11* (13), 2045–2050.

3. Mottweiler, J.; Rinesch, T.; Besson, C.; Buendia, J.; Bolm, C., *Green Chemistry* **2015,** *17* (11), 5001–5008.

4. Stärk, K.; Taccardi, N.; Bösmann, A.; Wasserscheid, P., *ChemSusChem* **2010,** *3* (6), 719–723.

5. Ringena, O.; Lebioda, S.; Lehnen, R.; Saake, B., *Journal of Chromatography A* **2006,** *1102* (1–2), 154–163.

6. Stark, N. M.; Yelle, D. J.; Agarwal, U. P., Techniques for characterizing lignin. In *Lignin in Polymer Composites*, Omar Faruk, M. S., Ed. Elsevier: Oxford, UK, 2016; pp 49–66.

7. Anthony, J. L.; Maginn, E. J.; Brennecke, J. F., *The Journal of Physical Chemistry B* **2002,** *106* (29), 7315–7320.

8. Neale, A. R.; Li, P.; Jacquemin, J.; Goodrich, P.; Ball, S. C.; Compton, R. G.; Hardacre, C., *Physical Chemistry Chemical Physics* **2016,** *18* (16), 11251–11262.

9. Gillet, S.; Aguedo, M.; Petitjean, L.; Morais, A.; da Costa Lopes, A.; Łukasik, R.; Anastas, P., *Green Chemistry* **2017,** *19* (18), 4200–4233.

10. Zhang, C.; Li, H.; Lu, J.; Zhang, X.; MacArthur, K. E.; Heggen, M.; Wang, F., *ACS Catalysis* **2017,** *7* (5), 3419–3429.

11. Brebu, M.; Vasile, C., *Cellulose Chemistry and Technology* **2010,** *44* (9), 353–363.

12. Yuan, Z.; Cheng, S.; Leitch, M.; Xu, C. C., *Bioresource Technology* **2010,** *101* (23), 9308–9313.

13. Villar, J. C.; Caperos, A.; García-Ochoa, F., *Journal of Wood Chemistry and Technology* **1997,** *17* (3), 259–285.

14. Villar, J.; Caperos, A.; Garcia-Ochoa, F., *Wood Science and Technology* **2001,** *35* (3), 245–255.

15. Waghmode, S. B.; Mahale, G.; Patil, V. P.; Renalson, K.; Singh, D., *Synthetic Communications* **2013,** *43* (24), 3272–3280.

16. Sun, Z.; Fridrich, B. l.; de Santi, A.; Elangovan, S.; Barta, K., *Chemical Reviews* **2018,** *118* (2), 614–678.

Chapter 4

Structure elucidation of the bulk aromatic depolymerization products

4.1 Introduction

The ideal analytical approach for investigating lignin depolymerization comprises molar mass determination (SEC discussed in Chapter 3), a separation technique to deconvolute the monomeric and oligomeric compounds according to chemical functionality (using liquid or gas chromatography coupled to suitable detectors e.g. mass spectrometry) and structure elucidation (using ESI-MS, NMR spectroscopy and FTIR spectroscopy).[1–4] From the results obtained from SEC, the product mixtures obtained by the oxidative depolymerization of lignin using nitrobenzene and DMSO/HBr showed the highest shifts towards low molar mass compounds. This chapter, therefore, focuses on deducing structure information of the depolymerized products from these two oxidation systems using LC-MS, GC-MS, ESI-MS, NMR spectroscopy and FTIR spectroscopy. In addition, the structure of the aromatic compounds formed by the depolymerization of Kraft lignin and the SAPPI lignosulfonate are compared.

4.2 Experimental

Materials

Methanol (MeOH, HPLC grade, ≥99.9%, Sigma Aldrich, Saint-Quentin-Fallavier, France), deionized water (H_2O), from a laboratory Millipore purification system, acetic acid (AA, HPLC grade, ≥99.8%, Sigma Aldrich, Buchs, Switzerland), DMSO/HBr and nitrobenzene product mixtures, guaiacol (natural ≥99%, Sigma Aldrich, Sigma Aldrich, Hong Kong, China), vanillin (99%, Sigma Aldrich, Hong Kong, China), 4-hydroxybenzaldehyde (98%, Alfa Aesar, Lancaster, UK), phenol (99%, Labchem, Gauteng, South Africa), benzaldehyde (≥99%, Sigma Aldrich, St. Louis, USA), syringaldehyde (≥98%, Sigma Aldrich, Hong Kong, China), catechol (≥99%, Sigma Aldrich, St. Louis, USA) and eugenol (99%, Sigma Aldrich, St. Louis, USA), deuterated water (≥99.9% NMR, Merck, KGaA, Darmstadt, Germany), deuterated dimethyl sulfoxide (99.8% NMR, Merck, KGaA, Darmstadt, Germany), potassium trifluoroacetate (KFTA, 98%, Sigma Aldrich, Buchs, Switzerland) were used as received.

Analyses

4.2.1 FTIR analysis

Attenuated total reflectance (ATR)–FTIR measurements of lignin and its depolymerized products were carried out on a Thermo Scientific Nicolet iS10 spectrometer (Thermo Scientific, Massachusetts, USA). Spectra recorded from 4000 to 650 cm^{-1} were obtained from a collection of 32 scans at a resolution of 4 cm^{-1} with automatic background subtraction. Thermo Scientific OMNIC software (version 8.1) was used for data collection and processing.

4.2.2 ^{1}H NMR analysis

All ^{1}H NMR spectra were acquired using a 400 MHz Varian *Unity* Inova instrument. (Varian Inc, Mulgrave, Australia). The chemical shifts are reported in parts per million (ppm) in a binary solvent of deuterated water and deuterated dimethyl sulfoxide with tetramethylsilane (TMS) as a reference.

4.2.3 ESI-MS

1 mg of each sample was dissolved in 1 mL methanol (HPLC ≥99.9%, Romil Ltd, Cambridge, UK), followed by a further 10-fold dilution into methanol. 2 µL of sample was injected into a stream of methanol flowing at 0.3 mL/min, using a Waters ultrahigh pressure liquid chromatograph (UPLC) (Waters, Milford, USA) which conveyed the sample to a Waters Synapt G2 quadrupole time-of-flight (QTOF) mass spectrometer used for high-resolution accurate mass analysis. Data were acquired in scan mode, the mass spectrometer was optimized for best sensitivity, a cone voltage of 15 V was used, and desolvation gas was nitrogen at 650 L/hr at a desolvation temperature of 275 °C. The scan range was between 100–1500g/mol.

4.2.4 GC-MS

All GC-MS measurements were carried out on a Thermo Scientific TSQ 8000 Triple Quadrupole GC-MS equipped with 2B FFAP 13 m×0.25 mm ×0.25 µm capillary column. Helium at a flowrate of 1 mL/min was used as carrier gas. The injector temperature used was 250 °C and the detector temperature was 150 °C. The oven temperature program illustrated in Fig. 4.1 was used.

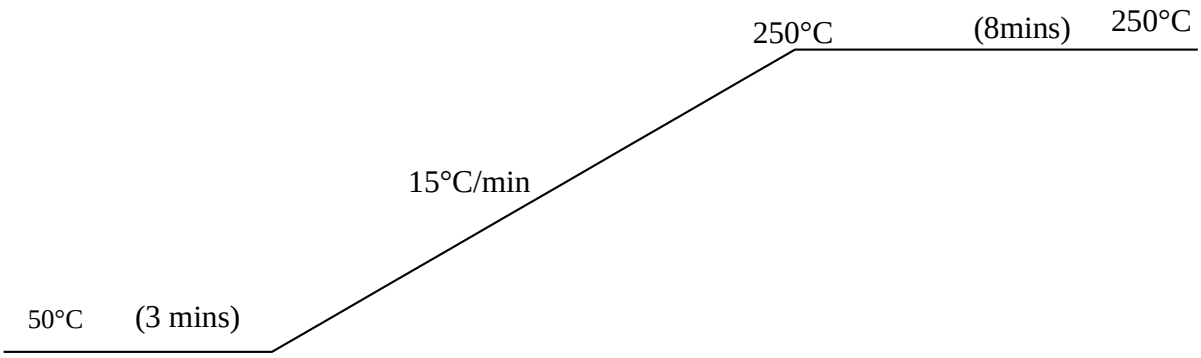

Fig. 4.1: Oven temperature program for GC-MS

4.2.5 HPLC analysis

Instrumentation and stationary phases

An Agilent 1200 HPLC instrument (Agilent Technologies, Waldbronn, Germany) comprising the following: autosampler, on-line degasser, quaternary pump unit and a thermostated column compartment set to 30 °C was used. The detectors used were: Agilent VWD ultraviolet (UV) detector at 277 nm and a 6120B single quadrupole MS detector. The MS data were acquired using the atmospheric pressure electrospray ionization (AP-ESI). Samples were analyzed in the positive scan mode at a mass range 10 to 1000 Da and in positive SIM mode. The fragmentor voltage was set to 150 V with a threshold of 150 using a gain of 1.0. The following columns were used: Macherey–Nagel Nucleosil C_{18} 50–5 column, with the following dimensions: 250 mm x 4.6 mm i.d, and Macherey–Nagel Nucleosil C_{18} 100–5 column with the following dimensions: 150 mm x 2 mm i.d. The methods that were applied on the above columns are tabulated in Table 4.1.

Table 4.1: Chromatographic methods used to separate the DMSO/HBr product mixture

Method I	Isocratic mode Column: C_{18} (length: 150 mm, internal diameter: 2 mm) Mobile phase: MeOH: H_2O: AA (30:68:2 (v/v)) Pump flow rate: 0.4 mL/min Detector: UV at 277 nm
Method II	Isocratic mode Column: C_{18} (length: 250 mm, internal diameter: 4.6 mm) Mobile phase: MeOH: H_2O: AA (30:68:2 (v/v)) Pump flow rate: 0.4 mL/min Detector: UV at 277 nm
Method III	Gradient elution (see gradient elution timetable in Table 4.2) Column: C_{18} (length: 250 mm, internal diameter: 4.6 mm) Mobile phase: H_2O:AA (98:2 (v/v)) (Solvent A), MeOH:AA (98:2 (v/v)) (Solvent B) Pump flow rate: 0.4 mL/min Detectors: UV at 277 nm, MS using API-ES ionization 0.1 M KFTA was used as the ionizing agent

Table 4.2: Gradient elution timetable for Method III

Time (min)	Solvent A	Solvent B
0	100	0
7	100	0
75	0	100
80	0	100
95	100	0

4.3 Results and discussion

4.3.1 FTIR analysis

FTIR spectroscopy is a non-destructive, non-invasive, highly sensitive and rapid analytical technique that has been widely used for the analysis of lignin, its derivatives and

depolymerization products. In this work, FTIR spectroscopy was used to establish a correlation between the structure of the lignin and the depolymerized aromatic products.

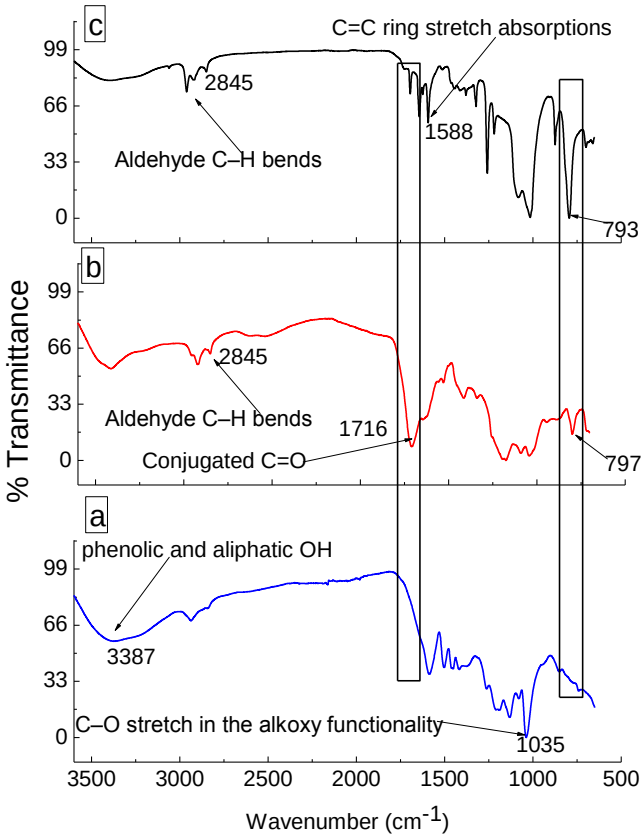

Fig 4.2: FTIR spectra of (a) Kraft lignin and depolymerization products from (b) DMSO/HBr oxidative and (c) nitrobenzene oxidative reactions

Fig. 4.2 shows the stacked FTIR spectra for native Kraft lignin, and the crude products from the nitrobenzene and DMSO/HBr depolymerization reactions. The appearance of an intense peak at a wavenumber of 1716 cm^{-1} is attributed to the presence of carbonyl (C=O) functional groups for the DMSO/HBr reactions (see Fig. B1.1 in Appendix B for SAPPI DMSO/HBr FTIR spectrum) and confirms the successful oxidation of alcohols to aldehyde or ketone groups as per the modified Swern oxidation mechanism proposed in this work and discussed in Chapter 3. The peaks at 797 cm^{-1} and 793 cm^{-1} for DMSO/HBr and nitrobenzene reactions also served to confirm the successful depolymerization of lignin into simpler aromatic compounds. These peaks suggest a para-substituted ring with out-of-plane bend vibrations common in depolymerized products of lignin such as syringaldehyde, vanillin, syringic acid and p-hydroxybenzaldehyde.[5–6] The CH_3 peak at 2960 cm^{-1} appears to be overlapping with the

aldehyde CH bands that are observed in the 2860–2800 cm^{-1} region and these peaks are more intense in the depolymerized products compared to Kraft lignin (also highlighting successful oxidative depolymerization). The peaks observed between 1012 cm^{-1} and 1261 cm^{-1} are characteristic for C–O stretching assigned to alcohols, ethers, carboxylic acids and esters. Taking into consideration the structure of lignin, these peaks tend to be assigned mainly to ether and alcohol groups.[7]

Broad peaks observed for all spectra between 3364 and 3408 cm^{-1} can be attributed to the phenolic and aliphatic hydroxyl group. A careful look at the nitrobenzene reaction spectrum (c) shows that the intensity of peaks at 1016 and 1265 cm^{-1} corresponding to alkoxy groups has increased, indicating that the presence of $–OCH_3$ groups has increased after depolymerization. The signals between 1534–1588 cm^{-1} are C=C aromatic ring stretch absorptions. Similar groups were observed for the SAPPI DMSO/HBr product mixture, see Appendix B for the peak assignments.

4.3.2 ^{1}H NMR analysis

^{1}H NMR spectroscopy was used to provide complimentary information on the structure of the aromatic depolymerization products. Figs. 4.3a–c show the ^{1}H NMR spectra for native Kraft lignin, crude nitrobenzene depolymerization products and crude DMSO/HBr products, respectively.

^{1}H NMR spectroscopy confirmed successful oxidative depolymerization of lignin as there was a shift towards narrow peaks for the reaction products compared to the broad peaks observed in the Kraft lignin. This can be explained by the rapid Brownian motion of small molecules which averages out dipolar and other anisotropic magnetic interactions (molecular tumbling), hence leading to narrow lines in the NMR spectra. In polymers, molecular tumbling is slow relative to the timescale of the NMR, therefore, broadening the NMR resonance lines of the spectra.[1, 8] ^{1}H NMR spectroscopy helped to establish that the few functional groups and the aromaticity present in lignin are retained in the products.[7] This is important because a good depolymerization technique is one that preserves the aromatic character of the fragments and gives functionalized compounds.

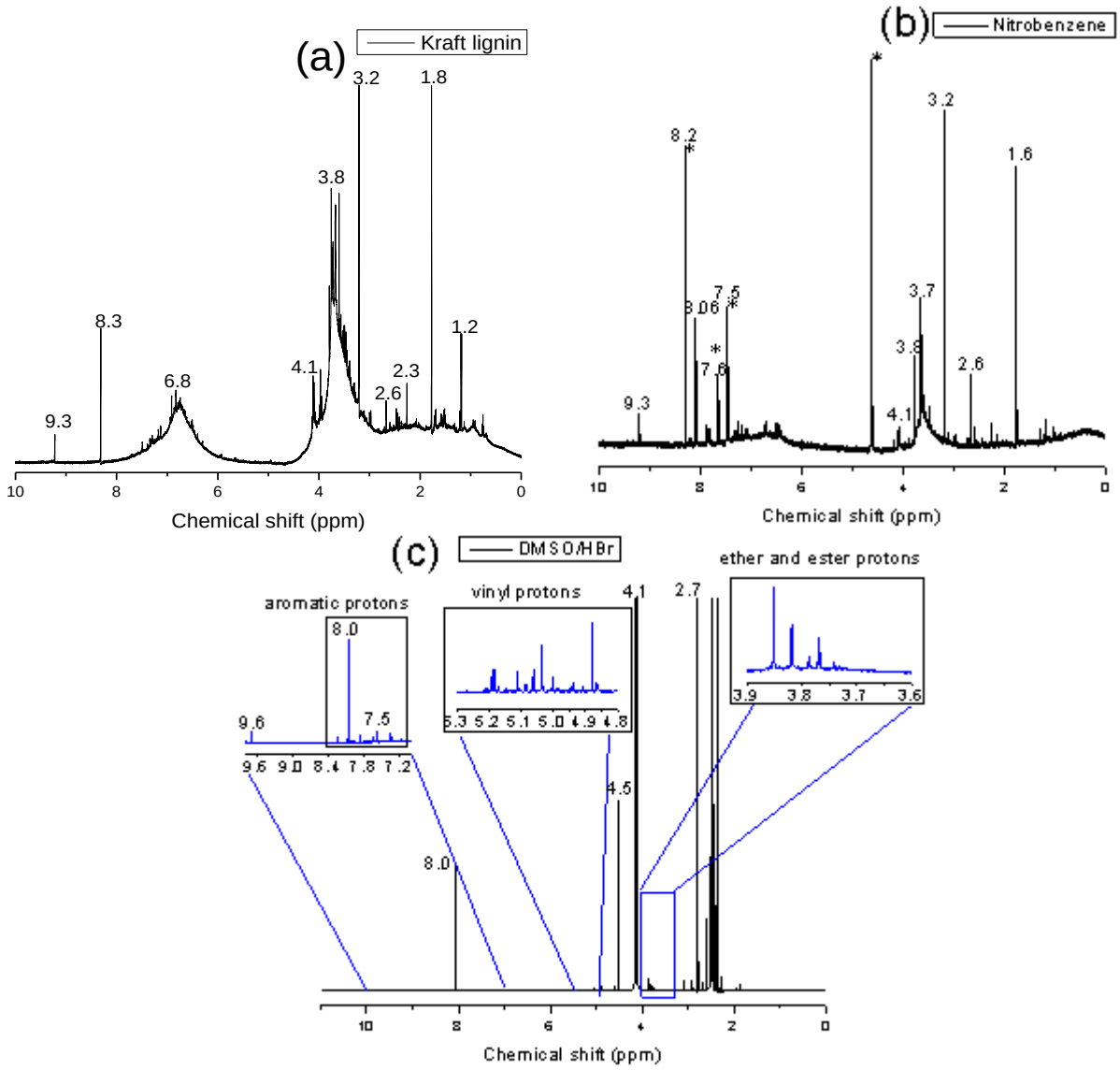

Fig. 4.3: ^{1}H NMR analysis of Kraft lignin (a), nitrobenzene product mixture (b) and DMSO/HBr product mixture (c)

The asterisks in all the ^{1}H NMR spectra denote signals due to residual DMSO and water (2.5 ppm and 4.7 ppm, respectively). The signals of the formyl protons are between 9 and 10 ppm. Between 9.55 and 9.75 ppm (observed in the DMSO/HBr reaction, see Fig. 4.3c) signals are detected that confirm the presence of the aldehyde group that is conjugated with vinyl moieties typical of structure A (see Fig. 4.4 for the structures), e.g. 4-hydroxy-3-methoxyphenylprop-2-enal (coniferaldehyde).[9–10] The resonance signals between 9.3 and 9.5 ppm (observed in the nitrobenzene reaction (b) Kraft lignin (a)), can be assigned to formyl protons in non-conjugated aldehyde groups typical of structure B.[9–10]

The signals observed between 6.5 and 8.5 ppm are due to the presence of aromatic protons. The largest chemical shifts within the aromatic region (7.5–8.3 ppm) observed for all spectra are typical of ring protons where electron withdrawing groups are attached, e.g. in structure D. The resonance signals of residual nitrobenzene were observed at 7.5, 7.6 and 8.2 ppm.

The presence of vinyl groups was indicated by the presence of the signals between 4.8 and 5.2 ppm in the NMR spectrum for DMSO/HBr depolymerization products. The ester (O–CO–C**H**$_2$CH$_3$) and ether proton signals were observed between 3.2 and 4.2 ppm. Taking into consideration the structure of lignin, the signals between 3.6 and 3.8 ppm are typical of methoxy protons (O–C**H**$_3$), see structures A, C, D and E in Fig. 4.4. The signals between 3.8 and 4.2 ppm are typical of the ester hydrogens on the carbon attached to the oxygen which are deshielded due to the electronegativity of oxygen typical of structure G.

The signal observed at 4.5 ppm for DMSO/HBr product can be ascribed to the methylene protons in cinnamyl alcohol, see structure F. The signals between 2.06 and 2.8 ppm can be assigned to the proton in α-position to the aryl carbonyl group or the benzylic proton, see structure C. [7]

The signals that are observed at the range 1.4–1.8 ppm could be assigned to CH_2 or CH_3 moieties. The many small peaks present in the NMR spectra could have been a result of various substitutions on aromatic rings, but due to the complex structure of lignin it would have been very difficult to assign all the peaks.[1, 11] ^{1}H NMR and FTIR analysis in synergy helped to corroborate the functionality of the compounds of lignin depolymerization which are later discussed in this section. SAPPI lignosulfonate and SAPPI DMSO/HBr had similar groups discussed above, see Appendix C for the signal assignments.

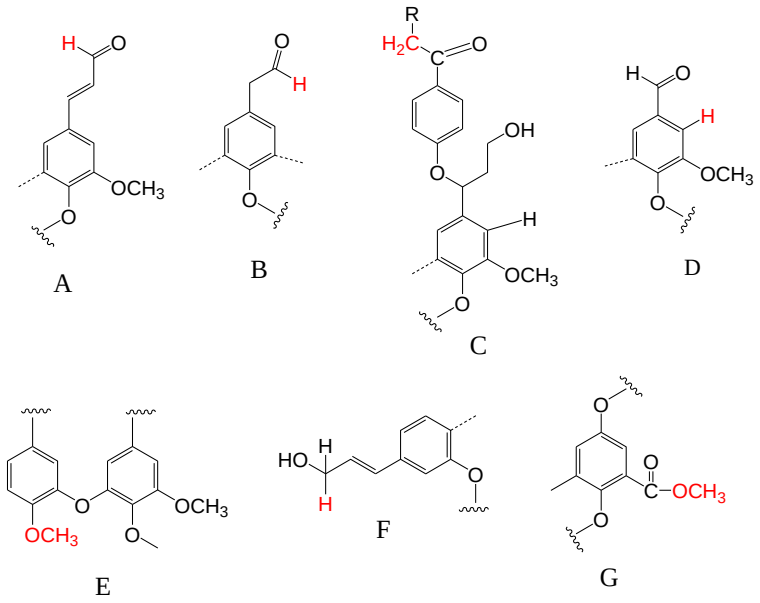

Fig. 4.4: Lignin substructures[12]

4.3.3 ESI-MS analysis

ESI-MS was used to get more detailed structural information of the depolymerized products of lignin (DMSO/HBr, nitrobenzene and SAPPI DMSO/HBr product mixtures). It was also used as a complementary technique to GC-MS (later discussed), as it was possible to obtain the full molar mass range for the depolymerized products of lignin. However, due to the high complexity and the large number of products, it is not practical to determine all monomeric compounds after depolymerization.[4] Therefore, the obtained ESI-MS spectra could only be interpreted to a limited degree. ESI-MS was carried out in positive mode, hence, typically a $[M+H]^+$ or $[M+Na]^+$ or $[M+K]^+$ (due to the alkali metal contaminants and the ionizing salt) ions are observed.

4.3.3.1 Structural elucidation of crude DMSO/HBr product mixture by ESI-MS

Fig. 4.5 shows the ESI mass spectrum for the crude DMSO/HBr depolymerization product. The peaks with the highest abundance of m/z 123 and 245 were assigned to hydroxybenzaldehyde (**E1**) and 4-(hydroxy(4-hydroxyphenyl)methoxy)benzaldehyde (**E21**) (please refer to Table 4.3 for their respective structures). **E21** is a dimer of **E1** formed via a nucleophilic addition reaction to form a hemiacetal type of compound. The catalyst for the formation of hemiacetals is acid; therefore, the formation of a hemiacetal was possible during depolymerization since HBr was used in the reaction.[13]

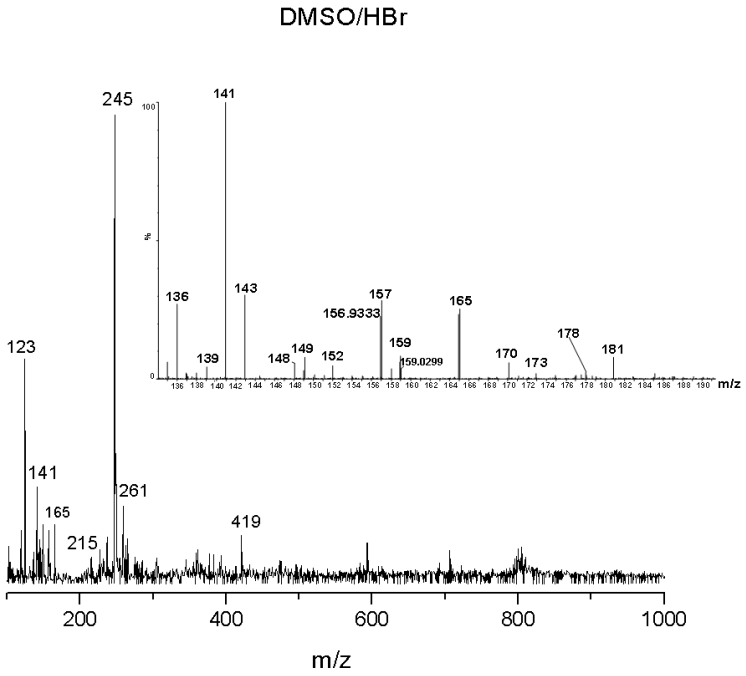

Fig. 4.5: Positive ESI-MS ($[M+H]^+$ or $[M+Na]^+$) mass chromatogram for DMSO/HBr

A zoom into a selected region of the mass spectrum (m/z 125–190) shows the presence of more compounds of interest and these include: 1-(2-hydroxyphenyl)ethanone (**E3**), 2-methoxy-4-methylphenol (4-methylguaiacol) (**E4**), 3-methoxybenzene-1,2-diol (3-methoxycatechol) (**E5**), 4-methylbenzaldehyde (**E6**), (E)-3-(4-hydroxyphenyl)prop-2-enal (4-hydroxyacinnamaldehyde) (**E8**), 4-hydroxy-3-methoxybenzaldehyde (vanillin) (**E10**), 3-phenylpropanal (**E11**), 3-methoxybenzaldehyde (**E12**), 2-methoxy-4-prop-2-enylphenol (eugenol) (**E13**), (E)-3-(4-hydroxy-3-methoxyphenyl)prop-2-enal (coniferaldehyde) (**E14**) and 4-[(E)-3-hydroxyprop-1-enyl]-2-methoxyphenol (coniferyl alcohol) (**E15**).

Coniferyl alcohol is one of the main monomers in the synthesis of lignin when copolymerized with p-coumaryl alcohol and sinapyl alcohol.[14] The m/z values of 261 and 419 were assigned to 4-(1-hydroxy-2-(2-methoxyphenoxy)ethyl)phenol (**E22**) and 4-(4-(4-hydroxy-3,5-dimethoxyphenyl)-hexahydrofuro[3,4-c]furan-1-yl)-2-methoxy-6-methylphenol (**E26**), respectively. The majority of the products determined by ESI-MS align to the proposed mechanism of oxidative depolymerization by DMSO/HBr discussed in Chapter 3.

4.3.3.2 Structural elucidation of nitrobenzene crude product mixture by ESI-MS

The dimeric species (**E21**) and hydroxybenzaldehyde (**E1**) observed in the DMSO/HBr product mixture were also identified in the nitrobenzene product mixture (see Fig. 4.6). In addition peaks at m/z values of 359 and 537 were observed and these were assigned to 1-(4-(1-(4-hydroxy-3-methoxyphenyl)prop-1-en-2-yloxy)-3,5-dimethoxyphenyl)ethanone (**E25**) and 4-(3-hydroxy-1,2-bis(4-((E)-3-hydroxyprop-1-enyl)-2-methoxyphenoxy)propyl)-2-methoxy-phenol (**E27**).

A zoom into a selected region of the mass spectrum (m/z 125–190) shows the presence of more compounds of interest and these include: 4-methylbenzaldehyde (**E6**), 4-phenyl-2-buten-1-al (**E7**), (E)-3-(4-hydroxyphenyl)prop-2-enal (4-hydroxyacinnamaldehyde) (**E8**), 4-ethenyl-2-methoxyphenol (vinylguaiacol) (**E9**), 3-methoxybenzaldehyde, 2-methoxy-4-prop-2-enylphenol (eugenol) (**E13**), 4-hydroxy-3-methoxybenzaldehyde (vanillin) (**E10**), 4-[(E)-3-hydroxyprop-1-enyl]-2-methoxyphenol (coniferyl alcohol) (**E15)**.

An oligomeric pattern of dimethylsiloxane oligomers, -Si(CH_3)$_2$-O-, Δ=74 Da, attributed to silicon oil contaminant is observed between 537 and 1055.

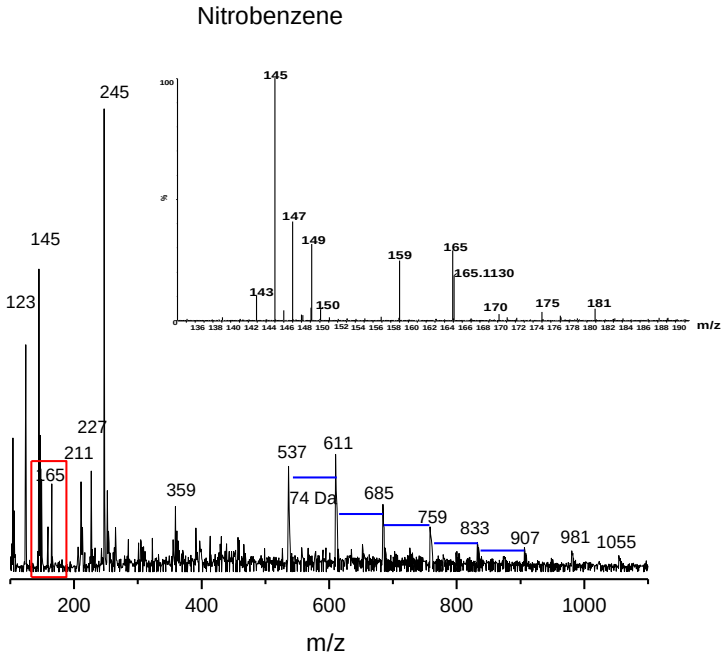

Fig. 4.6: Positive ESI-MS ([M+H]$^+$ or [M+Na]$^+$) mass chromatogram for nitrobenzene

4.3.3.3 Structural elucidation of SAPPI lignosulfonate product mixture by ESI-MS

The lignin monomeric compounds determined by ESI-MS for the SAPPI DMSO/HBr product mixture were also synonymous to those highlighted in the DMSO/HBr and nitrobenzene product mixtures (Fig. 4.7). FTIR and NMR results showed the possibility of compounds having vinyl moieties in the product mixtures and this was in agreement with what was obtained from ESI-MS i.e. 3,5-trimethoxycinnamaldehyde (**E19**), coniferaldehyde (**E14)** and 4-hydroxycinnamaldehyde (**E8)**).

The additional compounds determined by ESI-MS for SAPPI DMSO/HBr include: guaiacol (**E2**), hydroxybenzaldehyde (**1**), 1-(2-hydroxyphenyl)ethanone (**E3**), 2-methoxy-4-methylphenol (4-methylguaiacol) (**E4**), (E)-3-(4-hydroxyphenyl)prop-2-enal (4-hydroxyacinnamaldehyde (**E8**), 4-hydroxy-3-methoxybenzaldehyde (vanillin) (**E10**), 3-phenylpropanal (**E11**), 3-methoxybenzaldehyde (**E12**), (E)-3-(4-hydroxy-3-methoxyphenyl)prop-2-enal (coniferaldehyde) (**E14**), 2-formyl-5-methoxyphenyl acetate (**E16**), ethyl 2-(4-hydroxy-3-methoxyphenyl)acetate (ethyl homovanillate) (**E17**), (Z)-3-(3,4,5-trimethoxyphenyl)prop-2-enal (3,5-trimethoxycinnamaldehyde) (**E19**), 2-hydroxy-4,4'-diethoxybenzophenone (**E23**), ethyl 4-methoxyphenyl isophthalate (**E24**) and 1-(4-(1-(4-hydroxy-3-methoxyphenyl)prop-1-en-2-yloxy)-3,5-dimethoxyphenyl)ethanone (**E25**).

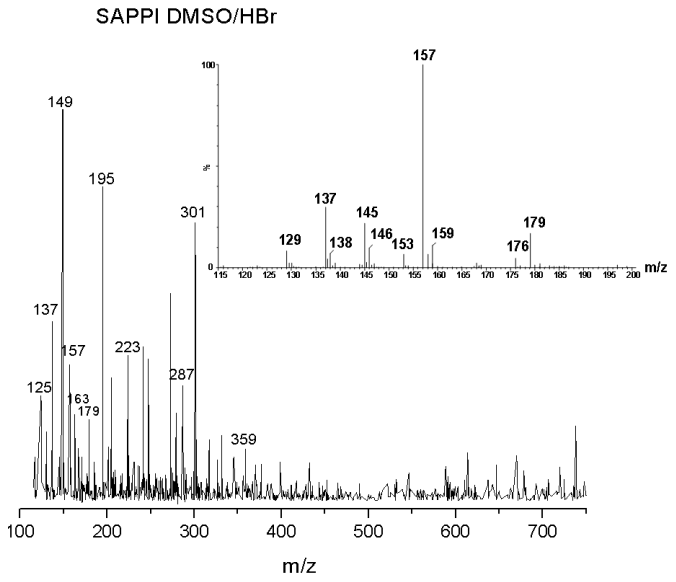

Fig. 4.7: Positive ESI-MS ($[M+H]^+$ or $[M+Na]^+$) mass chromatogram for SAPPI DMSO/HBr

NMR, FTIR and ESI-MS were in corroboration in structurally elucidating the depolymerized product mixtures as the compounds identified in ESI-MS confirmed the functionalities highlighted by NMR and FTIR. ESI-MS was also in agreement with SEC, as species with molar mass greater than 1000 g/mol were observed in the crude product mixtures. Table 4.3 tabulates the compounds determined by ESI-MS for the different product mixtures with their respective m/z ratios and theoretical masses.

Table 4.3: Summary of compounds determined by ESI-MS for the product mixtures

[a]m/z	[b]*M* (g/mol)	Structure
123, 145	122	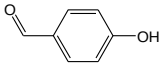 p-hydroxybenzaldehyde **(E1)**
125	124	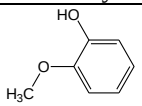 2-methoxyphenol (guaiacol) **(E2)**
136, 137	136	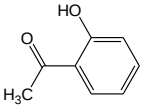 1-(2-hydroxyphenyl)ethanone (2-hydroxyacetophenone) **(E3)**
138	138	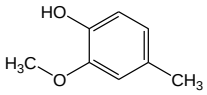 2-methoxy-4-methylphenol (4-methyl guaiacol) **(E4)**
141	140	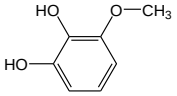 3-methoxybenzene-1,2-diol (3-methoxycatechol) **(E5)**
143 ($M+Na^+$)	120	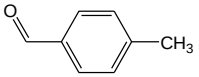 4-methylbenzaldehyde **(E6)**
147	146	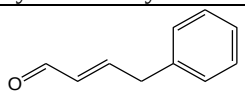 4-phenyl-2-buten-1-al **(E7)**
149	148	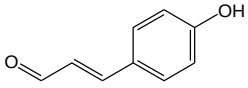 (E)-3-(4-hydroxyphenyl)prop-2-enal (4-hydroxyacinnamaldehyde) **(E8)**
150	150	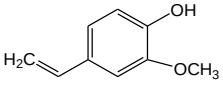 4-ethenyl-2-methoxyphenol (vinylguaiacol) **(E9)**
152, 153, 175	152	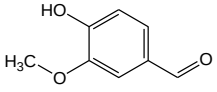 4-hydroxy-3-methoxybenzaldehyde (vanillin) **(E10)**

157 ($M+Na^+$)	134	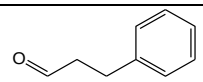 3-phenylpropanal **(E11)**
159 ($M+Na^+$)	136	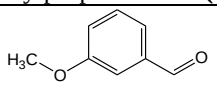 3-methoxybenzaldehyde **(E12)**
165	164	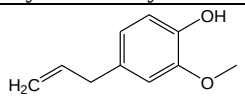 2-methoxy-4-prop-2-enylphenol (eugenol) **(E13)**
178, 179	178	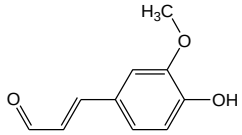 (E)-3-(4-hydroxy-3-methoxyphenyl)prop-2-enal (coniferaldehyde) **(E14)**
181	180	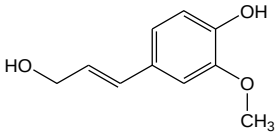 4-[(E)-3-hydroxyprop-1-enyl]-2-methoxyphenol (coniferyl alcohol) **(E15)**
195	194	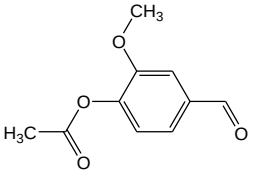 (4-formyl-2-methoxyphenyl) acetate **(E16)**
211	210	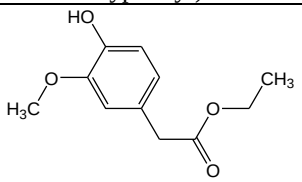 ethyl 2-(4-hydroxy-3-methoxyphenyl)acetate (ethyl homovanillate) **(E17)**
215	214	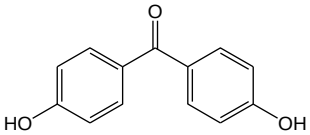 bis(4-hydroxyphenyl)methanone **(E18)**
223	222	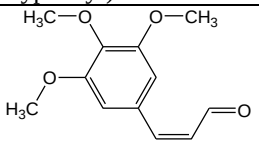 (Z)-3-(3,4,5-trimethoxyphenyl)prop-2-enal (3,5-trimethoxycinnamaldehyde) **(E19)**
227	226	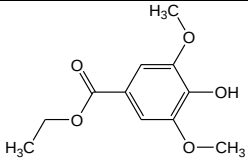 ethyl 4-hydroxy-3,5-dimethoxybenzoate (ethyl syringate) (**E20)**
245	244	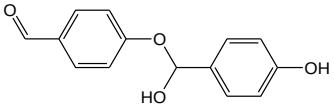 4-(hydroxy(4-hydroxyphenyl)methoxy)benzaldehyde **(E21)**

261	260	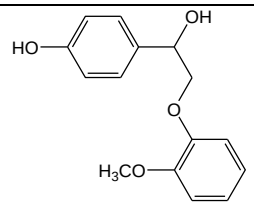 4-(1-hydroxy-2-(2-methoxyphenoxy)ethyl)phenol **(E22)**
287	286	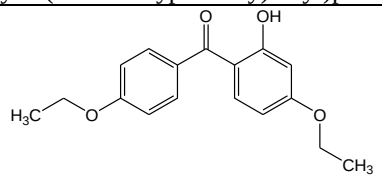 2-Hydroxy-4,4'-diethoxybenzophenone **(E23)**
301	300	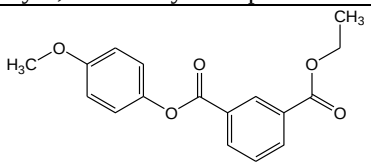 ethyl 4-methoxyphenyl isophthalate **(E24)**
359	358	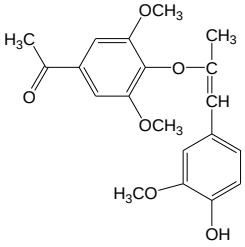 1-(4-(1-(4-hydroxy-3-methoxyphenyl)prop-1-en-2-yloxy)-3,5-dimethoxyphenyl)ethanone **(E25)**
419	418	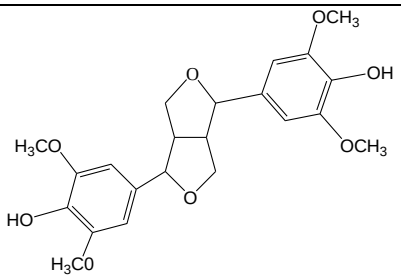 4-(4-(4-hydroxy-3,5-dimethoxyphenyl)-hexahydrofuro[3,4-c]furan-1-yl)-2-methoxy-6-methylphenol **(E26)**
537	536	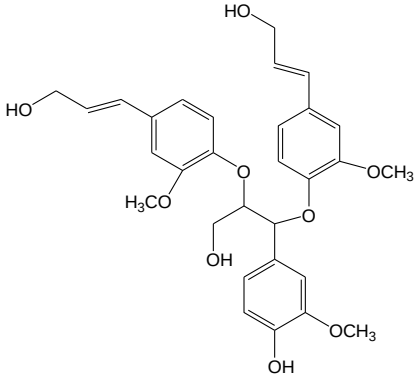 4-(3-hydroxy-1,2-bis(4-((E)-3-hydroxyprop-1-enyl)-2-methoxyphenoxy)propyl)-2-methoxyphenol **(E27)**

611	610	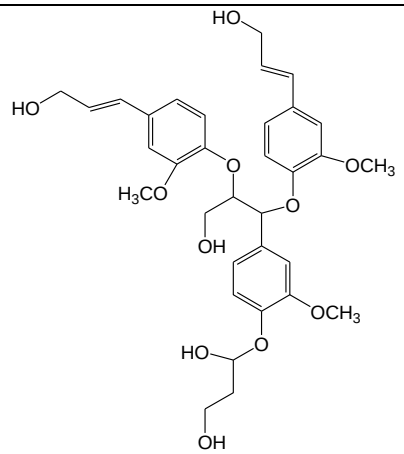 1-(4-(3-hydroxy-1,2-bis(4-((E)-3-hydroxyprop-1-enyl)-2-methoxyphenoxy)propyl)-2-methoxyphenoxy)propane-1,3-diol **(E28)**

[a] m/z observed, $[M+H]^+$ or $[M+Na]^+$ or $[M+K]^+$, Theoretical mass (M) [b]. The letter E before a number is used to denote structures obtained from ESI-MS

4.3.4 GC-MS analysis for the depolymerized products of lignin.

GC-MS was used to identify and confirm aromatic monomer formation in the respective product mixtures. The compounds of lignin depolymerization are relatively polar, therefore in this study, the product mixtures of lignin depolymerization were analyzed on a polar column (poly(ethylene) glycol modified with nitroterephthalic acid as stationary phase). Using a polar column avoided sample derivatization (sample derivatization is often a last resort in analysis and method development), because derivatization requires sensitive and attentive sample handling as most methods are moisture sensitive and can also adversely modify the chemistry of analyte if the reaction is not carried out properly.

This type of column is recommended in the analysis of phenols, phenolic derivatives and aldehydes, hence it was an ideal choice in this study since lignin produces a plethora of phenolic compounds and aldehyde functionalized compounds by oxidative depolymerization.[15–17] The ideal principle of separation on a polar stationary phase is that relatively non-polar compounds elute first followed by the polar compounds. Other secondary interactions, which are non-specific dispersion interactions (Van der Waals), and hydrogen bonding can contribute to the overall order of elution of the compounds.

From the GC-MS full scan elugrams in Fig. 4.8 and 4.10, relatively less polar compounds eluted first with relatively polar compounds eluting later. The ionization technique used in

these GC-MS experiments was electron impact ionization (EI). Compared to ESI-MS, EI provides mass spectral libraries for convenient elucidation, the NIST WebBook spectral library was used. The compounds identified by full scan GC-MS for the product mixtures (DMSO/HBr and SAPPI DMSO/HBr) with their respective retention times and characteristic ions are summarized in the tables and elution profiles that follow.

4.3.4.1 GC-MS analysis (full scan) of DMSO/HBr product mixture

The ESI-MS results were in corroboration with the GC-MS (full scan) results. This is because some of the compounds identified by positive ESI-MS were also identified by GC-MS, these include: 3-methoxy catechol (**G18**), vanillin (**G21**), p-hydroxybenzaldehyde (**G12**) and 4-methylbenzaldehyde (**G8**) (see Fig. 4.8). p-hydroxybenzaldehyde (**G12**) was one of the compounds with the highest relative abundance which was in agreement with positive ESI-MS (see Appendix G for the non-segmented DMSO/HBr GC-MS full scan chromatogram). The compounds identified by GC-MS were also in agreement with the results from FTIR and NMR analysis (most compounds identified are predominantly carbonyl functionalized, see Table 4.4). To improve selectivity and identification of more monomers within the product mixtures, single reaction monitoring (SRM) was employed (later discussed).

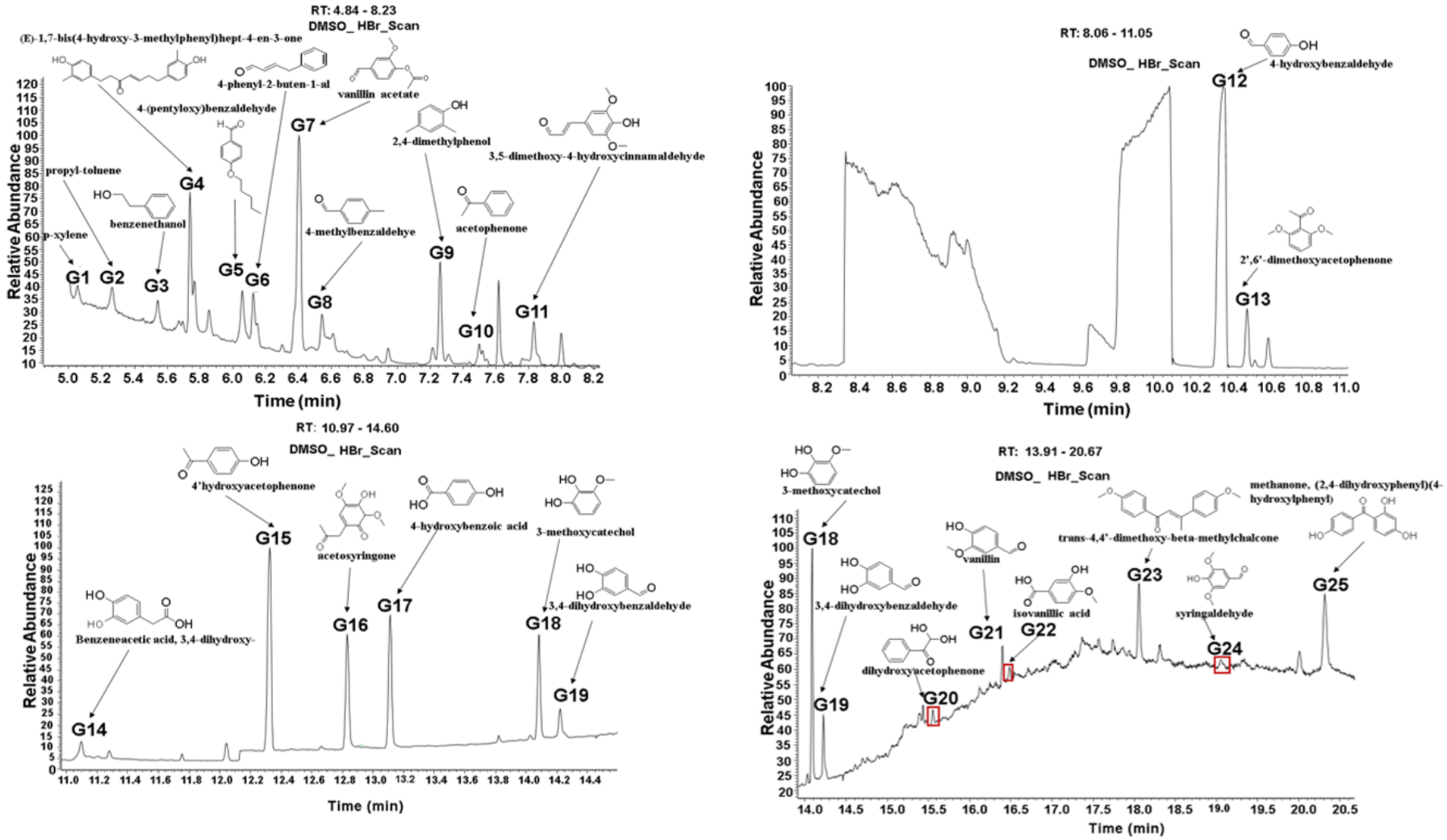

Fig. 4.8: Segmented GC-MS full scan total ion chromatogram of DMSO/HBr product mixture

Table 4.4: Compounds identified by GC-MS (full scan) in the DMSO/HBr product mixture

Product	Retention time (min)	Characteristic ions (m/z)
P-xylene **(G1)**	5.06	43, 61, 91, 106
Propyl-toluene (1-methyl-4-propylbenzene) **(G 2)**	5.26	61, 96, 105, 134
Benzeneethanol (2-phenylethanol) **(G3)**	5.55	91, 106, 122
(E)-1,7-bis(4-hydroxy-3-methylphenyl)hept-4-en-3-one **(G4)**	5.73	73, 267, 355, 356
4-(pentyloxy)benzaldehyde **(G5)**	6.06	42, 121, 123, 192
4-phenyl-2-buten-1-al **(G6)**	6.12	45, 87, 146
Vanillin acetate ((4-formyl-2-methoxyphenyl) acetate) **(G7)**	6.40	43, 107, 152 194
4-methylbenzaldehyde **(G8)**	6.54	63, 75, 119, 120
2,4-dimethylphenol **(G9)**	7.26	45, 62, 107, 122
Acetophenone (1-phenylethanone) **(G10)**	7.50	43, 61, 90, 120
3,5-dimethoxy-4-hydroxycinnamaldehyde ((E)-3-(4-hydroxy-3,5-dimethoxyphenyl)prop-2-enal) **(G11)**	7.83	43, 61, 78, 126, 151, 208
p-hydroxybenzaldehyde **(G12)**	10.38	39, 43, 79, 93, 122
2,6'-dimethoxyacetophenone **(G13)**	10.50	45, 65, 119, 120
2-(3,4-dihydroxyphenyl)acetic acid **(G14)**	11.10	51, 63, 77, 123, 168
4'-hydroxyacetophenone **(G15)**	12.32	63, 78, 94, 136
Acetosyringone (1-(4-hydroxy-3,5-dimethoxyphenyl)ethanone) **(G16)**	12.83	63, 81, 110, 126, 196
4-hydroxybenzoic acid **(G17)**	13.11	47, 77, 93, 121, 138
3-methoxycatechol (3-methylbenzene-1,2-diol) **(G18)**	14.09	79, 123, 140
3,4-dihydroxybenzaldehyde **(G19)**	14.26	79, 109, 138
Dihydroxyacetophenone (2,2-dihydroxy-1-phenylethanone) **(G20)**	15.55	77, 105, 122, 152
Vanillin (4-hydroxy-3-methoxybenzaldehyde) **(G21)**	16.40	81, 109, 151, 152
Isovanillic acid (3-hydroxy-4-methoxybenzoic acid) **(G22)**	16.48	121, 151, 153, 168
trans-4,4'-dimethoxy-beta-methylchalcone **(G23)**	18.06	79, 239, 267, 282
Syringaldehyde (4-hydroxy-3,5-dimethoxybenzaldehyde) **(G24)**	19.06	45, 88, 181, 182
(2,4-dihydroxyphenyl)-(4-hydroxyphenyl)methanone **(G25)**	20.31	51, 79, 135, 230

4.3.4.2 GC-MS analysis (full scan) of SAPPI DMSO/HBr product mixture

There were similarities in elution profiles of the crude product mixtures with regard to the compounds identified (see Table 4.4 and 4.5). The compounds identified by GC-MS (full scan) in SAPPI DMSO/HBr which were not identified in DMSO/HBr include veratraldehyde (**G31**), furfural (**G27**), ethyl caffeate (**G34**), methylhydroquinone (**G33**), 3,4-dihydroxyphenyl-2-propanone (**G28**) and 2-hydroxy-5-methoxybenzoic acid (**G35**). **G26** was identified as acetic acid (based on the fragmentation pattern) with characteristic ions being 45 and 60 Da only. Acetic acid was assumed to be a probable fragment for another unknown compound within the product mixture. The compounds not identified in SAPPI DMSO/HBr but identified in DMSO/HBr include: isovanillic acid (**G22**), vanillin acetate (**G7**), acetosyringone (**G16**), 3-methoxycatechol (**G18**), 4-phenyl-2-buten-1-al (**G6**), 3,4-dihydroxybenzaldehyde (**G19**) (2,4-dihydroxyphenyl)-(4-hydroxyphenyl)methanone (**G25**), trans-4,4'-dimethoxy-beta-methylchalcone (**G23**), 4-(pentyloxy)benzaldehyde (**G5**), p-hydroxybenzaldehyde (**G12**) and 3,5-dimethoxy-4-hydroxycinnamaldehyde (**G11**).

Some of the compounds identified in both product mixtures possessed either a guaiacyl nucleus (e.g vanillin, vanillin acetate, isovanillic acid) or a syringyl nucleus (e.g syringaldehyde and acetosyringone) which are typical nuclei in the structure of lignin.

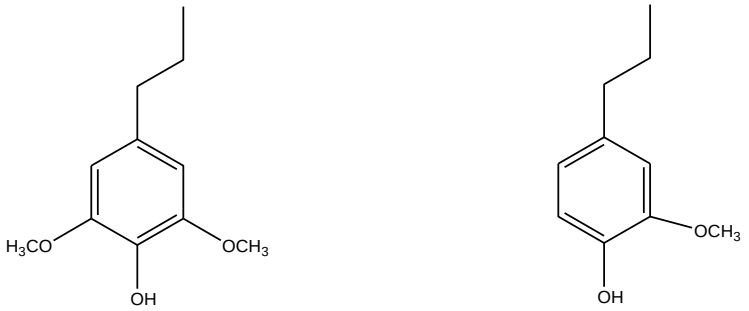

Syringyl unit Guaiacyl unit

Fig. 4.9: Guaiacyl unit and Syringyl unit

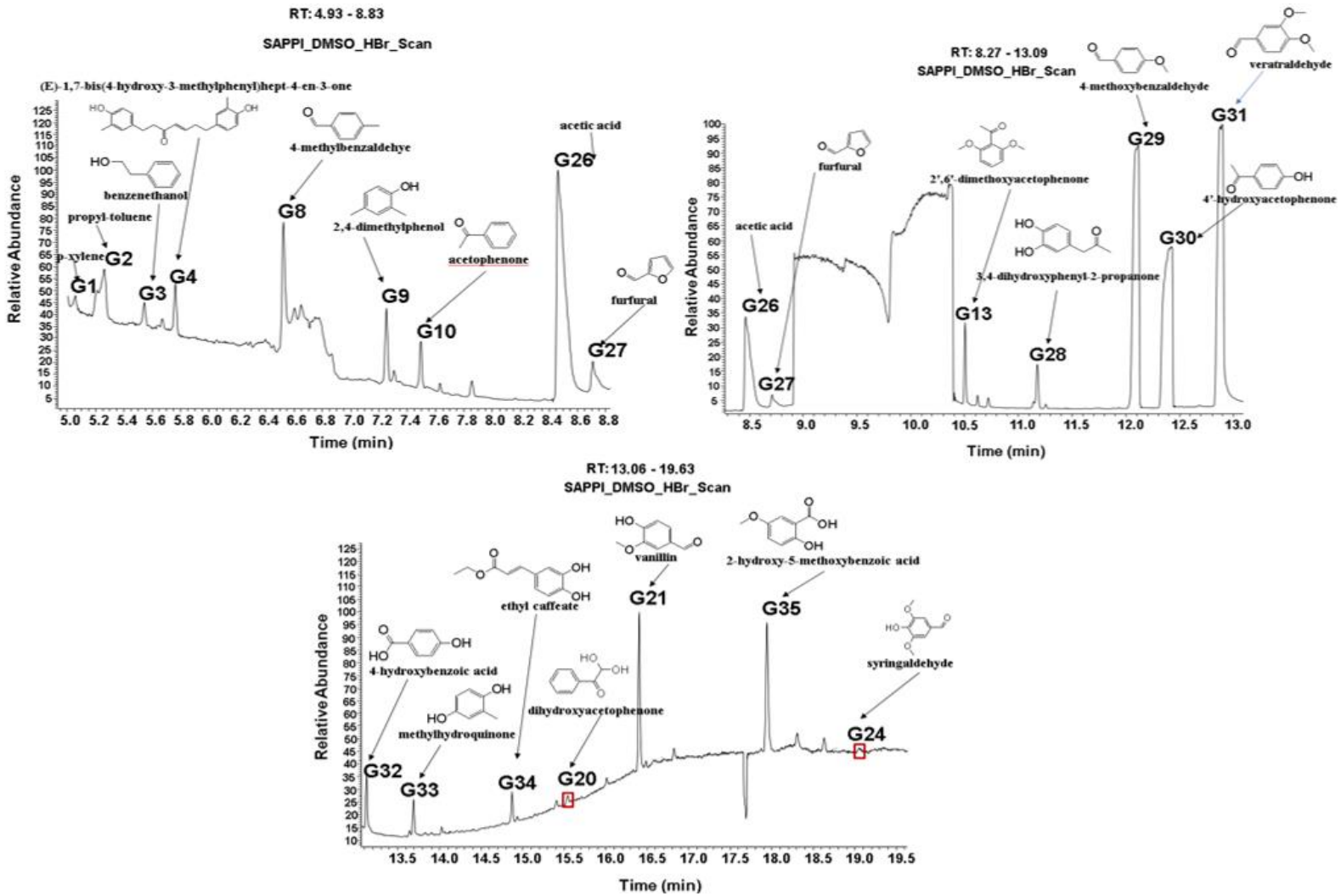

Fig. 4.10: Segmented GC-MS total ion chromatogram scan of SAPPI DMSO/HBr product mixture

Table 4.5: Compounds identified by GC-MS (full scan) in the SAPPI DMSO/HBr product mixture

Product	Retention time (min)	Characteristic ions (m/z)
P-xylene **(G1)**	5.06	43, 61, 91, 106
Propyl-toluene (1-methyl-4-propylbenzene) **(G2)**	5.26	61, 96, 105, 134
Benzeneethanol (2-phenylethanol) **(G3)**	5.55	91, 106, 122
(E)-1,7-bis(4-hydroxy-3-methylphenyl)hept-4-en-3-one **(G4)**	5.73	73, 267, 355, 356
4-methylbenzaldehyde **(G8)**	6.54	63, 75, 119, 120
2,4-dimethylphenol **(G9)**	7.26	45, 62, 107, 122
Acetophenone (1-phenylethanone) **(G10)**	7.50	43, 61, 90, 120
Acetic acid **(G26)**	8.47	45, 60
Furfural **(G27)**	8.71	67, 96
2,6'-dimethoxyacetophenone **(G13)**	10.50	45, 65, 119, 120
3,4-dihydroxyphenyl-2-propanone **(G28)**	11.18	77, 93, 123, 166
4'-methoxybenzaldehyde **(G29)**	12.10	63, 77, 94, 112, 136
4'-hydroxyacetophenone **(G30)**	12.32	63, 78, 94, 136
Veratraldehyde (3,4-dimethoxybenzaldehyde) **(G31)**	12.90	47, 63 79, 81, 110, 126, 166
4-hydroxybenzoic acid **(G32)**	13.11	47, 77, 93, 121, 138
Methylhydroquinone (2-methylbenzene-1,4-diol) **(G33)**	13.69	45, 61, 63, 124
Ethyl caffeate (ethyl (E)-3-(3,4-dihydroxyphenyl)prop-2-enoate) **(G34)**	14.87	45, 61, 89, 139, 208
Dihydroxyacetophenone (2,2-dihydroxy-1-phenylethanone) **(G20)**	15.55	77, 105, 122, 152
Vanillin (4-hydroxy-3-methoxybenzaldehyde) **(G21)**	16.40	81, 109, 151, 152
2-hydroxy-5-methoxybenzoic acid **(G35)**	17.94	45, 108, 123, 151, 168
Syringaldehyde (4-hydroxy-3,5-dimethoxybenzaldehyde) **(G24)**	19.06	45, 88, 181, 182

4.3.4.3: Single reaction monitoring (SRM)

Single reaction monitoring (SRM) was also used to identify some of the known compounds of depolymerization of lignin, as this technique allows the mass spectrometer to detect specific compounds with very high sensitivity. SRM is a non-scanning mass spectrometry technique

performed on triple quadrupole instruments in which collision-induced dissociation is used as a means to increase sensitivity and selectivity. SRM experiments were carried out using a set method targeting the following compounds: furfural, 5 methyl furfural, methyl guaiacol, ethyl guaiacol, m-cresol, eugenol, 5-hydroxy methyl furfural, vanillin, syringaldehyde and coniferaldehyde. SRM clearly shows the peak corresponding to the analyte of interest, which is either partially or completely obscured in the full scan GC-MS, see Fig. 4.11.

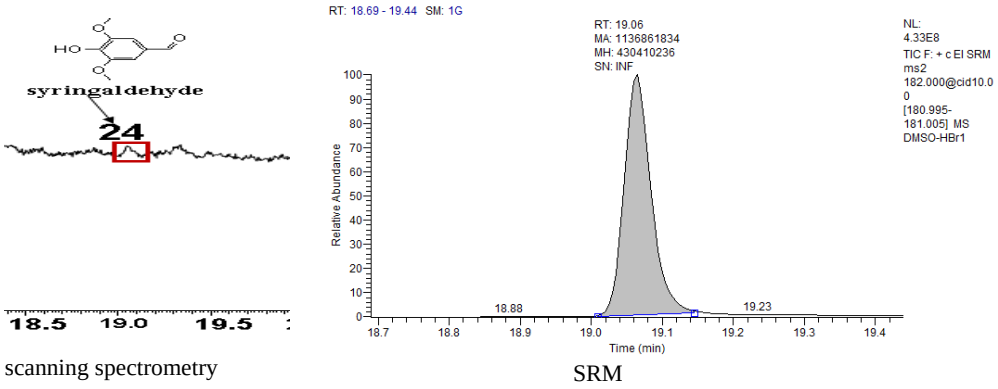

Fig. 4.11: Scanning spectrometry technique vs SRM

Table 4.6 tabulates the list of the compounds that were targeted by the SRM method in the depolymerized product mixtures for DMSO/HBr and SAPPI DMSO/HBr with their respective retention times and % relative abundances. Guaiacol, methyl guaiacol, ethyl guaiacol and eugenol are common known lignin monomeric compounds which were not identified from the respective experiments (due to relatively low % abundance and possible interference within the sample matrix). This ascertains or highlights increased sensitivity in SRM in detecting specific compounds for complex sample matrices). Vanillin and syringaldehyde for the targeted monomers (by SRM) showed higher relative abundance compared to other targeted monomeric compounds. For both sets of reactions, there was a higher percentage abundance of vanillin, this can be used as a probable tool to give an insight to the syringyl/guaiacyl (S/G) ratio of the lignin samples in question. Furfural and its derivatives are contaminants derived from cellulose. The SRM elution profiles are outlined in the Appendix section (Appendix D and E). The % abundance reported in Table 4.6 is not representative of the whole sample, but with respect to the compounds targeted by the SRM method.

Table 4.6: Compounds identified by GC-MS (SRM mode) in the crude product mixtures

	DMSO/HBr		SAPPI DMSO/HBr	
	RT	% Abundance	RT	% Abundance
Furfural	8.71	9.60	8.72	4.3
5-Methyl furfural	9.70	4.01	9.70	1.5
Guaiacol	11.92	0.59	11.92	0.24
Methyl guaiacol	12.67	0.11	12.59	0.06
Ethyl guaiacol	13.09	0.03	13.08	0.007
m-Cresol	13.40	0.014	13.41	0.002
Eugenol	13.98	0.04	13.98	0.007
5-Hydroxymethyl furfural	16.02	1.42	16.02	0.19
Vanillin	16.42	44.1	16.42	59.0
Syringaldehyde	19.06	40.0	19.06	34.3
Coniferaldehyde	21.45	0.01	21.45	0.003

4.3.5 Analysis of the depolymerized products of lignin by HPLC coupled to mass spectrometry

Reversed phase liquid chromatography (RP-LC) has been widely used in the analysis of the depolymerized products of lignin[3, 18–19] because of its enhanced selectivity compared to normal phase liquid chromatography (NP-LC). Separation in RP-LC is according to hydrophobicity, with the more polar compounds interacting less with the stationary phase and eluting first followed by the less polar compounds which are retained more and elute later.[3, 20] In the first part of this HPLC study, a method for efficiently separating the depolymerization products was developed by carefully studying and optimizing the separation of eight lignin model monomeric compounds. Catechol (L1), p-hydroxybenzaldehyde (L2), phenol (L3), vanillin (L4), syringaldehyde (L5), guaiacol (L6), benzaldehyde (L7) and eugenol (L8), structures shown in Fig. 4.12, were injected individually and as a stock solution on the Macherey–Nagel Nucleosil C_{18} column with the following size 150 × 2.0 mm i.d. and analyzed using the conditions given in Method I. The recovery for these compounds was >98%.

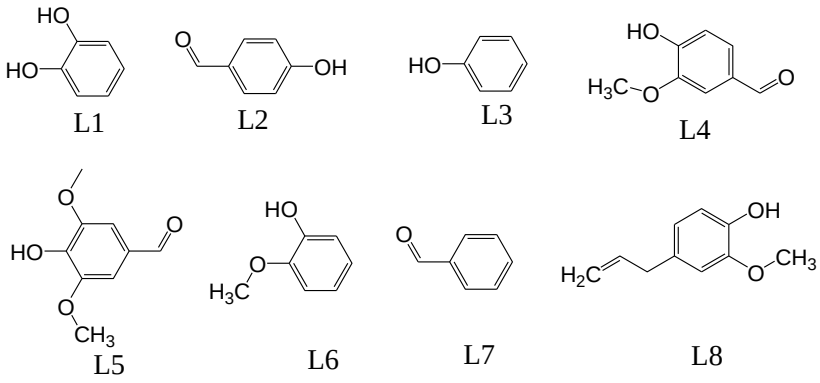

Fig. 4.12: Lignin monomeric compounds

The most polar of the compounds (catechol (L1)) with the two hydroxyl groups (electron withdrawing groups) eluted first and the least polar (eugenol (L8)) eluted last, due the stronger hydrophobic interactions of the alkyl group with the non-polar stationary phase, see Fig 4.13a. This confirmed that separation was indeed according to hydrophobicity. Although compounds L2–L7 were also eluting according to decreasing polarity, the challenge was that compounds, L3 and L4 as well as L5 and L6 had poor resolution and were co-eluting. Attempts were, therefore made to improve the separation of these compounds through altering the experimental conditions.

In principle, the resolution of a chromatographic separation is dependent on the column efficiency (plate number, N), selectivity factor (α), and retention factor (k), see Equation 4.1

$$R_s = \frac{\sqrt{N}}{4}\left(\frac{\alpha-1}{\alpha}\right)\left(\frac{\boldsymbol{ki}}{\boldsymbol{ki+1}}\right) \qquad (4.1)$$

where R_s is the resolution, N is the theoretical number of plates, α is the selectivity factor, K_i is the retention factor.

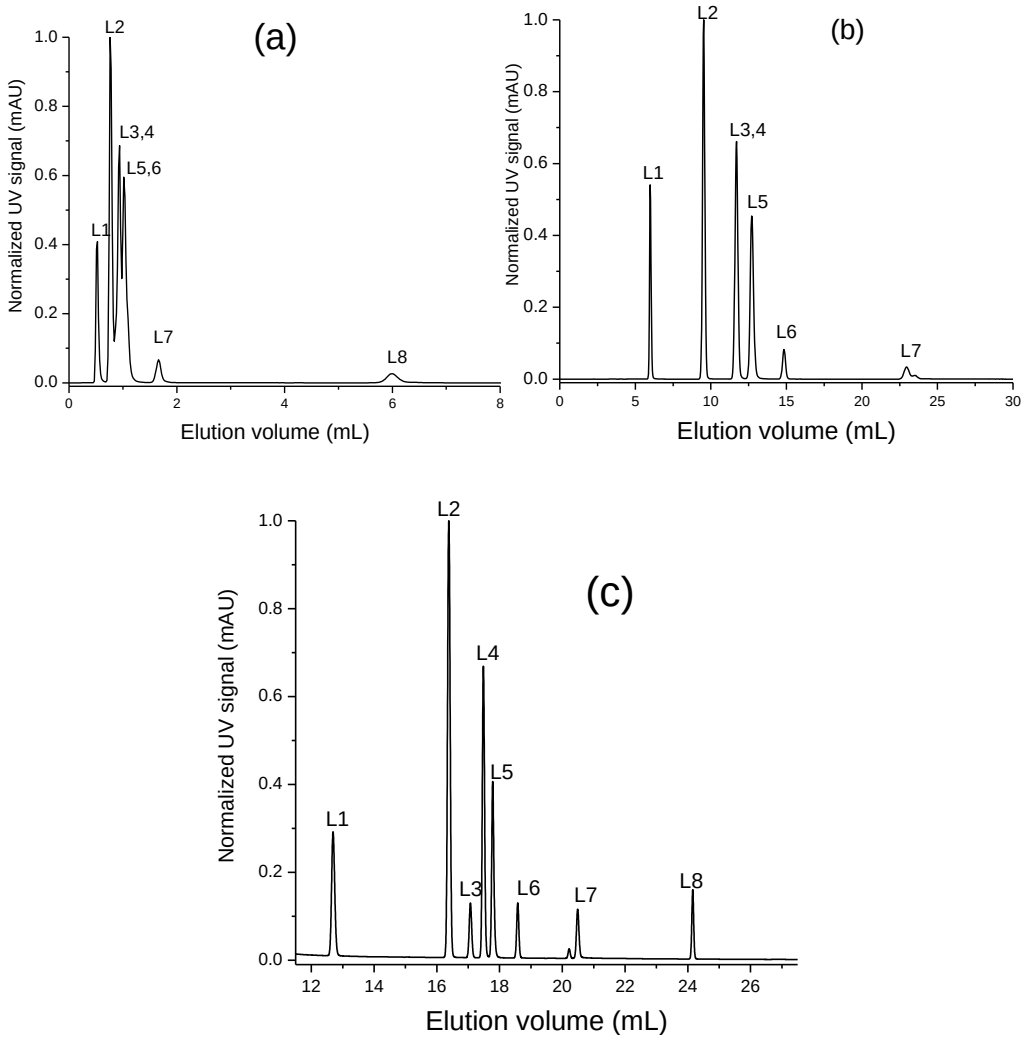

Fig. 4.13: a) Chromatogram of lignin model monomeric compounds analyzed using Method I, (b) Separation of lignin monomeric compounds on a longer C_{18} column (using method II) (c) Separation of lignin monomeric compounds on a longer C_{18} column by gradient elution (using method III)

Attempts to improve the separation efficiency were made by using a longer C18 column (250 mm x 4.6 mm i.d, recoveries at 80%) and analyzing the samples using Method II. Increasing the column length increases the number of theoretical plates consequently improving resolution. Better resolution was observed with compounds L5 and L6 that no longer co-eluted. However, two challenges still remained, compounds L3 and L4 still co-eluted, and compound L8 took longer to elute due to the enhanced interactions with the stationary phase, see Fig. 4.13b.

Solvent gradient elution chromatography was then explored in order to improve the selectivity of the separation i.e. to sufficiently separate compounds L3 and L4 and to ensure that all sample

components are eluting from the column within a reasonable time. Fig. 4.13c shows the chromatogram for the separation of compounds L1–L8 using Method III.

Although, peak identification of the stock solution was made through comparing the retention times of the individually injected standards with the eluting peaks, MS detection was used for further verification. Fig. 4.14 shows an overlay of the UV elugrams and positive scan total ion count (TIC) of the standards. Compounds L3 and L6 (phenol and guaiacol) were not observed in the positive scan TIC. As highlighted in GC-MS, there is low sensitivity which is accustomed to full scan analysis as some peaks can be partially or completely obscured in full scan mode. This is due to ionizability challenges of the respective compounds usually referred to as ionization suppression. Ionization suppression is when the extent of ionization for an analyte is decreased due to the competition between the sample matrix components and the analyte within the atmospheric pressure ion source.[21]

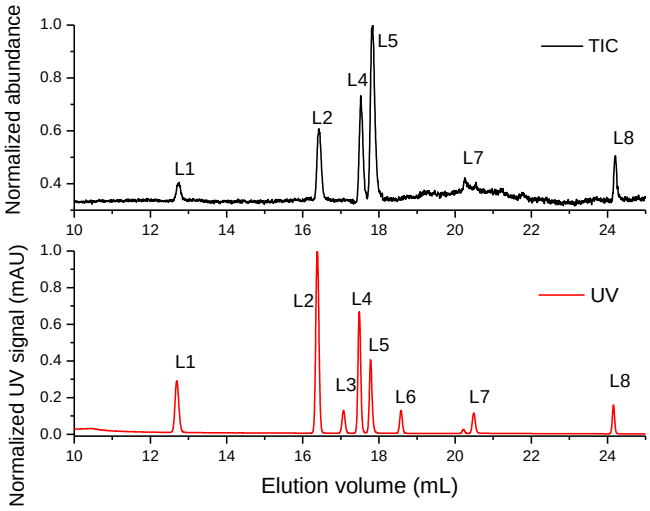

Fig. 4.14: Chromatograms of stock solution LC-UV and positive scan TIC

Since ESI-MS was set in positive mode, typically observed ions would be $[M+H]^+$ or $[M+Na]^+$ or $[M+K]^+$. Table 4.7 tabulates the ions observed for the stock solution.

Table 4.7: Compounds identified by LC-MS (full scan) for standards

Compound	Elution volume (mL)	(m/z)	[a]*M* (g/mol)
Catechol (L1)	12.7	111, 149	110
p-Hydroxybenzaldehyde (L2)	16.4	123, 145	122
Vanillin (L4)	17.5	153, 175	152
Syringaldehyde(L5)	17.9	183, 205, 221	182
Benzaldehyde (L7)	20.6	107, 129	106
Eugenol (l8)	24.2	165, 187, 203	165

[a]*M:* theoretical mass

Reversed phase liquid chromatography of DMSO/HBr depolymerization products

After successfully developing a separation protocol for selected lignin model monomeric compounds, the product from the DMSO/HBr procedure was also analyzed.

The chromatograms of the stock solution and DMSO/HBr product mixture were stacked in order to qualitatively elucidate the compounds present in the DMSO/HBr mixture, see Fig. 4.15.

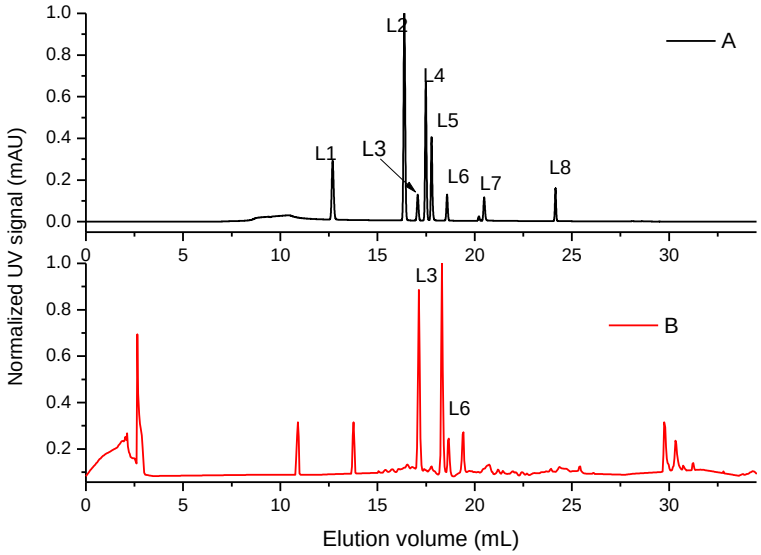

Fig. 4.15: LC-UV traces of (A) Lignin model monomeric compounds stock solution and (B) DMSO/HBr depolymerization products

Based on the elution volumes of the standards in the stock solution, only phenol and guaiacol could be identified in the product mixture. In order to further identify the other compounds present, LC-MS was used.

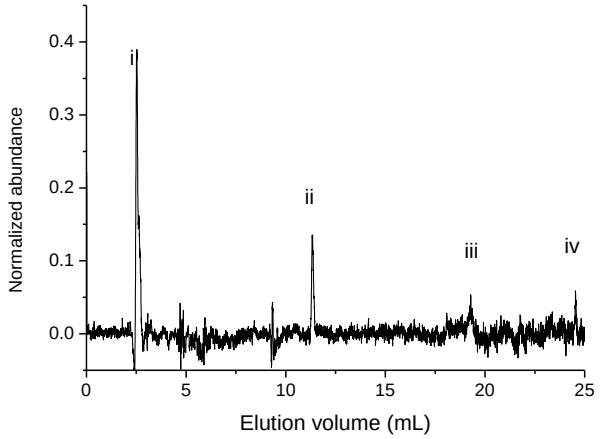

Fig. 4.16: HPLC-MS TIC elution profile for DMSO/HBr product mixture

The signal to noise ratio of the MS detector for the analysis of DMSO/HBr, see Fig. 4.16 was low, hence sensitivity was compromised. Significantly less peaks were observed in the positive scan TIC and this did not improve even after increasing the sample concentrations and injection volumes to 2.5 mg/mL and 100 µL, respectively.

The peaks labelled (i) to (iv) coincided with those observed in the UV chromatogram. Peak i eluted outside the void volume of the column (3.1 mL) and did not interact much with the stationary phase. This could mean that this compound is very polar. The data obtained from MS detection and from the m/z of the observed ions showed that peak i was most likely attributed to the following compound 4-(3-hydroxy-1,2-bis(4-((E)-3-hydroxyprop-1-enyl)-2-methoxyphenoxy)propyl)-2-methoxyphenol, see structure in Table 4.8. This compound has a theoretical molecular mass of 536 g/mol. The m/z value of 537 (compound i) was in agreement with the results reported by ESI-MS earlier.

Peak ii with an m/z of 127 was attributed to phloroglucinol with a theoretical molecular mass of 126 Da. Peak ii elutes earlier than catechol (L1) (11 mL vs 12.5 mL) making it more polar than catechol. In addition, the m/z for this peak is 127 which is in agreement with the substitution of an Ar-**H (aryl-H linkage)** with a more polar OH group. Phloroglucinol was reported as one of the compounds of lignin valorization in 1924 by Hagglund and Bjorkman.[22]

Peaks iii and iv with m/z 185 and 213, respectively, are attributed to compounds relatively less polar than guaiacol and eugenol, respectively, see Fig. 4.16. 3,4,5-trimethoxy phenol (iii) and 2,3-dihydroxypropyl 2-hydroxybenzoate (iv) with theoretical molar masses of 184 g/mol and 212 g/mol are most likely attributed to the observed peaks.

Phenol and guaiacol which had been previously observed in the LC-UV trace were not observed in the TIC, most likely due to the poor ionizability of these compounds under the given conditions. Single ion monitoring (SIM) experiments were carried out to enhance the sensitivity of the detector towards these ions and confirm their presence. Fig. 4.17 shows the positive SIM TIC for these compounds.

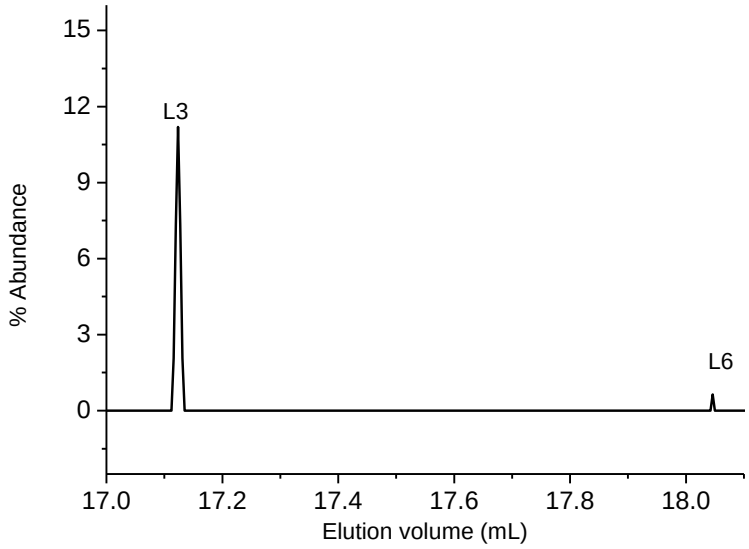

Fig. 4.17: SIM elugram showing phenol and guaiacol in the DMSO/HBr product micture

Table 4.8: Possible compounds assigned to the peaks in the TIC elution profile

Compound	Elution volume (mL)	(m/z)	[a]*M* (g/mol)
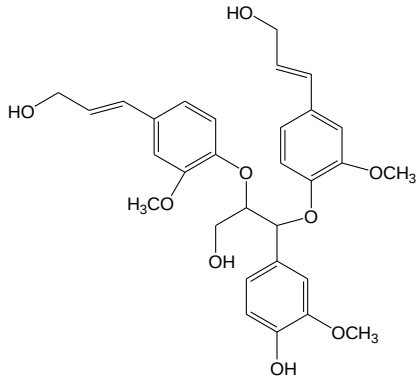 4-(3-hydroxy-1,2-bis(4-((E)-3-hydroxyprop-1-enyl)-2-methoxyphenoxy)propyl)-2-methoxyphenol (i)	2.69	537	536
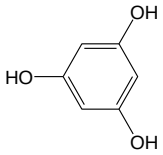 Phloroglucinol (ii)	11.1	127	126
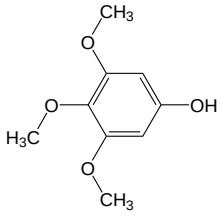 3,4,5-timethoxyphenol (iii)	19.4	185	184
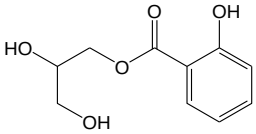 2,3-dihydroxypropyl2-hydroxybenzoate (iv)	24.5	213	212

[a]*M:* theoretical mass

4.4 Conclusion

Structural elucidation of the depolymerization products was successfully carried out by LC-MS, GC-MS, ESI-MS, NMR and FTIR spectroscopy. FTIR confirmed the oxidation of alcohols to aldehyde or ketone (typified by an intense peak at approximately 1716cm^{-1}) as per the modified Swern oxidation mechanism proposed and discussed in Chapter 3. ^{1}H NMR confirmed successful oxidative depolymerization of lignin by nitrobenzene and DMSO/HBr,

evident by a transition from broad polymer peaks of lignin to narrower peaks typical of monomeric and oligomeric species. The ^{1}H NMR spectra were difficult to accurately explain because of the complex product mixtures characterized by signal overlap.

ESI-MS was used as a complementary technique to GC-MS, as it was possible to obtain the full molar mass range for the depolymerization products of lignin. However, due to the high complexity of the large number of products, it was not practical to determine all the monomeric compounds after depolymerization. Therefore, the obtained ESI-MS spectra could only be interpreted to a limited degree. GC-MS was successfully used to identify and confirm aromatic monomer formation in the respective product mixtures.

The compounds identified by GC-MS were also in agreement with the results from FTIR and NMR analysis (most compounds identified were predominantly carbonyl functionalized, which is evidence of oxidative depolymerization). To enhance detector sensitivity in GC-MS, SRM was effectively used. SRM clearly showed the peak corresponding to the analyte of interest which is either partially or completely obscured in the full scan GC-MS. The main shortcoming of GC-MS was that it was a challenge to analyze oligomeric species due to the low volatility. Therefore, to avoid this effect, product mixtures were successfully analyzed by ESI-MS and LC-MS.

HPLC analysis of depolymerized products was successfully carried out. A separation protocol for efficiently separating the depolymerization products was developed by carefully studying and optimizing the separation of eight lignin model monomeric compounds by RP-HPLC. The developed separation protocol was applied on the DMSO/HBr product mixture. Hyphenating HPLC to ESI-MS (online) provided more information with regard to the structural and qualitative analysis of the DMSO/HBr product mixture. Poor signal-to-noise ratio of the ESI-MS detector in full scan mode prompted the use of single ion monitoring. The compounds identified from DMSO/HBr product mixture included: phenol, guaiacol, phloroglucinol, 3,4,5-trimethoxy phenol, 2,3-dihydroxypropyl-2-hydroxybenzoate and 4-(3-hydroxy-1,2-bis(4-((E)-3-hydroxyprop-1-enyl)-2-methoxyphenoxy)propyl)-2-methoxy-phenol.

However, peaks due to a few products which can be observed in GC-MS analysis could not be observed in HPLC analysis, probably due to overlapping of peaks for a few other lignin monomeric compounds. [7] It was important to quantitatively elucidate the complex product mixture (DMSO/HBr) by HPLC analysis, but the complexity of the product mixture played a

significant role for the prevalence of overlapping peaks, hence, quantitative analysis was a challenge. Therefore, vacuum distillation (later discussed in Chapter 5) was carried out in order to fractionate the complex DMSO/HBr product mixture into less complex fractions in pursuit of quantitatively determining the amounts of the lignin monomeric compounds produced during depolymerization.

4.5 References

1. Dier, T. K.; Rauber, D.; Durneata, D.; Hempelmann, R.; Volmer, D. A., *Scientific Reports* **2017,** *7* (1), 1–12.

2. Ringena, O.; Lebioda, S.; Lehnen, R.; Saake, B., *Journal of Chromatography A* **2006,** *1102* (1–2), 154–163.

3. Jiang, Z.; Zhu, J.; Li, X.; Lian, Z.; Yu, S.; Yong, Q., *Chinese Journal of Chromatography* **2011,** *29* (1), 59–62.

4. Xia, G.-G.; Chen, B.; Zhang, R.; Zhang, Z. C., *Journal of Molecular Catalysis A: Chemical* **2014,** *388*, 35–40.

5. Boeriu, C. G.; Bravo, D.; Gosselink, R. J.; van Dam, J. E., *Industrial Crops and Products* **2004,** *20* (2), 205–218.

6. Zhao, X.; Liu, D., *Industrial Crops and Products* **2010,** *32* (3), 284–291.

7. Deepa, A. K.; Dhepe, P. L., *ACS Catalysis* **2014,** *5* (1), 365–379.

8. Bovey, F. A.; Mirau, P. A., 1 - Fundamentals of Nuclear Magnetic Resonance. In *NMR of Polymers*, Bovey, F. A.; Mirau, P. A., Eds. Academic Press: San Diego, 1996; pp 1–115.

9. Evtuguin, D. V.; Neto, C. P.; Silva, A. M.; Domingues, P. M.; Amado, F. M.; Robert, D.; Faix, O., *Journal of Agricultural and Food Chemistry* **2001,** *49* (9), 4252–4261.

10. Lundquist, K., Proton (^{1} H) NMR Spectroscopy. In *Methods in Lignin Chemistry*, Lin S.Y, D. C. W., Ed. Springer-Verlag Berlin Heidelberg Germany: Springer-Verlag 1992; pp 242–249.

11. Wen, J.-L.; Sun, S.-L.; Xue, B.-L.; Sun, R.-C., *Materials* **2013,** *6* (1), 359–91.

12. Capanema, E. A.; Balakshin, M. Y.; Kadla, J. F., *Journal of Agricultural and Food Chemistry* **2004,** *52* (7), 1850–1860.

13. Diebold, J. P. *A review of the chemical and physical mechanisms of the storage stability of fast pyrolysis bio-oils*; National Renewable Energy Lab., Golden, CO (US): 1999; pp 1–59.

14. Quideau, S.; Ralph, J., *Journal of Agricultural and Food Chemistry* **1992,** *40* (7), 1108–1110.

15. Poole, C. F.; Li, Q.; Kiridena, W.; Koziol, W. W., *Journal of Chromatography A* **2000,** *898* (2), 211–226.

16. Horka, M.; Janak, K.; Kahle, V.; Tesařík, K., *Chromatographia* **1987,** *23* (8), 553–556.

17. Poole, C. F.; Poole, S. K., *Journal of Chromatography A* **2008,** *1184* (1–2), 254–280.

18. Lobbes, J. r. M.; Fitznar, H. P.; Kattner, G., *Analytical Chemistry* **1999,** *71* (15), 3008–3012.

19. Sun, M.; Sandahl, M.; Turner, C., *Journal of Chromatography A* **2018,** *1541*, 21–30.

20. Ingalls, A. E.; Ellis, E. E.; Santos, G. M.; McDuffee, K. E.; Truxal, L.; Keil, R. G.; Druffel, E. R., *Analytical Chemistry* **2010,** *82* (21), 8931–8938.

21. Mannur, V.; Patel, D.; Mastiholimath, V.; Shah, G., *International Journal of Pharmaceutical Sciences Review and Research* **2011,** *6* (1), 34–37.

22. Hagglund, E.; Bjorkman, C., *Biochemische Zeitschrift* **1924,** *147*, 74–89.

Chapter 5

Fractionation and characterization of DMSO/HBr depolymerized product mixture

5.1 Introduction

Separating complex mixtures of depolymerized products of lignin into single or two components is a huge challenge thus far.[1–2] This is because of the similarities in properties such as chemical composition and boiling points of the monomeric compounds within the complex mixture. The challenge in separating these complex mixtures has, therefore, prompted researchers to exploit the molecular diversity of the complex mixtures to synthesize complex multicomponent polymers.

Different methods of isolating monomeric compounds obtained by lignin depolymerization have been explored and the respective shortcomings of each method have been emphasized. These methods include solvent extraction, column chromatography and distillation.[3–4] Solvent extraction is most often used as an initial step in the purification of the crude product mixtures but it is plagued by low selectivity. Co-elution has been reported as one of the challenges in purification of these monomeric compounds by column chromatography. Simple fractional distillation could cause decomposition of these crude product mixtures as they are characterized by high boiling point monomeric components.

Vacuum distillation was carried out in this study, in order to fractionate the complex DMSO/HBr product mixture into less complex fractions in pursuit of quantitatively determining the amounts of the lignin monomeric compounds produced during depolymerization. The complexity of the product mixture played a significant role to the prevalence of overlapping peaks (as discussed in Chapter 4), hence quantitative analysis was a challenge. Due to the high boiling points of the lignin monomeric compounds, conventional fractional distillation would have initiated the further degradation of the depolymerized product mixture upon using high temperatures hence vacuum distillation was carried out.

5.2 Experimental

Materials

Methanol (HPLC grade, ≥99.9%, Sigma Aldrich, Saint-Quentin-Fallavier, France), deionized water from a laboratory Millipore purification system, acetic acid (HPLC grade, ≥99.8%, Sigma Aldrich, Buchs, Switzerland), DMSO/HBr product mixture (from the depolymerization of lignin by DMSO/HBr), guaiacol (natural ≥99%, Sigma Aldrich, Hong Kong, China), vanillin (99%, Sigma Aldrich, Hong Kong, China), 4-hydroxybenzaldehyde (98%, Alfa Aesar, Lancaster, UK), phenol (99%, Labchem, Gauteng, South Africa), benzaldehyde (≥99%, Sigma Aldrich, St. Louis, USA), syringaldehyde (≥98%, Sigma Aldrich, Hong Kong, China), catechol (≥99%, Sigma Aldrich, St. Louis, USA) and eugenol (99%, Sigma Aldrich, St. Louis USA), phloroglucinol (99%, Riedel-de Haen AG, Hannover, Germany) and 2,4-dihydroxybenzaldehyde (98%, Sigma Aldrich, Gillingham, UK), deuterated trifluoro acetic acid (TFA-*d*), (≥995.%, Sigma Aldrich, St. Louis, USA) were used as received.

5.2.1 Vacuum distillation of DMSO/HBr

The DMSO/HBr product was distilled under vacuum and fractions collected at the following temperatures: 100–130 °C, 140–150 °C, 160 °C and 180 °C, see Table 5.1. After all the fractions were collected they were quantified gravimetrically. The fraction that contained the un-distilled product was also quantified gravimetrically. The percentage recovered sample was calculated according to the following equation:

$$\% \text{ of recovered sample} = \frac{\text{weight of fraction}}{\text{weight of crude DMSO/HBr}} \times 100\% \qquad (5.1)$$

where *Weight of fraction* is the mass of the recovered sample (mass of fraction) at a particular temperature by vacuum distillation of the crude DMSO/HBr product mixture and *Weight of crude DMSO/HBr* is the mass of the crude DMSO/HBr product mixture before vacuum distillation.

Table 5.1: Gravimetric quantification of fractions

Fraction number	Description	Recovered sample (g)	% of recovered sample
1	100–130 °C (phase 1)	1.84	12.3
2	100–130 °C (phase 2)	2.73	18.2
3	**140–150 °C (phase 1)**	0.98	6.50
4	140–150 °C (phase 2)	3.84	25.6
5	160 °C (phase 1)	1.56	10.4
6	**160 °C (phase 2)**	0.42	2.8
7	**180 °C (phase 1)**	0.96	6.40
8	180 °C (phase 2)	0.44	2.93
Un-distilled fraction	–	0.83	5.53
Solid char	–	1.4g	9.33

5.2.2.1 LC-MS analysis

The experimental procedure was described in section 4.2.5 in Chapter 4.

Quantification of lignin monomeric compounds by LC-MS analysis.

The quantification of the respective lignin monomeric compounds in the fractions was carried out using a single point external calibration method with the ESI-MS detector in positive SIM mode. The amount of injected analyte was calculated using Equations 5.2 and 5.3.

$$\text{Response factor} = \frac{\text{Peak Area}}{\text{Concentration } (\frac{\text{mg}}{\text{mL}})} \quad (5.2)$$

$$\text{Concentration of analyte} = \frac{\text{Peak Area}}{\text{Response Factor}} \quad (5.3)$$

The method used for quantification is tabulated in Table 5.2. The following pure lignin monomeric compounds vanillin, p-hydroxybenzaldehyde, syringaldehyde, catechol, guaiacol, benzaldehyde, phenol, eugenol, phloroglucinol, 2,4-dihydroxybenzaldehyde which were readily available from different suppliers were used as standards for calibration. The positive SIM ions for each compound were set at $[M+H]^+$ and $[M+Na]^+$ ions respectively (see Table 5.2), where *M* is theoretical mass of a compound.

Table 5.2: Experimental parameters for the HPLC-ESI-MS Positive SIM mode method

V_e (mL)	Group	*M*	SIM ION	Fragmentor	Gain
10.96	phloroglucinol	126	127.10	150	1.00
			149.00		
12.69	catechol	110	111.10	150	1.00
			133.00		
16.43	p-hydroxybenzaldehyde	122	123.10	150	1.00
			145.10		
16.85	phenol	94	95.10	150	1.00
			117.00		
17.15	3,4-dihydroxybenzaldehyde	138	139.10	150	1.00
			161.00		
17.50	vanillin	152	153.10	150	1.00
			175.00		
17.80	syringaldehyde	182	183.1	150	1.00
			205.00		
18.576	guaiacol	124	125.10	150	1.00
			147.00		
20.22	benzaldehyde	106	107.10	150	1.00
			129.00		
20.54	eugenol	164	165.10	150	1.00
			187.00		

5.2.2.2 FTIR analysis

The experimental procedure was described in Section 4.2.1 in Chapter 4.

5.2.2.3 ^{1}H-NMR and ^{13}C NMR analysis

NMR spectra were acquired using a Varian 400 MHz Varian *Unity* Inova instrument. (Varian Inc, Mulgrave, Victoria Australia). TFA-*d* was used as the solvent and tetramethylsilane (TMS) as the reference.

5.3 Results and discussion

The main objectives of this chapter were to positively identify and quantify lignin monomeric compounds obtained by the depolymerization of lignin. The fractions collected at each temperature range consisted of two phases, 1 and 2 (liquid and solid phases). The limitations of the full scan mode in LC-MS analysis have been highlighted and discussed in Chapter 4. Therefore, a SIM mode experiment was setup and was applied on all fractions to deconvolute the monomeric compounds with reference to the pure compounds that were available. The distilled fractions that exhibited positive responses to the lignin monomer standards set in the

SIM method in Table 5.2 include: 140–150 °C (phase 1), 160 °C (phase 2), 180 °C (phase 1) and the un-distilled fraction. Therefore, these fractions are the ones fully discussed in this section. The compounds identified and quantified in these fractions aligned with the theoretical boiling point trends of the standards.

Due to possible ionization suppression when using mass spectrometry, UV at a wavelength of 277 nm was also used. Quantification in HPLC-UV was performed by peak area. This method is a semi-quantitative approach as peak areas are dependent on the UV absorption properties of compounds. Therefore absolute quantification was done by a single point calibration using ESI-MS detector in SIM mode as highlighted above. Fractions 100–130 °C (phase 1 and 2), 140–150 °C phase 2, 160 °C phase 1 and 180 °C phase 2 did not absorb UV light in the range of 250–280 nm where aromatic compounds normally absorb. The possible explanation was that, these fractions contained linear compounds which possibly formed due to the degradation of the crude DMSO/HBr product mixture during distillation e.g. breaking of susceptible linkages in oligomeric species due to high temperatures (see Appendix I for the ^{1}H NMR analysis of these fractions as no aromatic signals were observed).

5.3.1 Analysis of fraction 140-150 °C (phase 1)

Fig. 5.1 shows the SIM elugram of Fraction 1 (140–150 ^{o}C, phase 1). The compounds that were positively identified and quantified by means of injected mass were syringaldehyde eluting at 17.8 mL and benzaldehyde which eluted at 20.2 mL.

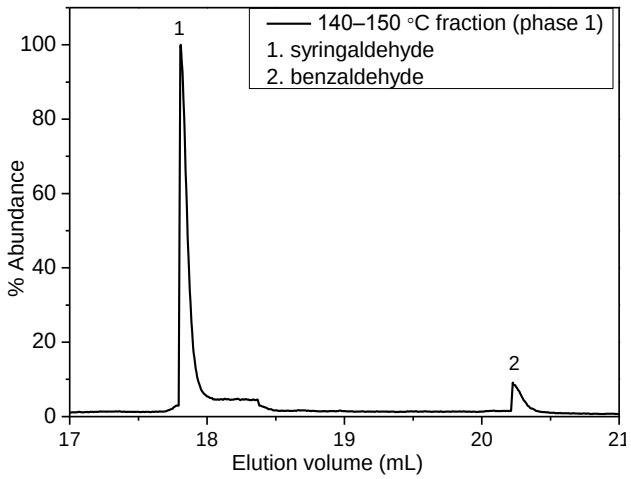

Fig. 5.1: SIM elugram of the 140–150 °C fraction (phase 1)

Fig 5.2 to 5.3 show the mass spectra of syringaldehyde and benzaldehyde, respectively, which confirmed the identification of the compounds. The theoretical masses (*M*) of syringaldehyde and benzaldehyde are 182 and 106 g/mol, respectively. H^+ and Na^+ adducts were observed for both compounds (183.1 and 205 for syringaldehyde, 107.1 and 129 for benzaldehyde). The compounds were present in the following quantities 31.1% and 6.4% by single point calibration.

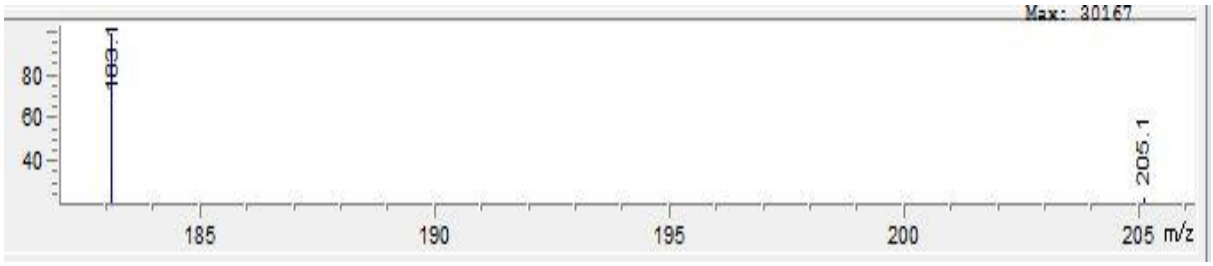

Fig. 5.2: Mass spectrum of syringaldehyde with characteristic $[M+H]^+$ and $[M+Na]^+$

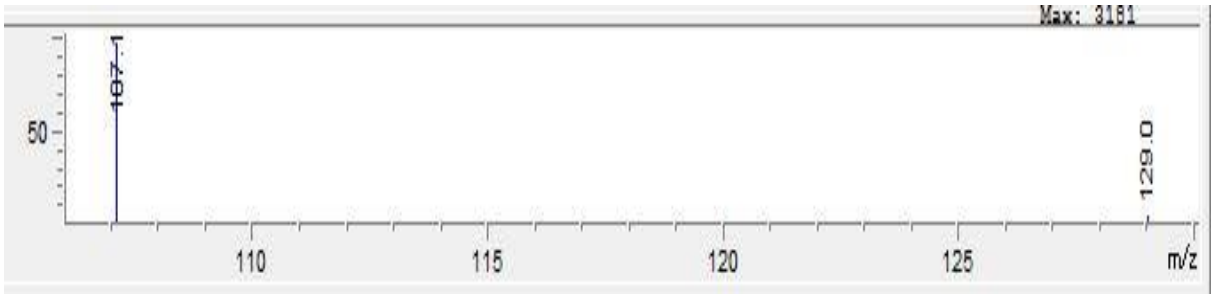

Fig. 5.3: Mass spectrum of benzaldehyde with characteristic $[M+H]^+$ and $[M+Na]^+$

Other peaks that were not qualitatively and quantitatively determined from this fraction by LC-MS positive SIM mode are observed in the HPLC-UV chromatogram at the following elution volumes: 17.2 mL (compound more polar than both syringaldehyde and benzaldehyde) and at 19.4 mL, see Fig. 5.4. When full MS scan was carried out, these compounds were not identified, probable due to ion suppression discussed in Chapter 4. Quantification in HPLC-UV was carried out by peak area. This method is a semi-quantitative approach as peak areas are dependent on the UV absorption properties of compounds. The peak area percentages of each compound using HPLC-UV are: 4.8% (unknown compound eluting at 17.2 mL), 70.7% (syringaldehyde), 2.1% (unknown compound eluting at 19.4 mL) and 22.4% (benzaldehyde).

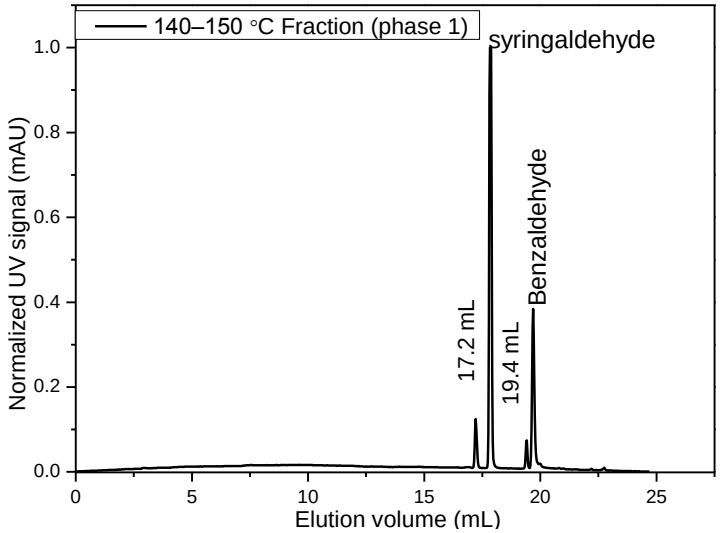

Fig. 5.4: HPLC-UV elugram of the 140–150 °C: fraction (phase 1)

Fig. 5.5 shows the ^{13}C NMR spectrum for the 140–150 °C fraction (phase 1). The results supported the results of LC-MS. A typical aldehyde carbon (Ar-**C**O-H) was observed at approximately 201 ppm which is synonymous with the aldehyde carbon found in syringaldehyde and benzaldehyde. Another carbonyl carbon is also observed at a resonance signal of 170 ppm which is probably due to the presence of the unquantified compounds in the 140–150 °C fraction.

The resonance signal between 120 and 140 ppm is typical of aromatic ring carbons. The alkoxy region is elucidated at 50–90 ppm (based on the structure of syringaldehyde the alkoxy region can be attributed to the CH_3–O moiety). Between 22 and 50 ppm, aliphatic carbon resonance is prevalent. The TFA-*d* solvent peaks are marked by an asterisk. A splitting pattern (quartet) for TFA is observed between 110–125 ppm due to heteronuclear coupling caused by the attachment of the fluorine atoms to carbon atom.[5]

The fraction was also analyzed by ^{1}H NMR spectroscopy, see Fig. 5.6. A greater magnitude of deshielding was observed most likely (resonance approximately 10–12 ppm) due to hydrogen bonding within molecules as proposed by Lampman and co-authors[5], see structure in Fig. 5.6. The formyl protons (Ar-CO-**H**) (typical of syringaldehyde and benzaldehyde) were observed at between 9.25–10 ppm. The resonance signals between 7.6 and 8.3 ppm are typical of aromatic ring protons where electron withdrawing groups are attached to the ring e.g in syringaldehyde. Higher resonance vinylic protons typical of 4-hydroxycinnamaldehyde and coniferaldehyde (refer to Table 4.3 for structures) are observed between 5.5 and 6.5 ppm. The

signal at approximately 3.5 ppm is typical of methoxy signals. The TFA-*d* solvent peak is marked by an asterisk at approximately 11.5 ppm.

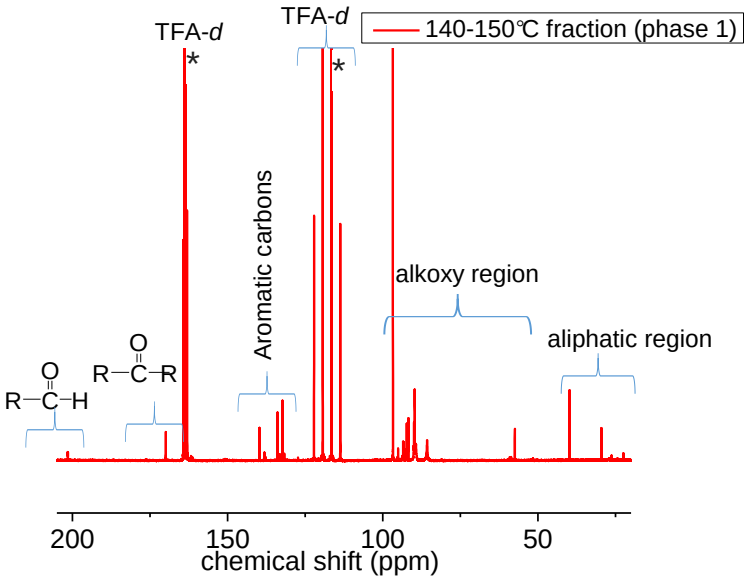

Fig. 5.5: ^{13}C NMR spectrum of the 140–150 °C fraction (phase 1)

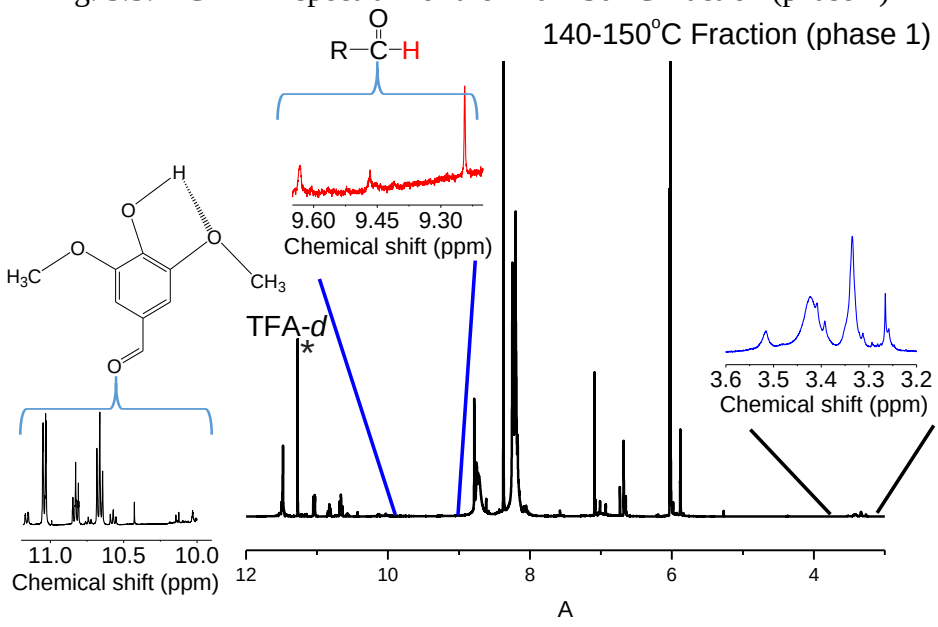

Fig. 5.6: ^{1}H NMR spectrum of the 140–150 °C fraction (phase 1)

The results obtained from FTIR analysis were in agreement with LC-MS. A broad peak at around 3357 cm^{-1} was attributed to the phenolic group present in syringaldehyde, see Fig. 5.7. A conjugation of C=O with phenyl, at 1710 cm^{-1} for C=O and 1620 cm^{-1} for aromatic ring was observed typical in syringaldehyde and benzaldehyde. The C–O stretch (1083 cm^{-1}) in the alkoxy functionality region is typical of the methoxy group in syringaldehyde. The peak at 690 cm^{-1} suggests a para-substituted ring with out-of-plane bend vibrations.

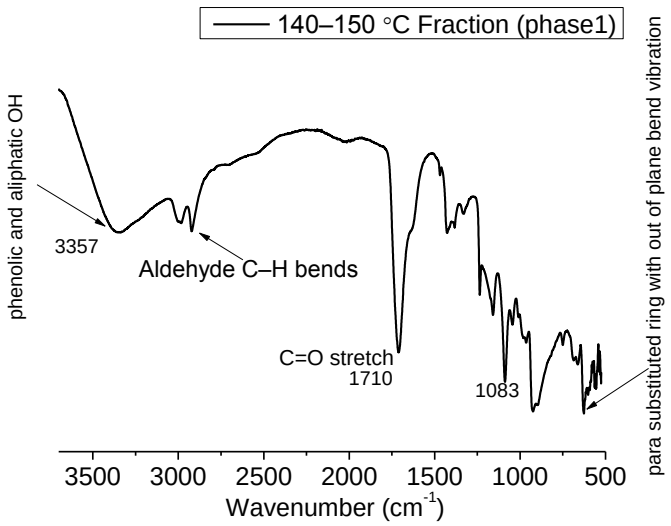

Fig. 5.7: FTIR spectrum of the 140–150 °C fraction (phase 1)

5.3.2 Analysis of 160 °C fraction (phase 2)

Eugenol (V_e: 23.5 mL) is the only compound that was quantified and identified from the 160 °C fraction (phase 2) by LC-MS in positive SIM mode and was quantified at 21.8% (by mass of injected sample) using single point calibration, see Fig. 5.8. Fig 5.9 shows the mass spectrum of eugenol highlighting the $[M+H]^+$and $[M+Na]^+$ions, respectively.

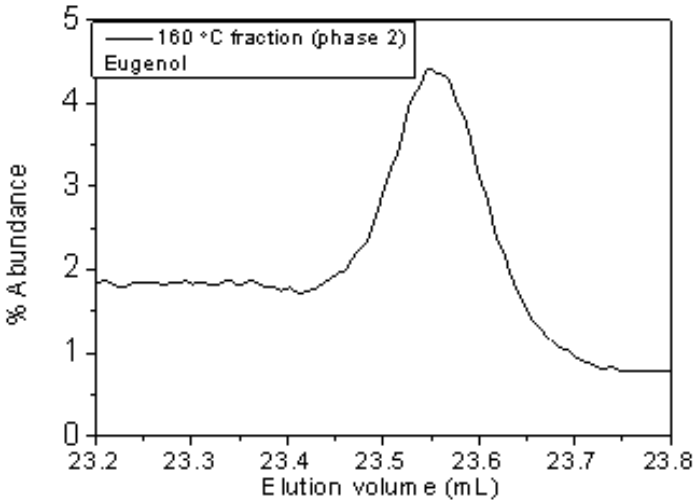

Fig. 5.8: SIM elugram of the 160 °C fraction (phase 2)

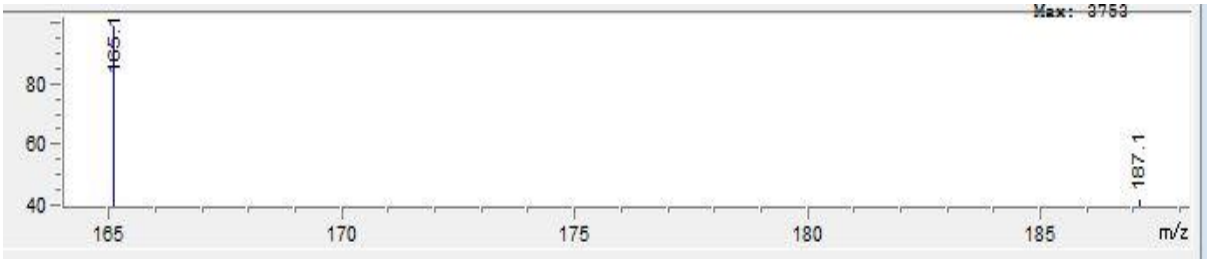

Fig. 5.9: Mass spectrum of eugenol with characteristic $[M+H]^+$ and $[M+Na]^+$

Peaks at the following elution volumes were also observed from the UV chromatogram (see Fig. 5.10): 2.3, 2.8, 3.0, 22.7 and 24.9 mL. The peaks eluting between 2.8 and 3.0 mL signified the presence of highly polar compounds. When a full MS scan was carried out, coniferaldehyde was identified based on the mass spectrum observed at 22.7 mL (see Fig. F1.1 in Appendix F). The peak area percentages of each compound using HPLC-UV are: 64.5% (eugenol), 18.4% (unknown compound eluting at 24.8 mL), 6.8% (coniferaldehyde) and 10.3% (highly polar compounds eluting between 2.3 and 3.0 mL)

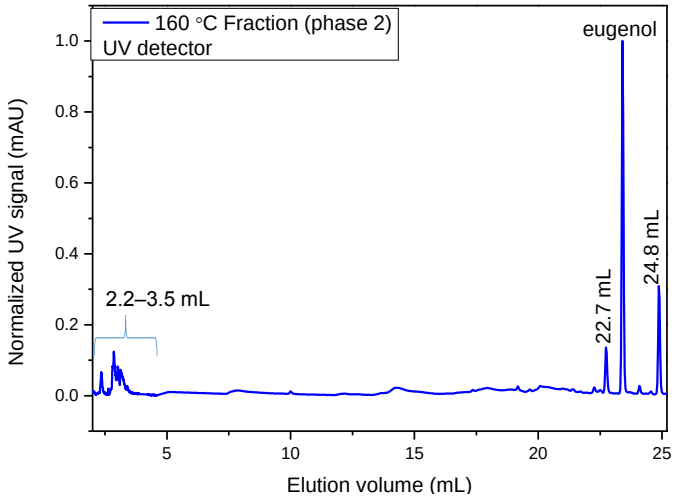

Fig. 5.10: HPLC-UV elugram of the 160 °C: fraction (phase 2)

FTIR results (see Fig. 5.11) presenting the following wavenumbers confirmed the presence of eugenol in the fraction: 3394 cm^{-1} (phenolic hydroxyl group), 3100 cm^{-1} (C=H stretch in alkenes), 1620cm^{-1} (C=C aromatic ring stretch absorptions), 1433cm^{-1} (CH_2 bend absorptions) 1039cm^{-1} (C–O stretch in the alkoxy functionality). ^{1}H NMR analysis also confirmed the presence of vinylic protons between 4–6 ppm, see Fig. 5.12. After a careful look into the ^{13}C NMR results, the vinylic signals could not be visibly identified because there was possible overlapping of the sample peaks with the solvent peaks (between 110 to 125 ppm) (see Fig

5.13). A carbonyl signal from ^{13}C NMR and ^{1}H NMR results (170 ppm and 2.27 ppm respectively) was an indication of the presence of other compounds within the fraction.

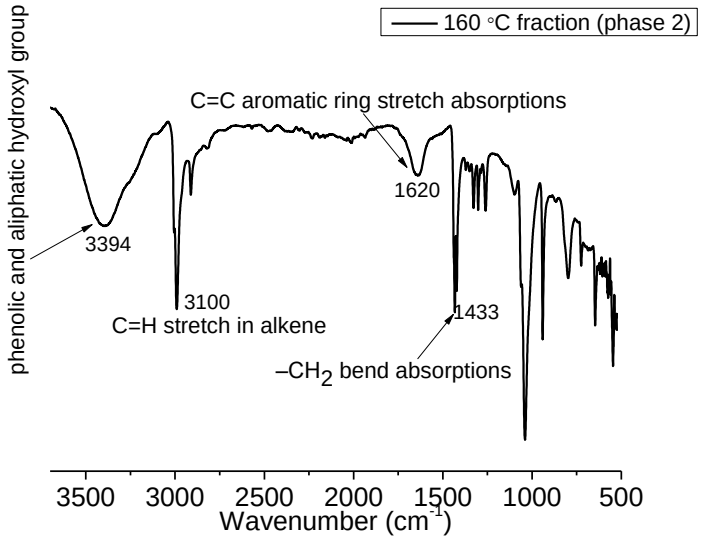

Fig. 5.11: FTIR spectrum of the 160 °C fraction (phase 2)

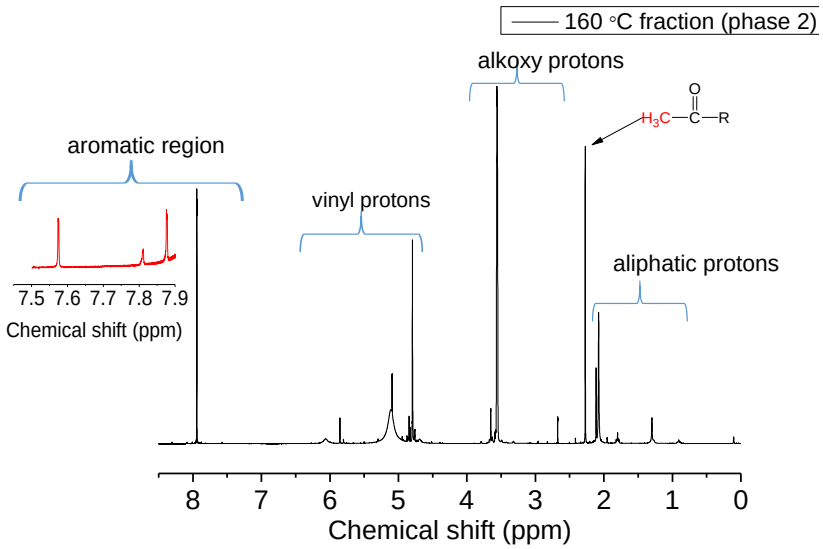

Fig. 5.12: ^{1}H NMR spectrum of the 160 °C fraction (phase 2)

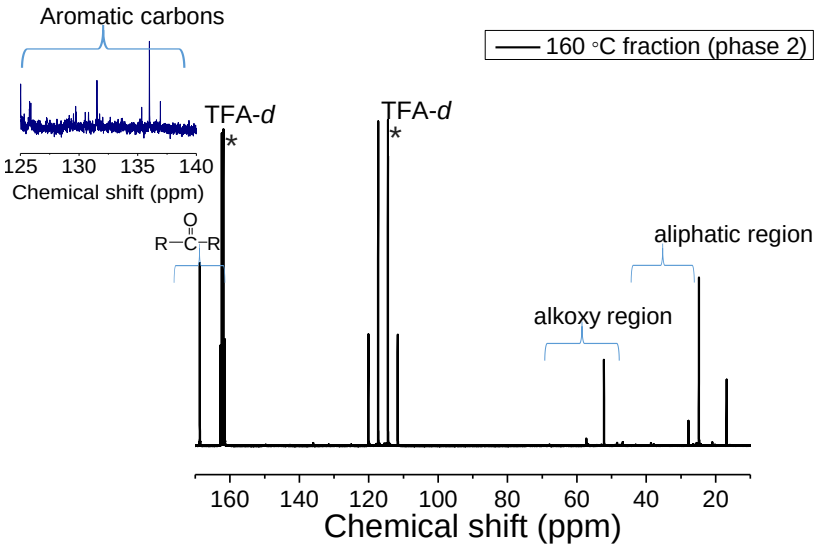

Fig. 5.13: ^{13}C NMR spectrum of the 160 °C fraction (phase 2)

5.3.3 Analysis of fraction 180 °C (phase 1)

Vanillin (V_e: 17.5 mL) and p-hydroxybenzaldehyde (V_e: 16.4 mL) were identified from the 180°C (phase 1) fraction by LC-MS in positive SIM mode. Fig 5.14 highlights the HPLC elugram showing the presence of vanillin and p-hydroxybenzaldehyde and Fig. 5.15 and 5.16 show the respective mass spectra of the deconvulated compounds (with characteristic m/z values of $[M+H]^+$). Vanillin (32.4%, by single point calibration) has a higher percentage contribution than p-hydroxybenzaldehyde (13.6%), which is typical of oxidative depolymerization reactions.[6–7]

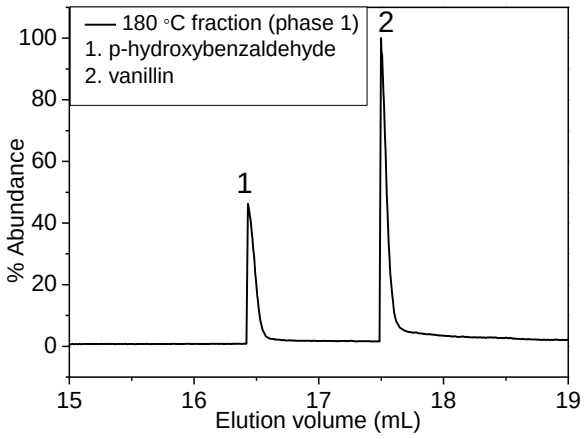

Fig. 5.14: SIM elugram of the 180°C fraction (phase 1)

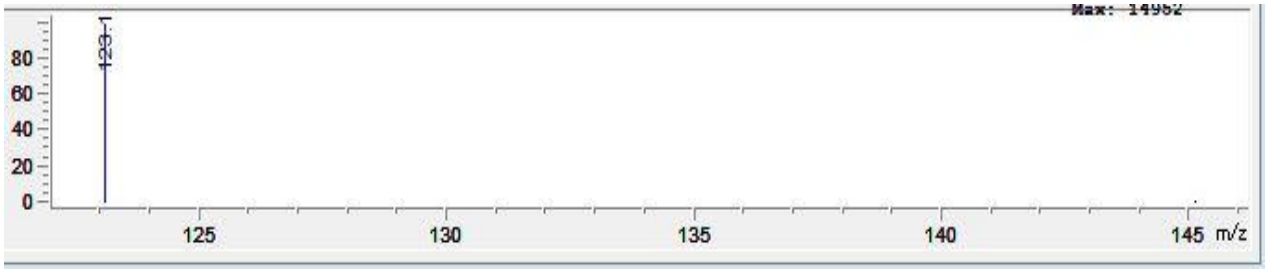

Fig. 5.15: Mass spectrum of p-hydroxybenzaldehyde with characteristic $[M+H]^+$

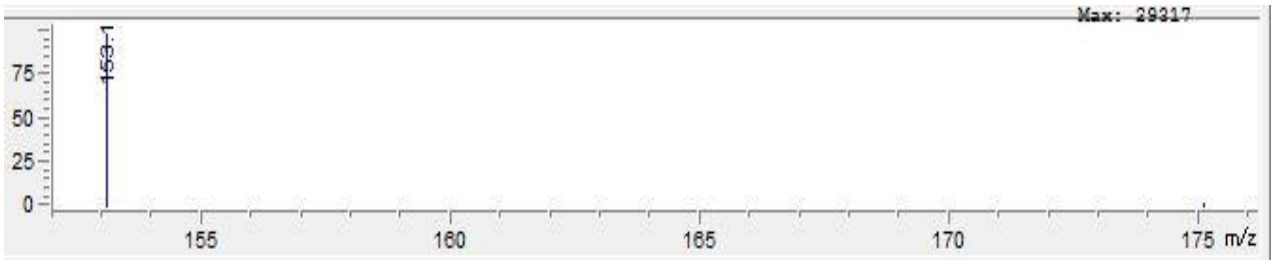

Fig. 5.16: Mass spectrum of vanillin with characteristic $[M+H]^+$

In addition to these compounds, other peaks emphasizing the presence of other compounds in the fraction were observed in the highly polar region, see Fig. 5.17, showing the HPLC-UV chromatogram. Higher m/z values of 604 and 650 at 2.3 and 4.8 mL respectively were observed when a full MS scan was conducted (see Fig. F1.3 and F1.4 for the mass spectra). The mass spectrum at 2.8 ml showed a plethora of peaks highlighting possible co-elution, see Fig. F1.2 in Appendix F). Highly polar compounds eluting between 2.3 and 4.8 mL were quantified at 63.7% by peak area, vanillin and p-hydroxybenzaldehyde were quantified at 19.6 and 16.7%, respectively.

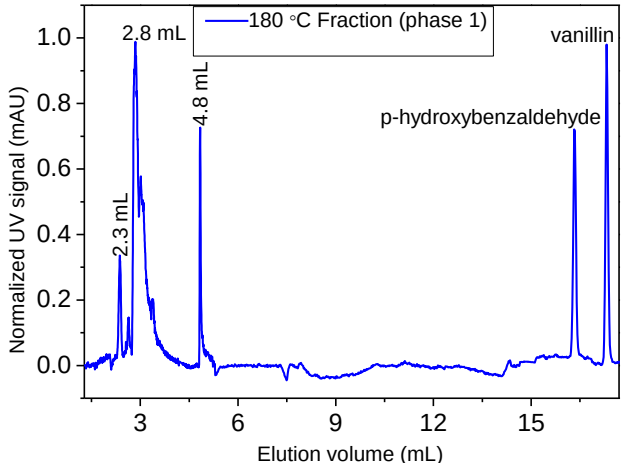

Fig. 5.17: HPLC-UV elugram of the 180 °C: fraction (phase1)

FTIR results (see Fig. 5.18) showing the following wavenumbers confirmed the presence of vanillin and p-hydroxybenzaldehyde in the fraction: 3350 cm^{-1} (phenolic hydroxyl group), 1704 cm^{-1} (C=O stretch in carbonyl functionalized compounds), 1620cm^{-1} (C=C aromatic ring stretch absorptions), 1433cm^{-1} (CH_2 bend absorptions) 1037cm^{-1} (C–O stretch in the alkoxy functionality typical of the CH_3–O moiety in vanillin).

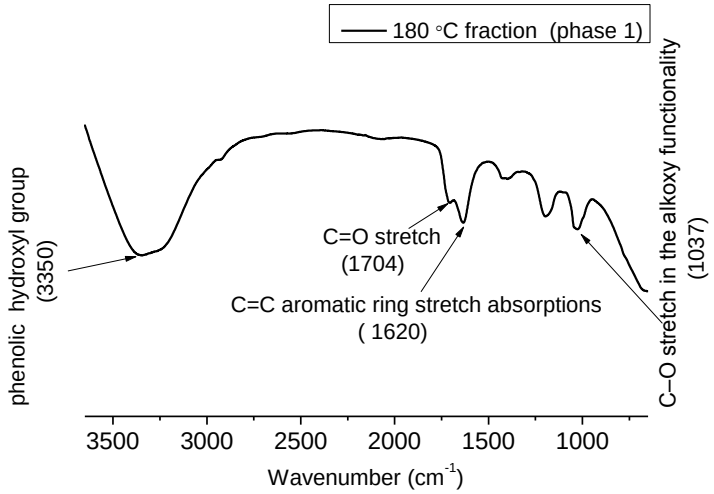

Fig. 5.18: FTIR spectrum of the 180 °C fraction (phase 1)

Both ^{1}H NMR and ^{13}C NMR were also carried out to corroborate the results with the findings of LC-MS. Solubility studies were carried out on this fraction particularly in the widely used solvents (acetone, DMSO, chloroform) but dissolved in TFA-*d* (highlighting the high polarity of the fraction). A similar deshielding effect towards high resonances (between 10–12 ppm) was observed which was earlier highlighted as due to hydrogen bonding. When carefully looking into the ^{13}C NMR spectrum (see Fig. 5.20), overlapping of the sample peaks with the solvent is observed in the aromatic region, as the quartet signals of TFA-d are predominant. Therefore, to confirm presence of aromatic signals, a careful look in the ^{1}H NMR spectrum (between 7 and 8.3 ppm) showed aromatic signals, see Fig. 5.19. These aromatic proton signals are typical of aromatic ring protons where electron withdrawing groups are attached to the ring e.g in vanillin and p-hydroxybenzaldehyde.

The formyl protons (Ar-CO-**H**) (typical of vanillin and p-hydroxybenzaldehyde) were observed at between 9.25–10 ppm. Higher resonance vinylic protons typical of 4-hydroxycinnamaldehyde and coniferaldehyde (refer to Table 4.3 for structures) are observed between 5.5 and 6.5 ppm. The signal at approximately 3.5 ppm is typical of methoxy signals,

which also in agreement with ^{13}C NMR results (alkoxy region observed between 50 and 90 ppm typical of vanillin methoxy group). The majority of the signals observed in the 140–150 °C were observed in the 180 °C fraction, signifying co-relation in functionality of the elucidated compounds.

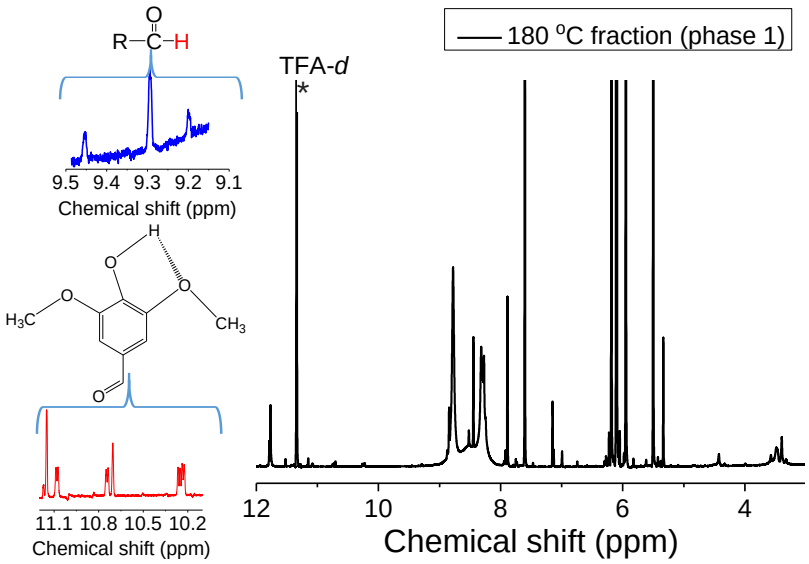

Fig. 5.19: ^{1}H-NMR spectrum of the 180 °C fraction (phase 1)

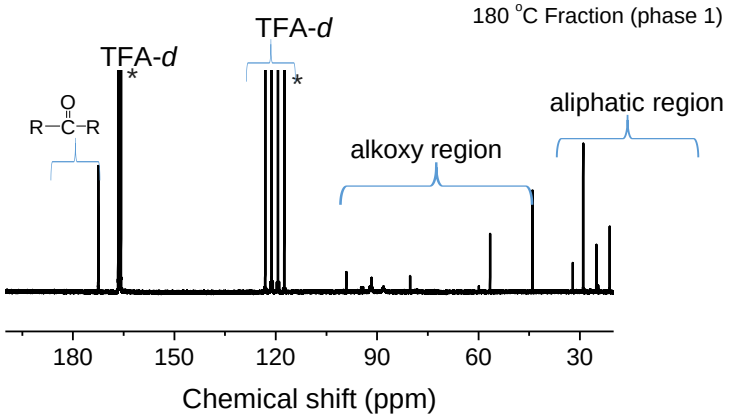

Fig. 5.20: ^{13}C NMR spectrum of the 180 °C fraction (phase 1)

5.3.4 Un-distilled fraction

Vacuum distillation was conducted up to temperatures of180 °C and the high boiling point fraction was isolated by decanting from the un-distilled fraction. Increasing temperature

beyond 180°C on the un-distilled bulk sample led to formation of solid char. The high boiling point fraction was also characterized by LC-MS in SIM mode only (see Fig. 5.21). Phloroglucinol (V_e: 10.96 mL, 5.5% by mass of injected sample) and 2,4-dihydroxybenzaldehyde (Ve: 17.15 mL, 12.3% by mass of injected sample) were identified and quantified in this fraction by single point calibration. Due to the very high boiling points of phloroglucinol and 2,4-dihydroxybenzaldehyde (343° C and 323 °C, respectively), it was challenge to isolate these by distillation as this would prompt degradation of the sample. Fig. 5.22 and 5.23 show the mass spectra of phloroglucinol and 2.4-dihydroxybenzaldehyde, respectively.

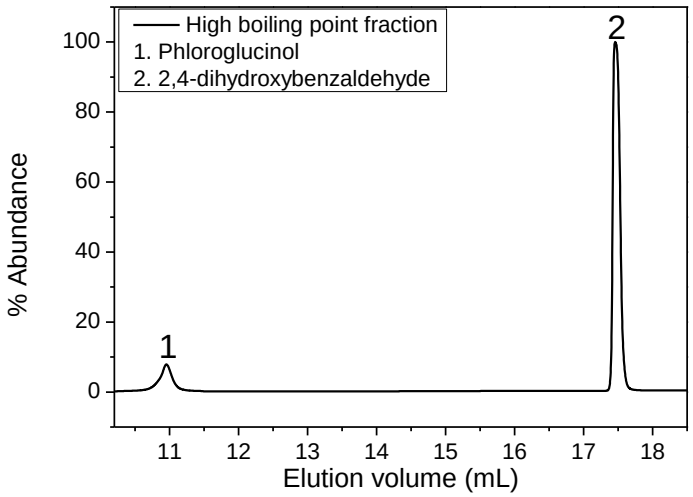

Fig. 5.21: SIM elugram of the high boiling point fraction

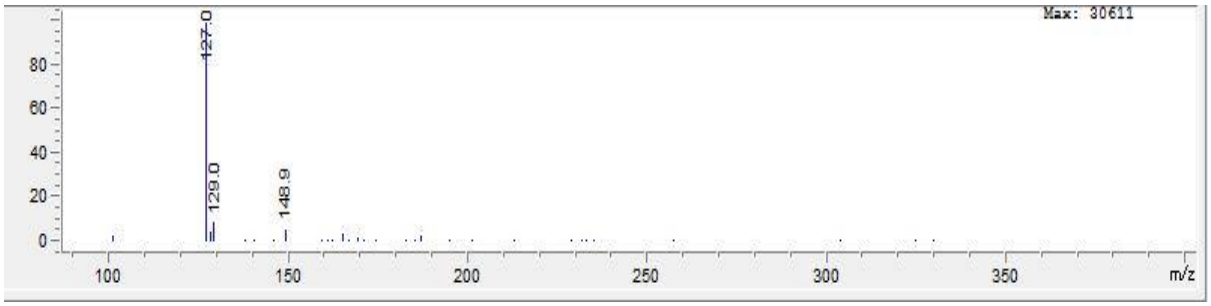

Fig. 5.22: Mass spectrum of phloroglucinol ($[M+H]^+$and $[M+Na]^+$)

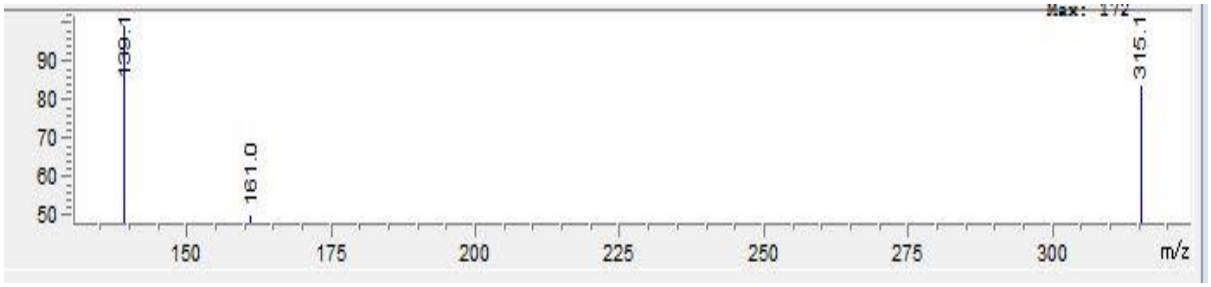

Fig. 5.23: Mass spectrum of 2,4-dihydroxybenzaldehyde ($[M+H]^+$, $[M+Na]^+$and $[M+M+K]^+$

In Chapter 4, phenol and guaiacol were qualitatively determined by LC-MS in SIM mode from the crude DMSO/HBr sample. Phenol (5.9%) and guaiacol (2.2%) were quantitatively determined from the crude DMSO/HBr in this section (see Fig. 5.24 for the SIM elugram and Fig. 5.25 and 5.26 for the mass spectra of phenol and guaiacol, respectively).

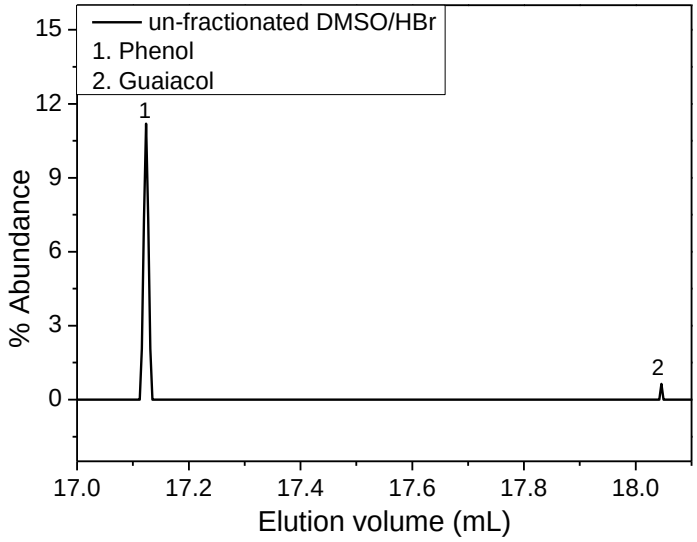

Fig. 5.24: SIM elugram of unfractionated DMSO/HBr

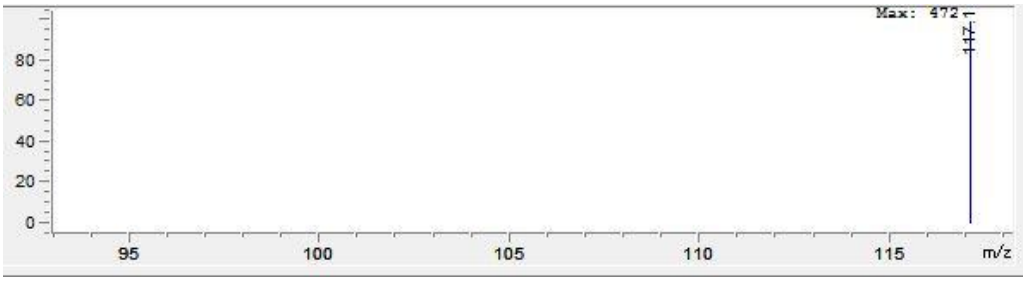

Fig. 5.25: Mass spectrum of phenol ($[M+Na]^+$)

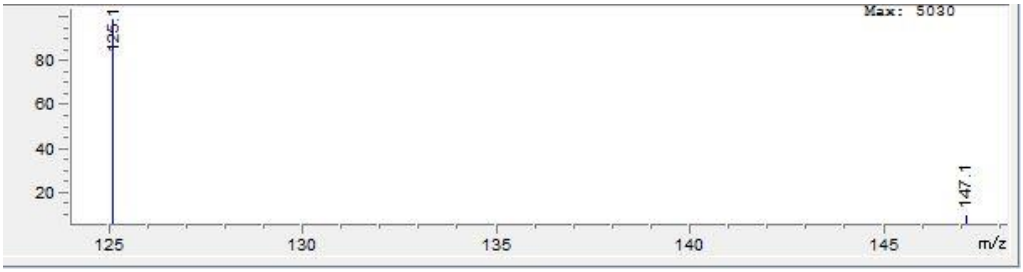

Fig. 5.26: Mass spectrum of guaiacol ($[M+H]^+$and $[M+Na]^+$)

The percentage values of the compounds quantified in each fraction by LC-MS in positive SIM mode were converted to masses per respective fraction and summarized in Table 5.3. The respective masses were summed up to give the total quantifiable monomeric count. Therefore, percentages based on the total quantifiable monomeric count for each monomer were calculated and recorded in Table 5.3.

Table 5.3: Weight % of monomeric compound per total quantifiable monomeric compounds

Quantified lignin monomeric compound	Weight (mg) by single point calibration	% of monomeric compound
Vanillin	311.0	29.5
Benzaldehyde	62.7	5.9
p-Hydroxybenzaldehyde	130.6	12.3
Syringaldehyde	304.8	28.8
Eugenol	9.2	0.9
Phloroglucinol	56.7	5.4
2,4-Dihydroxybenzaldehyde	102.1	9.6
Phenol	59.0	5.5
Guaiacol	22.0	2.1
Total quantifiable monomeric compounds	1058.1	100

Vanillin (29.5%) and syringaldehyde (28.8%) were the dominant phenolic compounds as shown in Table 5.3 and these findings were in agreement to the work by Jablonsky and co-workers who depolymerized lignin by nitrobenzene oxidation.[8, 9, 10] Vanillin was quantified at approximately 30% of the quantifiable lignin monomeric compounds by Deepa and co-workers,[3] which was in agreement with the % contribution of vanillin in the total quantifiable

monomeric compounds in this work. Phloroglucinol is not widely reported as a product of oxidative depolymerization of lignin, in this work it was quantified at approximately 5.4%.

90.7% of the native lignin that was depolymerized could be quantitatively recovered (only 23.5% of the compounds were positively analyzed). 23.5% was identified as phenolic-type compounds which included vanillin, p-hydroxybenzaldehyde, guaiacol, syringaldehyde and phloroglucinol. 67.2% of the depolymerized lignin could not be identified. Solid char was quantified at 9.3%. The following table shows the percentage by weight of monomer per weight of lignin and the quantities were compared to other oxidation reactions in literature. The monomeric quantities in this work are in agreement with other monomeric quantities per weight of lignin previously reported for other oxidative reactions, see Table 5.4.

Table 5.4: Weight % of monomeric compound per weight of lignin

Monomeric compound	% Weight of monomer per weight of lignin				
	[a] **1**	[b] **2**	[c] **3**	[d] **4**	[e] **5**
Vanillin	2.1	0.27	2.3	0.8–1.3	1.8–2.2
Benzaldehyde	0.4	–	–	–	–
p-Hydroxybenzaldehyde	0.9	–	0.28	–	0.1
Syringaldehyde	2.0	0.13	2.2	0.1–2.4	4.4–5.9
Eugenol	0.06	–	–	–	–
Phloroglucinol	0.4	–	–	–	–
2,4-Dihydroxybenzaldehyde	0.7	–	–	–	–
Phenol	0.4	–	–	–	0.03–0.2
Guaiacol	0.2	–	–	–	0.05–0.2

[a] DMSO/HBr, [b] nitrobenzene oxidation[8], [c] alkaline nitrobenzene oxidation[11], [d] H_2O_2/ microwave assisted oxidation[12], [e] nitrobenzene oxidation of Alcell lignin[13]

5.4 Conclusion

Vacuum distillation was successfully carried out for the fractionation of the complex DMSO/HBr product mixture into less complex fractions. A SIM method was successfully set-up with reference to the available pure compounds. The fractions that exhibited a positive response to the set SIM method include: 180 °C, 140–150 °C, 160 °C and high boiling point fraction (un-distilled fraction). The compounds identified and quantified in these fractions

aligned to the theoretical boiling point trends (that is from low boiling point to high boiling point fractions). Vanillin (29.5%) and syringaldehyde (28.8%) were the dominant phenolic compounds of the total quantifiable monomeric compounds. Phloroglucinol, not widely reported as a product of oxidative depolymerization of lignin, was quantified at approximately 5.4% of the total quantifiable monomeric compounds.

90.7% of the native lignin that was depolymerized could be quantitatively recovered. 23.5% was identified as phenolic-type compounds which included vanillin, p-hydroxybenzaldehyde, guaiacol, syringaldehyde and phloroglucinol. 67.2% of the depolymerized lignin could not be identified. Solid char was quantified at 9.3%. The monomeric quantities in this work are in agreement with other monomeric quantities per weight of lignin previously reported for other oxidative reactions e.g, vanillin (2.1%), syringaldehyde (2.0%) and p-hydroxybenzaldehyde (0.9%)

As highlighted by Fache and co-workers[1] it was a challenge to separate this complex product mixture into single or two component streams. Use of high distillation temperatures (>180 °C) led to the degradation of the product mixture into solid char. Less compounds than those observed from the bulk sample by GC-MS or ESI-MS were observed, but fractionation by distillation enhances the recovery of better defined materials from the obtained fractions.

5.5 References

1. Fache, M.; Boutevin, B.; Caillol, S., *Green Chemistry* **2016,** *18* (3), 712–725.

2. Stanzione III, J. F.; Giangiulio, P. A.; Sadler, J. M.; La Scala, J. J.; Wool, R. P., *American Chemical Society Sustainable Chemistry and Engineering* **2013,** *1* (4), 419–426.

3. Deepa, A. K.; Dhepe, P. L., *American Chemical Society Catalysis* **2014,** *5* (1), 365–379.

4. Stärk, K.; Taccardi, N.; Bösmann, A.; Wasserscheid, P., *ChemSusChem* **2010,** *3* (6), 719–723.

5. Lampman, G. M., Pavia, D.L, Kriz, G.S, Vyvyan, J.R, *Spectroscopy*. 4th ed.; Brooks/Cole Cengage Canada, 2010.

6. F. De Gregorio, G.; Prado, R.; Vriamont, C.; Erdocia, X.; Labidi, J.; Hallett, J. P.; Welton, T., *American Chemical Society Sustainable Chemistry & Engineering* **2016,** *4* (11), 6031–6036.

7. Di Marino, D.; Stöckmann, D.; Kriescher, S.; Stiefel, S.; Wessling, M., *Green Chemistry* **2016,** *18* (22), 6021–6028.

8. Jablonsky, M.; Haz, A.; Škulcova, A.; Dubinyova, L.; Šurina, I.; Kacik, F.; Kacikova, D., *Cellulose Chemistry & Technology* **2016,** *50* (7–8), 731–735.

9. Tarabanko, V. E.; Tarabanko, N., *International Journal of Molecular Sciences* **2017,** *18* (11), 1–29.

10. Leopold, B.; Malmstrom, I., *Acta Chem. Scand* **1952,** *6* (1), 49–54.

11. Sun, R.; Lawther, J. M.; Banks, W., *Industrial Crops and Products* **1995,** *4* (4), 241–254.

12. Gu, X.; Kanghua, C.; Ming, H.; Shi, Y.; Li, Z., *Maderas. Ciencia y tecnologia* **2012,** *14* (1), 31–41.

13. Hepditch, M. M.; Thring, R. K., *The Canadian Journal of Chemical Engineering* **1997,** *75* (6), 1108–1114.

Chapter 6

Functionalization of lignin monomeric compounds for polymerization (preliminary experiments for future work)

6.1 Introduction

The depolymerization of lignin by DMSO/HBr produced varying amounts of a wide array of functionalized aromatic compounds, namely hydroxybenzaldehyde, vanillin, 4-hydroxycinnamaldehyde, syringaldehyde and methylguaiacol that mimic common synthetic monomers which include bisphenol A and styrene, which are essential for polymer applications.[1–2] These natural compounds can be employed in the synthesis of new bio-based polymers with novel properties that are suitable for various applications. Due to a wide range of functional groups in the depolymerized products of lignin, different avenues of functionalization of these monomeric compounds can be explored for different types of polymerization reactions which include polycondensation reactions (for example bimolecular reactions) and radical polymerization reactions. [3]

In this chapter we focused on the functionalization of lignin monomeric compounds for conventional radical polymerization. The principle of radical polymerization is based on the presence of a vinyl group. Since most of the compounds produced by the depolymerization of lignin in this study are not vinyl-functionalized, the vinyl group has to be introduced. Some research has been carried out focusing on the modification of lignin model monomer compounds using methacrylic anhydride (non-renewable material) or methacryloyl chloride, both of which are derived from non-renewable feedstocks. This study focuses on preliminary results where itaconic anhydride (3-methylideneoxolane-2,5-dione) was used to modify lignin model monomeric compounds, and lignin depolymerization products to give fully bio-based monomers. Itaconic anhydride is produced from the fermentation of carbohydrates forming itaconic acid followed by dehydration to form the anhydride.[4]

6.2 Experimental

Materials

Guaiacol (natural ≥99%, Sigma Aldrich, Hong Kong, China), Tin octoate (≈95%, Sigma Aldrich, St. Louis USA), itaconic anhydride (95%, Sigma Aldrich, St. Louis USA), 1,4-dioxane (HPLC ≥99.8%, Merck KGaA, Darmstadt, Germany), chloroform (HPLC ≥99.8%, Sigma Aldrich, St. Louis USA), Hexane (HPLC ≥97%, Sigma Aldrich, St. Louis USA), N,N-dimethylacetamide (HPLC ≥99.8%, Sigma Aldrich, St. Louis USA), acetone-d6 (≥99.9% NMR, Merck, KGaA, Darmstadt, Germany), dimethyl sulfoxide-d6, (99.8% NMR, Merck, KGaA, Darmstadt, Germany) was used as received.

6.2.1 Functionalization of guaiacol by itaconic anhydride

A mixture of itaconic anhydride (1.0 g, 8.9×10^{-3} moles), guaiacol (1 mL, 8.9×10^{-3} moles), with tin octoate catalyst (0.073 g, 1.8×10^{-4} moles) in 5 mL of 1,4-dioxane solvent in a 50 mL reaction flask coupled with a refluxing cooler was reacted at 80 °C for 3 hours under argon. The reaction was stopped by cooling to room temperature. The reaction mixture was dissolved in chloroform, washed with 1N hydrochloric acid to remove the catalyst. The product which had two isomers and unmodified guaiacol still present was dried under vacuum. Yield: 80%, functionality: 70%.

ESI-MS (molar mass determination): theoretical molecular mass (*Mr*) = 236 g/mol, m/z values: 237 ($[M+H]^+$), 259 ($[M+Na]^+$), 275 ($[M+K]^+$) (see appendix H for spectrum)

^{13}C NMR ([Acetone-d_6)]: chemical shifts (δ in ppm) = 171.33, 168.42, 151.11, 140.19, 134.44, 128.19, 126.79, 122.72, 121.12, 115.03, 55.32, 36.84 (same resonance signals were observed for both isomers formed, see Appendix H for the spectrum)

^{1}H-NMR: ([Acetone-d_6)]: chemical shifts (δ in ppm): Isomer A, 7.3–6.75 (bm, 4H), 6.48 (s, 1H), 5.96 (s, 1H), 3.80 (s, 3H); Isomer B, 7.3–6.75 (bm, 4H), 6.35 (s, 1H), 5.92(s, 1H), 3.80 (s, 3H), Guaiacol, 6.96–6.75 (bm, 4H), 3.8 (s, 3H)

6.2.2 Functionalization of DMSO/HBr product mixture by itaconic anhydride

A mixture of itaconic anhydride (1.0 g, 8.9×10^{-3} moles), DMSO/HBr product mixture (0.5 g), with tin octoate catalyst (0.1 g, 2.5×10^{-4} moles) in 5 mL of 1,4-dioxane solvent in a 50 mL

reaction flask coupled with a refluxing cooler was reacted at 80 °C for 3 hours under argon. The reaction was stopped by cooling to room temperature. The reaction mixture was allowed to dissolve in chloroform. The product was isolated by drying under reduced pressure.

6.2.3 Polymerization of functionalized guaiacol

A dry Schlenk flask was charged with functionalized guaiacol (1 g, 4.23×10^{-3} moles), AIBN (14.2 mg, 8.65×10^{-5} moles) and 5 mL of 1,4-dioxane solvent and a magnetic stirrer bar was added. The mixture was thoroughly degassed by multiple successive freeze pump thaw cycles, backfilled with nitrogen, sealed and immersed into an oil bath preheated and thermostated at 70 °C. The reaction was stopped after stirring for 24 hours by opening the flask to allow termination of radicals by oxygen. The slightly viscous polymer was dissolved in chloroform and the solution poured into n-hexane to precipitate the polymer. The polymer was centrifuged and dried under vacuum. Conversion was determined gravimetrically.

6.2.4 Analyses

6.2.4.1 ^{1}H NMR analysis

All ^{1}H NMR spectra were acquired using a Varian VNMRS 400 MHz spectrometer. The chemical shifts are reported in parts per million (ppm) in deuterated acetone and deuterated dimethyl sulfoxide with tetramethylsilane (TMS) as a reference.

6.2.4.2 ESI-MS analysis

The experimental procedure was described in section 4.2.3 in Chapter 4.

6.2.4.3 SEC analysis

An Agilent 1200 HPLC instrument (Agilent Technologies, Waldbronn, Germany) comprising the following: autosampler, on-line degasser, quaternary pump unit and a thermostated column compartment set to 40 °C was used. The detectors used were: Agilent VWD ultraviolet (UV) detector at a UV wavelength of 277 nm and RI detector at 40 °C. Three 10 µm GRAM columns (with polyester copolymer as a stationary phase) with porosities of 100 Å and 3 000 Å and a 10 µm guard column were used. The eluent system used was DMAc (HPLC grade, BHT stabilized, with LiCl salt) at a flowrate of 0.8 mL/min. Calibration was carried out using narrow dispersed poly(methyl methacrylate) (Polymer Standards Service (PSS), Mainz, Germany) with peak maximum molecular weights (M_p) ranging between 800 g/mol and 2 200 000 g/mol.

Therefore, the SEC data obtained are reported as PMMA equivalents. PSS WinGPC Unichrom 8.2 software was used to acquire and process the data.

6.2.4.4 FTIR analysis

The experimental procedure was described in Section 4.2.1 in Chapter 4.

6.3 Results and discussion

6.3.1 Functionalization of guaiacol

Pure guaiacol was functionalized for the first time by itaconic anhydride in the presence of a catalytic amount of tin octoate at a temperature of 80 °C, see Scheme 6.1. No work has been reported on the functionalization of lignin monomeric compounds by itaconic anhydride. The method was adopted from Okuda and co-workers who synthesized itaconic anhydride-based copolymers with poly ($_L$-lactic acid) grafts.[5]

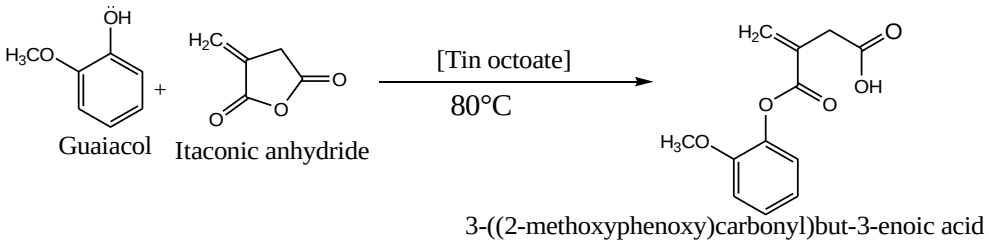

Guaiacol Itaconic anhydride 3-((2-methoxyphenoxy)carbonyl)but-3-enoic acid

Scheme 6.1: Reaction scheme of itaconic anhydride and guaiacol

The reaction between guaiacol and itaconic anhydride proceeded via an esterification reaction shown in Scheme 6.1 to form two isomers (3-((2-methoxyphenoxy)carbonyl)but-3-enoic acid and 4-(2-methoxyphenoxy)-2-methylene-4-oxobutanoic acid). To our best knowledge, itaconic anhydride has not been employed for the functionalization of lignin monomeric compounds, therefore, the proposed mechanism utilizes the reactive nature of itaconic anhydride of ring opening in an esterification reaction. The phenolic oxygen atom acts a nucleophile to attack the electrophilic carbon atom to form an intermediate alkoxide (1a), see Scheme 6.2. The redistribution of electrons induces ring opening to form intermediate 1b. The negatively charged oxygen formed as a result of ring opening, abstracts a proton from the electron-deficient oxygen within the molecule to form modified guaiacol (1c), see Scheme 6.2. The functionalization of pure guaiacol was used as a template for the modification of the

DMSO/HBr product mixture. DMSO/HBr was functionalized via the same conditions (outlined in the experimental section) used for the functionalization of pure guaiacol.

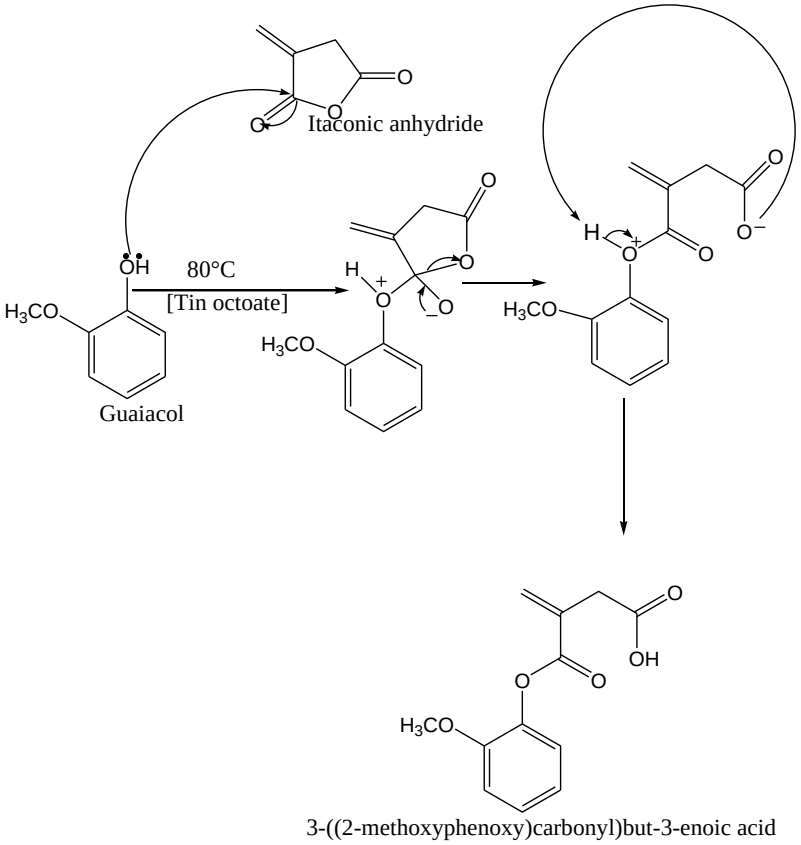

Scheme 6.2: Reaction mechanism of guaiacol and itaconic anhydride

6.3.1.1 ^{1}H NMR analysis of functionalized guaiacol

^{1}H NMR elucidated the formation of two isomers (3-((2-methoxyphenoxy)carbonyl)but-3-enoic acid and 4-(2-methoxyphenoxy)-2-methylene-4-oxobutanoic acid) upon the reaction of guaiacol and itaconic anhydride in the presence of tin octoate as catalyst, as can be observed at the alkene region of the ^{1}H NMR spectrum (see Fig. 6.1). This was elucidated by the resonance signals in the alkene region (5.7–6.5 ppm) which were typical isomeric signals. The vinyl protons directly attached to the double bond in isomer A (4-(2-methoxyphenoxy)-2-methylene-4-oxobutanoic acid) are more deshielded compared to those in isomer B (3-((2-methoxyphenoxy)carbonyl)but-3-enoic acid). This is because the vinyl protons in isomer A are α to the carboxylic group (highly electron withdrawing group) compared to the vinyl protons in isomer B which are β to the carboxylic group. The resonance at approximately 3.5 ppm is typical of ester protons, which further confirms a successful modification reaction by esterification. The resonance signals observed between 6.5 and 7.5 ppm are due to the presence

of aromatic protons. The methoxy proton resonance is observed at a resonance of approximately 3.8 ppm.

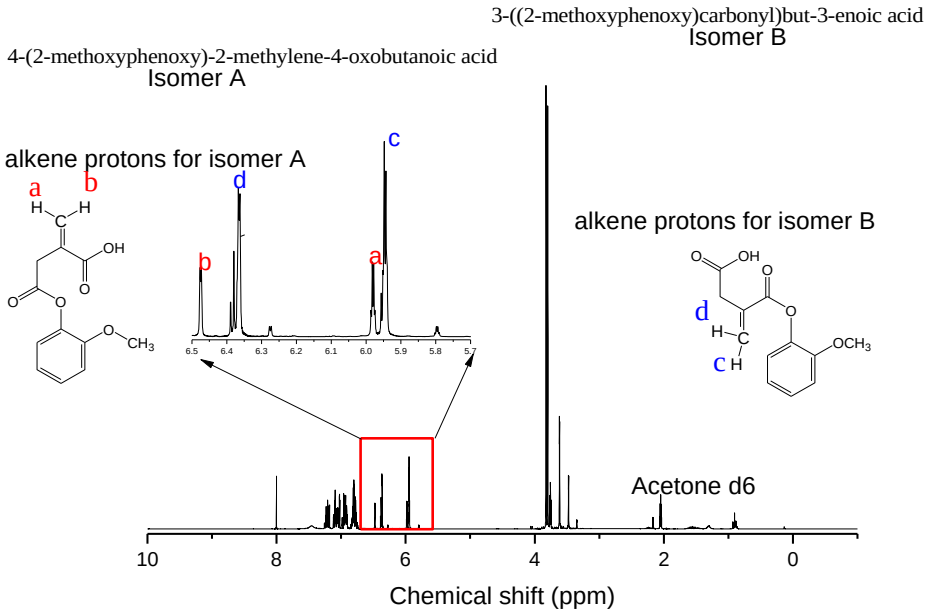

Fig. 6.1: ^{1}H-NMR spectrum of functionalized guaiacol

6.3.1.2 FTIR analysis of functionalized guaiacol

FTIR also helped to corroborate the functionalization of guaiacol by itaconic anhydride. The disappearance of the intense peak around 3470 cm^{-1} in guaiacol indicates the transformation of –OH groups to the ester groups. The intense peak observed in the –C=O stretch (1710 cm^{-1}) due to ester formation also served as an indicator for successful modification of guaiacol by itaconic anhydride (see Fig. 6.2). The appearance of vinyl bending at 652 cm^{-1} accustomed to vinyl groups further ascertained the successful attachment of the vinyl group during functionalization.[6–7]

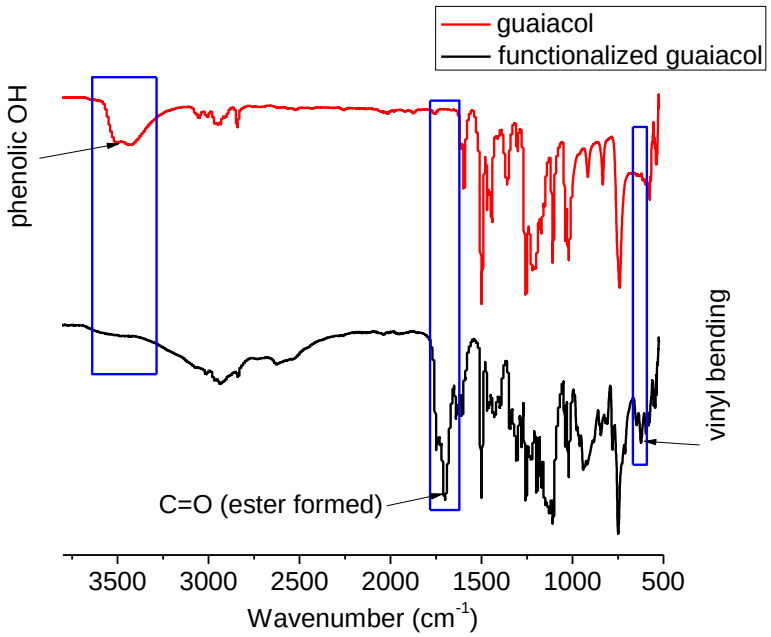

Fig. 6.2: FTIR spectrum of functionalized guaiacol

6.3.1.3 Determination of molar mass of functionalized guaiacol by ESI-MS

Positive ESI-MS was used to confirm the formation of the modified guaiacol by determining its molar mass and typical m/z values of the following adducts were observed $[M+H]^+$, $[M+Na]^+$ and $[M+K]^+$ (see Fig. H1.1 in Appendix H). From the observed m/z values highlighted in section 6.2.1, it was concluded that the molar mass of functionalized guaiacol was 236 g/mol which was in agreement with the expected theoretical value.

6.3.2 Polymerization of functionalized guaiacol by conventional radical polymerization

The vinyl-modified guaiacol was polymerised via radical polymerization using AIBN as the initiator and 1,4-dioxane as the solvent. The conversion was determined gravimetrically and was calculated to be 33%. The crude product was analyzed by ^{1}H NMR. The broad peaks observed in the ^{1}H NMR spectrum typical of polymers confirmed the formation of polymer by conventional radical polymerization. The resonance signals between 0.8 and 2.5 ppm are typical of the protons due to alkane groups (saturated polymer chains) due to the conversion of unsaturated aliphatic chains (alkenes) to saturated aliphatic chains. The resonance signals observed between 5.92 and 6.48 ppm in the spectrum highlighted the presence of residual

monomer, see Fig. 6.3. The ratio of the aromatic to vinyl protons for polymer and monomer is 8 to 1.

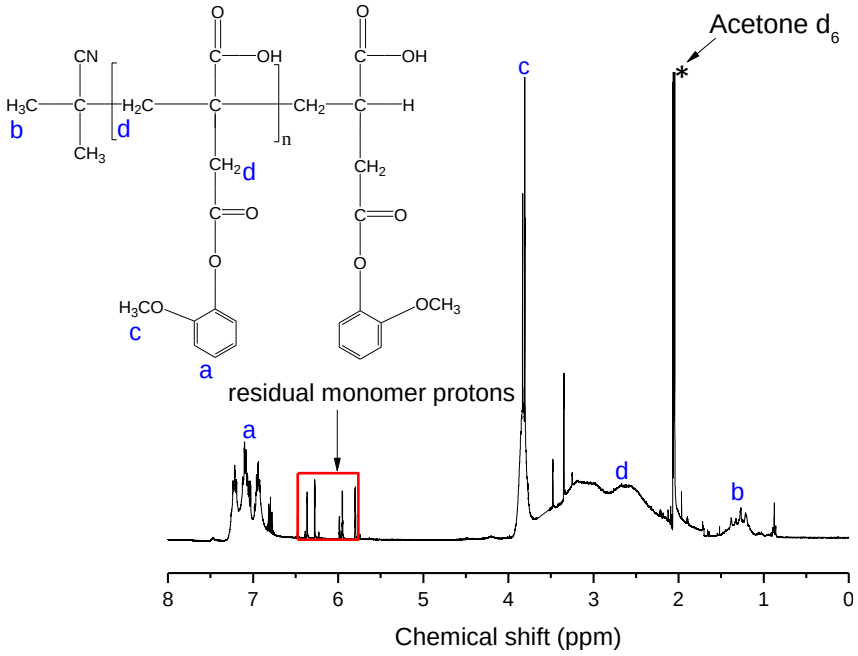

Fig. 6.3: ^{1}H-NMR spectrum of crude poly(guaiacyl itaconic acid)

Molar mass determination of the poly(guaiacyl itaconic acid) was carried out via SEC using conventional calibration. M_n was calculated as 3 400 g/mol which was in agreement with the theoretical molar mass at a conversion of 33%. A bimodal distribution (see Fig. 6.4) was observed due to possible bimolecular termination reactions, with termination by combination being predominant, as can be seen from the M_p values (2 700 and 5 350 g/mol) of the respective peaks.

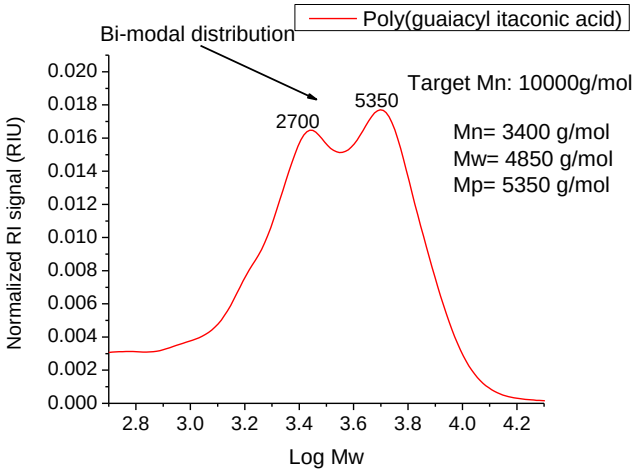

Fig. 6.4: Molar mass distribution of poly(guaiacyl itaconic acid)

6.3.3 Functionalization of the DMSO/HBr by itaconic anhydride

Separating complex mixtures of depolymerized products of lignin into single or two-component streams has been reported to be a challenge thus far. Therefore, in this study, the bulk DMSO/HBr product mixture was used to exploit the molecular diversity of the complex mixture in pursuit of synthesizing heteropolymers.[8]

The modification of pure guaiacol was used as a template for the modification of DMSO/HBr. The crude modified DMSO/HBr product mixture did not behave the same way as its template. Under the same reaction conditions, a polymer was formed within the crude modified DMSO/HBr as confirmed by the presence of broad ^{1}H NMR peaks (which are not observed in the unmodified DMSO/HBr spectrum, see Fig. 6.6) typical of polymers. This possibly signalled the occurrence of side reactions during the modification reaction attributed to bimolecular reactions.

However, typical isomeric signals in the alkene region (5.6–6.5 ppm) of the spectra were also observed to indicate successful modification, see Fig. 6.5. Compared to the unmodified DMSO/HBr spectrum, the vinyl protons of the modified DMSO/HBr are more deshielded because they are possibly attached to carbons bonded to electron withdrawing groups after the ring opening reaction of the itaconic anhydride with the hydroxyl groups of the depolymerized product mixture. The resonance at approximately 3.6 ppm is typical of ester protons which further confirms a successful modification reaction by esterification.

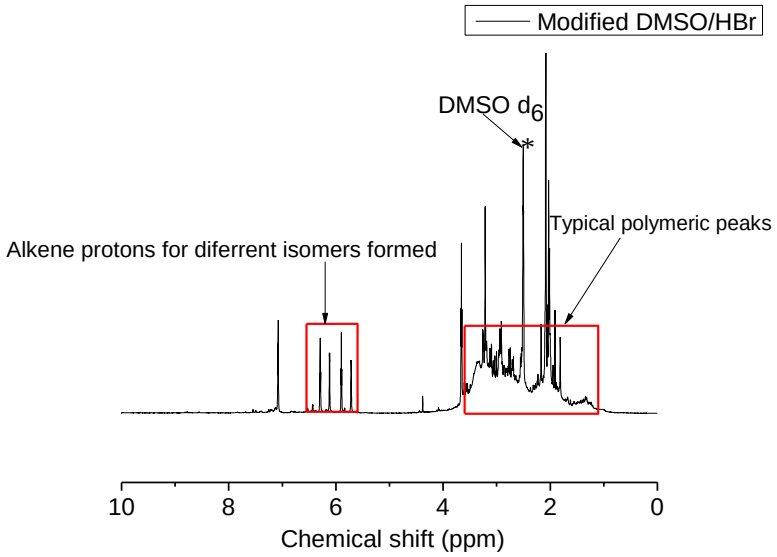

Fig. 6.5: ^{1}H-NMR spectrum of modified DMSO/HBr

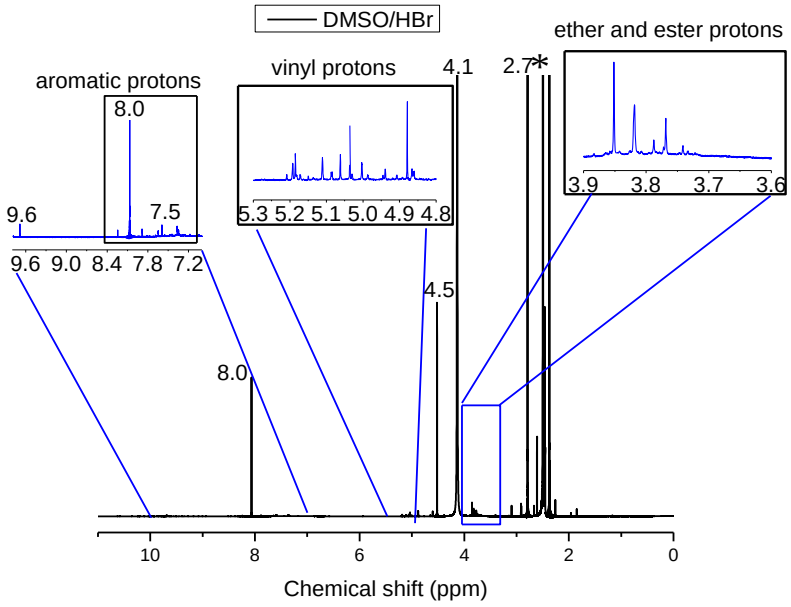

Fig. 6.6: ^{1}H-NMR spectrum of unmodified DMSO/HBr

6.4 Conclusion

Modification of guaiacol by itaconic anhydride (renewable anhydride) was successful producing two new fully bio-based isomeric monomers which are (3-((2-methoxyphenoxy)carbonyl)but-3-enoic acid and 4-(2-methoxyphenoxy)-2-methylene-4-oxobutanoic acid. The yield for the reaction was 80% and the degree of functionalisation 70%.

Although ESI-MS confirmed the formation of the desired product, additional 2D NMR experiments will be required to conclusively assign the different signals from the two isomers.

Vinyl-modified guaiacol was successfully polymerized by conventional radical polymerization as shown by the broad peaks in the ^{1}H NMR spectrum and a number average molar mass of 3 400 g/mol was determined by SEC. To improve or have control of the molar masses and other parameters such as composition, molar mass dispersity and chain architecture, reversible deactivation radical polymerization (RDRP) is a recommendation.

The modification of the crude DMSO/HBr reaction product showed traits of the formation of a polymeric species during modification as shown in Fig. 6.6 and this was attributed to the occurrence of side reactions during modification due to the presence of other functional groups that react under the same reaction conditions during modification. However, typical isomeric signals in the alkene region (5.6–6.5 ppm) of the spectra were also observed to indicate successful modification. To address the issue of side reactions, the use of other polymerization techniques as an alternative to radical polymerization can be investigated for example poly condensation since the DMSO/HBr product mixture is highly –OH functionalized. The use of less complex fractions obtained by vacuum distillation of DMSO/HBr discussed in Chapter 5 can also be used as an antidote for possible complex side reactions that occur during modification of the bulk complex depolymerized product mixture.

6.5 References

1. Stanzione, J. F.; Sadler, J. M.; La Scala, J. J.; Wool, R. P., *ChemSusChem* **2012,** *5* (7), 1291–1297.

2. Stanzione III, J. F.; Giangiulio, P. A.; Sadler, J. M.; La Scala, J. J.; Wool, R. P., *ACS Sustainable Chemistry and Engineering* **2013,** *1* (4), 419–426.

3. Mialon, L.; Pemba, A. G.; Miller, S. A., *Green Chemistry* **2010,** *12* (10), 1704–1706.

4. Carlsson, M.; Habenicht, C.; Kam, L. C.; Antal, M. J. J.; Bian, N.; Cunningham, R. J.; Jones, M. J., *Industrial and Engineering Chemistry Research* **1994,** *33* (8), 1989–1996.

5. Okuda, T.; Ishimoto, K.; Ohara, H.; Kobayashi, S., *Macromolecules* **2012,** *45* (10), 4166–4174.

6. Zhou, J.; Zhang, H.; Deng, J.; Wu, Y., *Macromolecular Chemistry and Physics* **2016,** *217* (21), 2402–2408.

7. Zhang, C.; Madbouly, S. A.; Kessler, M. R., *Macromolecular Chemistry and Physics* **2015,** *216* (17), 1816–1822.

8. Fache, M.; Boutevin, B.; Caillol, S., *Green Chemistry* **2016,** *18* (3), 712–725.

Chapter 7

Conclusions and recommendations

7.1 Summary

A method for oxidatively depolymerizing lignin into low molar mass compounds using mild oxidizing agents was developed and optimized. A novel DMSO/HBr oxidative depolymerization approach was used to depolymerize technical lignins (Kraft lignin and SAPPI lignosulfonate) into low molar mass compounds. The mechanism of this approach was proposed and discussed. Since there is not much information in published literature focusing on the oxidative depolymerization of lignin using DMSO as the oxidant, other well established oxidative depolymerization methods were carried out in this work for comparison (oxidative depolymerization using nitrobenzene and oxidative depolymerization in ionic liquid (1-ethyl-3-methylimidazolium trifluoromethanesulfonate) and water using oxygen as an oxidant). SEC subsequently confirmed the successful depolymerization of technical lignins by DMSO/HBr reaction and nitrobenzene oxidation as there was a considerable shift from high molar masses to low molar masses.

SEC only provided molar mass information on the respective bulk product mixtures. Therefore, to get more information, that is, chemical functionality and structural information with regard to the depolymerized products, advanced analytical techniques were employed. Separation techniques to deconvolute the monomeric and oligomeric compounds according to chemical functionality (using liquid or gas chromatography coupled to suitable detectors e.g. mass spectrometry (MS)) and structural elucidation techniques (ESI-MS, NMR spectroscopy, FTIR spectroscopy) further confirmed the successful depolymerization of lignin by DMSO/HBr and nitrobenzene. GC-MS and LC-MS results showed the presence of carbonyl-functionalized aromatic compounds in the bulk product mixtures and these results were in agreement with FTIR, NMR and ESI-MS results. The presence of carbonyl-functionalized compounds confirmed the successful oxidative depolymerization. [1]

The analysis of the DMSO/HBr product mixture by LC-MS showed possible overlapping and the challenges of full scan analysis were highlighted especially due to ionization suppression of certain compounds in the sample matrix, therefore, quantitative analysis of the monomeric compounds was a challenge. Vacuum distillation was, therefore, carried out in order to

fractionate the complex DMSO/HBr product mixture into less complex fractions in pursuit of quantitatively determining the amounts of the lignin monomeric compounds produced during depolymerization by DMSO/HBr. To reduce ionization suppression and low sensitivity issues in mass spectrometry, LC-MS in positive SIM mode was carried out on all fractions obtained by vacuum distillation. The distilled fractions that exhibited positive responses to the lignin monomer standards set in the SIM method include fractions obtained at distillation temperatures of 140–150 °C (phase 1), 160 °C (phase 2), 180 °C (phase 1) and the un-distilled fraction and they were successfully elucidated. The compounds identified and quantified in these fractions aligned to the theoretical boiling point trends (that is from low boiling point to high boiling point fractions). 90.7% of the native lignin that was depolymerized could be quantitatively recovered (only 23.5% of the compounds were positively analyzed). 23.5% was identified as phenolic-type compounds which included vanillin, p-hydroxybenzaldehyde, syringaldehyde and phloroglucinol. 67.2% of the depolymerized lignin could not be identified. Solid char was quantified at 9.3%. The monomeric quantities in this work are in agreement with other monomeric quantities per weight of lignin previously reported for other oxidative reactions e.g, vanillin (2.1%), syringaldehyde (2.0%) and p-hydroxybenzaldehyde (0.9%).

A novel fully bio-based monomer for radical polymerization was successfully synthesized by the reaction of itaconic anhydride and guaiacol via an esterification reaction as preliminary experiment for future work. The resultant monomer was polymerized by conventional radical polymerization (33% conversion by gravimetric analysis). M_n was determined as 3 400 g/mol which was agreement with the conversion of 33%. The modification of the bulk DMSO/HBr sample was used as a template for the modification of the bulk DMSO/HBr sample. A polymeric species was produced during modification.

7.2 Conclusions

A novel DMSO/HBr oxidative depolymerization approach was successfully developed and optimized to depolymerize technical lignins (Kraft lignin and SAPPI lignosulfonate) into low molar mass compounds. SAPPI lignosulfonate depolymerization by DMSO/HBr was used as a validation method to emphasize that the novel DMSO/HBr approach can be successfully employed on lignin from different sources. There was no evidence of repolymerization when this approach was used, which is normally one of the shortcomings of the reported techniques of lignin depolymerization.

The conversion of 46.3% when using the DMSO/HBr approach was in agreement with literature values and also in agreement with nitrobenzene reaction carried out in this study. [2, 3] A plethora of carbonyl functionalized compounds, which is typical of successful oxidative depolymerization was produced as elucidated by LC-MS, GC-MS, FTIR, ESI-MS and NMR.

Vanillin (29.5%) and syringaldehyde (28.8%) were the dominant phenolic compounds of the total quantifiable monomeric compounds (typical of oxidative depolymerization).[4–5] Phloroglucinol, not widely reported as a product of oxidative depolymerization of lignin, was quantified at approximately 5.4%.

Modification of guaiacol by itaconic anhydride (renewable anhydride) was successful producing two new fully bio-based isomeric monomers which are (3-((2-methoxyphenoxy)carbonyl)but-3-enoic acid and 4-(2-methoxyphenoxy)-2-methylene-4-oxobutanoic acid. Vinyl-modified guaiacol was successfully polymerized by conventional radical polymerization and a number average molar mass of 3 400 g/mol was determined by SEC. The modification of DMSO/HBr showed traits of the formation of a polymeric species during modification and this was attributed to the occurrence of bimolecular reactions during modification due to the presence of other functional groups which react under the same reaction conditions during modification.

7.3 Challenges and Recommendations

The lack of calibration standards with structural similarity to lignin impaired the accuracy of the molar masses that were determined by SEC especially with regard to SAPPI lignosulfonate. Lignin is a hyperbranched polymer, in contrast to linear pullulan standards that were used and possible differences in hydrodynamic volumes made molar mass calculation relative. Therefore, the use of MALLS for absolute molar mass determination can be explored.

The use of individual compounds from a depolymerized mixture is a challenge from a separation technology point of view. A potential way forward is to optimize isolation techniques like vacuum distillation and column chromatography to isolate these lignin monomeric compounds in their purest form and in good yields.

Although the assignment of the vinyl protons of the two isomeric compounds was straightforward, additional 2D NMR experiments would be required to conclusively assign the remaining signals. Polymerization of lignin monomeric compounds modified by itaconic

anhydride through reversible deactivation radical polymerization (RDRP) is a recommendation. RAFT or RITP can be explored in pursuit of synthesizing well-defined functional polymers.

7.4 References

1. Gao, R.; Li, Y.; Kim, H.; Mobley, J. K.; Ralph, J., *ChemSusChem* **2018,** *11* (13), 2045–2050.

2. Stärk, K.; Taccardi, N.; Bösmann, A.; Wasserscheid, P., *ChemSusChem* **2010,** *3* (6), 719–723.

3. Sun, Z.; Fridrich, B. l.; de Santi, A.; Elangovan, S.; Barta, K., *Chemical Reviews* **2018,** *118* (2), 614–678.

4. F. De Gregorio, G.; Prado, R.; Vriamont, C.; Erdocia, X.; Labidi, J.; Hallett, J. P.; Welton, T., *ACS Sustainable Chemistry and Engineering* **2016,** *4* (11), 6031–6036.

5. Di Marino, D.; Stöckmann, D.; Kriescher, S.; Stiefel, S.; Wessling, M., *Green Chemistry* **2016,** *18* (22), 6021–6028.

Appendix A

SEC elugrams highlighting effect of reaction time on the reaction for oxidative depolymerization by DMSO/HBr

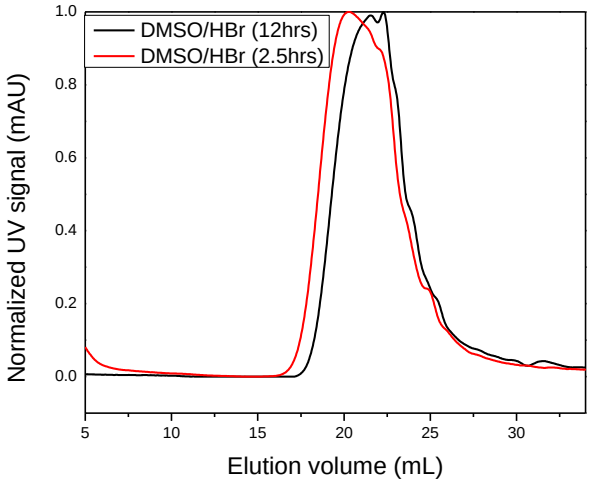

Fig. A1.1: SEC elugrams highlighting effect of residence time on the reaction

Appendix B

FTIR analysis of SAPPI lignosulfonate vs SAPPI DMSO/HBr

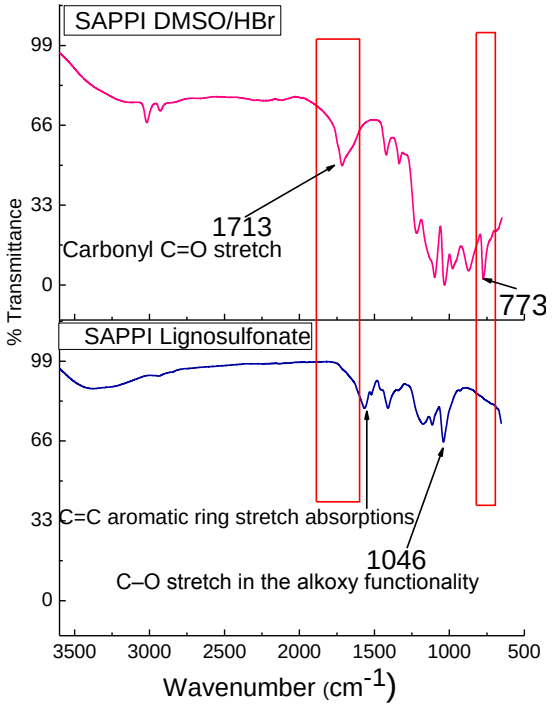

Fig. B1.1: FTIR spectrum of SAPPI lignosulfonate and SAPPI DMSO/HBr

Table B1.1: FTIR analysis of SAPPI lignosulfonate and SAPPI DMSO/HBr

Wavenumber (cm^{-1})	Elucidated information
3402–3354	Phenolic and aliphatic -OH
3000–2850	Alkane–CH stretch
2905	Aldehyde –CH stretch
1713	Conjugated –C=O (carbonyl functional group)
1575–1450	C=C aromatic ring stretch absorptions
1046–1030	C-O stretch in the alkoxy functionality
773	Para-substituted ring with out of plane bending vibrations

Appendix C

^{1}H NMR analysis of SAPPI lignosulfonate and SAPPI DMSO/HBr product mixture

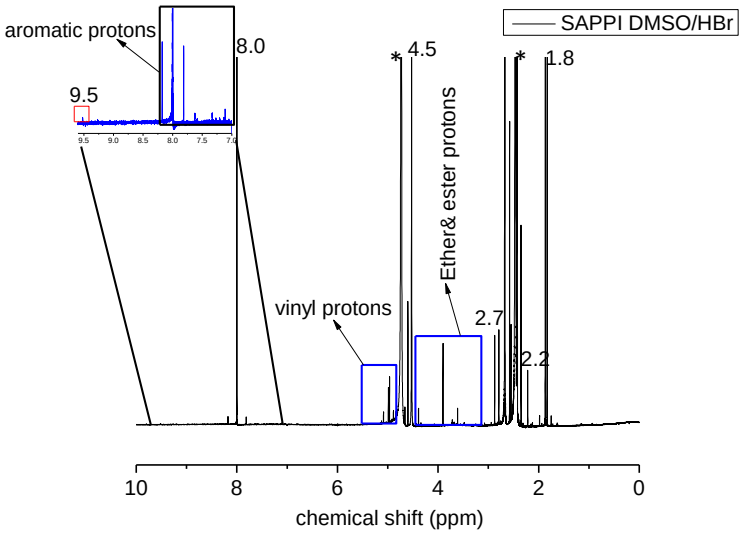

Fig. C1.1: ^{1}H NMR spectrum of the depolymerized products of SAPPI lignosulfonate (SAPPI DMSO/HBr)

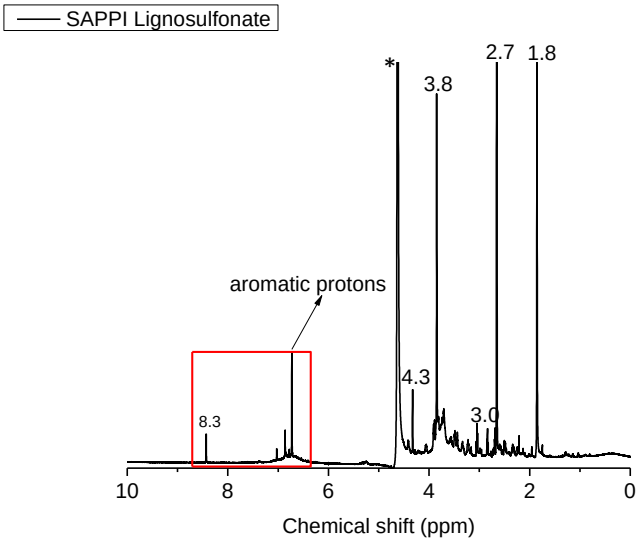

Fig. C1.2: ^{1}H NMR spectrum of SAPPI lignosulfonate

Appendix

Table C1.1: ^{1}H NMR analysis of SAPPI lignosulfonate and SAPPI DMSO/HBr

Chemical shift (ppm)	Peak assignment
9–10	Aldehyde protons
7.0–8.3	Aromatic protons
4.8–5.2	Vinylic protons
4.5	Methylene protons in a cinnamyl alcohol type of structure
3.8–4.2	Ester and ether protons
2.0–2.8	Proton α to the aryl carbonyl group
1.5–2.2	Aliphatic protons

Appendix D

Single reaction monitoring (SRM) elution profiles for DMSO/HBr product mixture

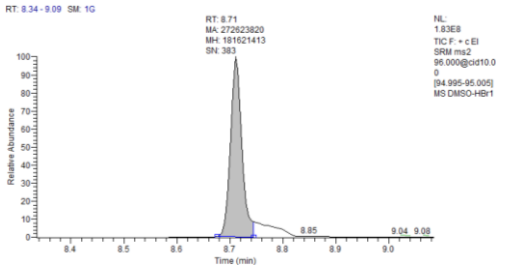

Fig. D1.1: SRM elution profile for furfural (DMSO/HBr product mixture)

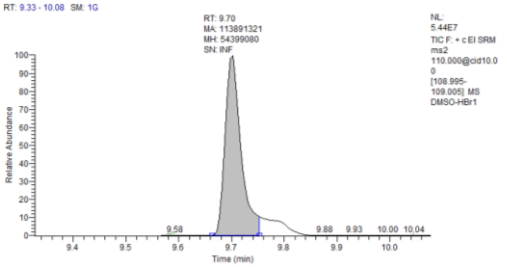

Fig. D1.2: SRM elution profile for 5-methylfurfural (DMSO/HBr product mixture)

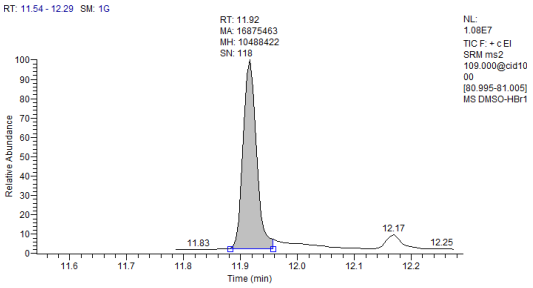

Fig. D1.3: SRM elution profile for guaiacol (DMSO/HBr product mixture)

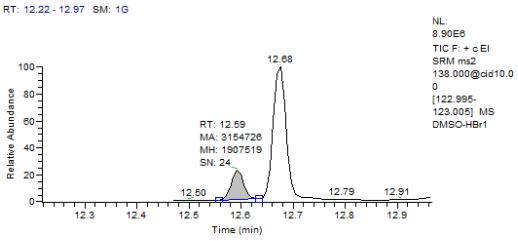

Fig. D1.4: SRM elution profile for 4-methylguaiacol (DMSO/HBr product mixture)

Appendix

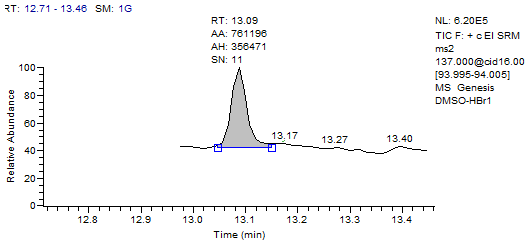

Fig. D1.5: SRM elution profile for 4-ethylguaiacol (DMSO/HBr product mixture)

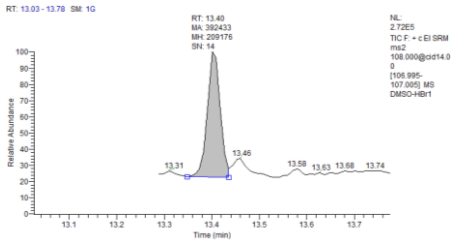

Fig. D1.6: SRM elution profile for m-cresol (DMSO/HBr product mixture)

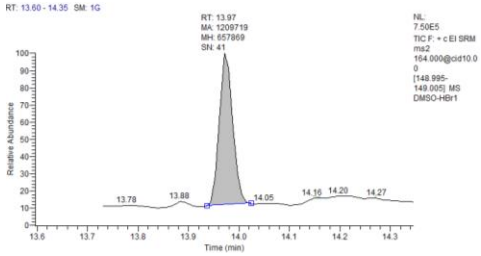

Fig. D1.7: SRM elution profile for eugenol (DMSO/HBr product mixture)

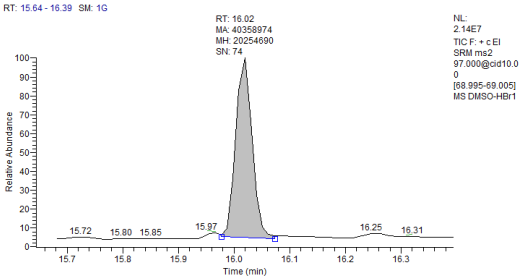

Fig. D1.8: SRM elution profile for 5-(hydroxymethyl)furfural (DMSO/HBr product mixture)

Appendix

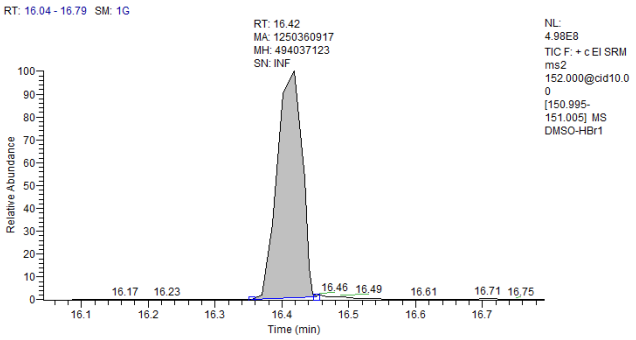

Fig. D1.9: SRM elution profile for vanillin (DMSO/HBr product mixture)

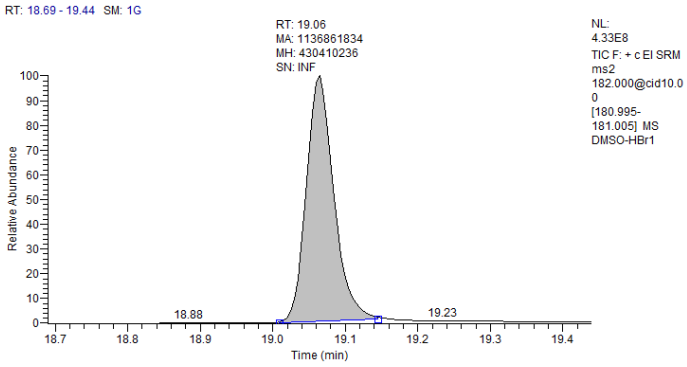

Fig. D1.10: SRM elution profile for syringaldehyde (DMSO/HBr product mixture)

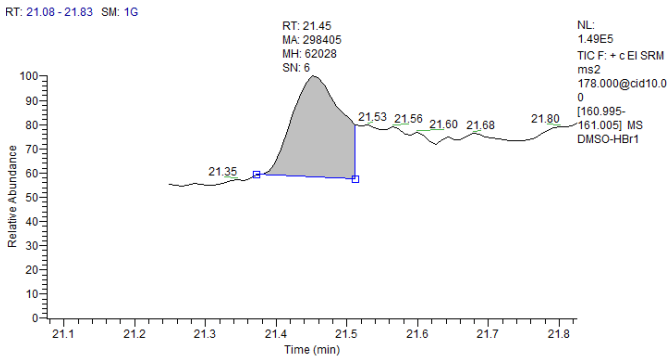

Fig. D1.11: SRM elution profile for coniferaldehyde (DMSO/HBr product mixture)

Appendix E

Single reaction monitoring (SRM) elution profiles for SAPPI DMSO/HBr product mixture

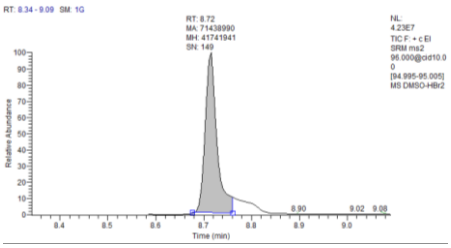

Fig. E1.1: SRM elution profile for furfural (SAPPI DMSO/HBr product mixture)

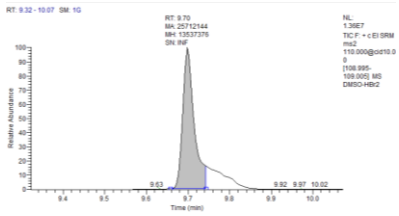

Fig. E1.2: SRM elution profile for 5-methylfurfural (SAPPI DMSO/HBr product mixture)

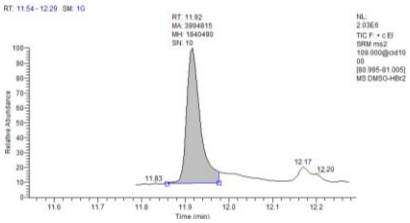

Fig. E1.3: SRM elution profile for guaiacol (SAPPI DMSO/HBr product mixture)

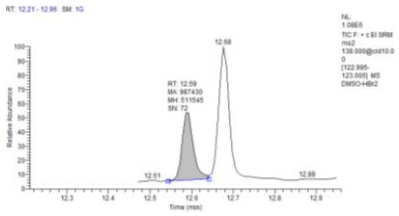

Fig. E1.4: SRM elution profile for 4-methylguaiacol (SAPPI DMSO/HBr product mixture)

Appendix

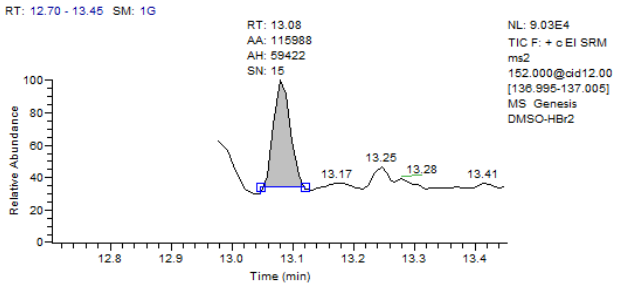

Fig. E1.5: SRM elution profile for 4ethylguiacol (SAPPI DMSO/HBr product mixture)

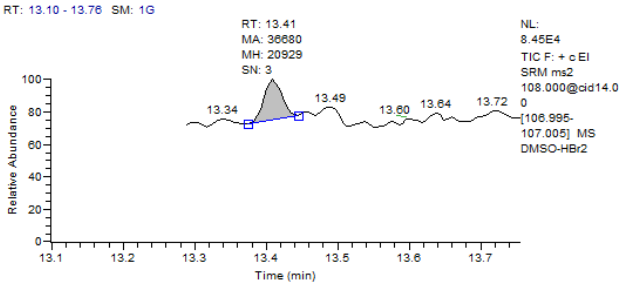

Fig. E1.6: SRM elution profile for m-cresol (SAPPI DMSO/HBr product mixture)

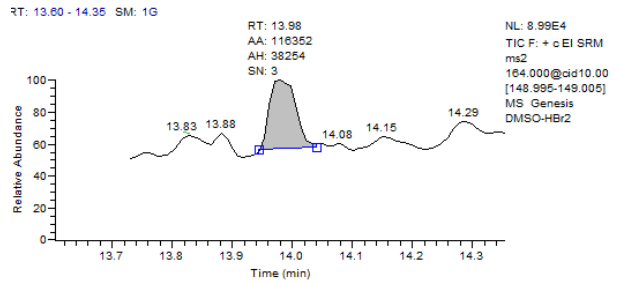

Fig. E1.7: SRM elution profile for eugenol (SAPPI DMSO/HBr product mixture)

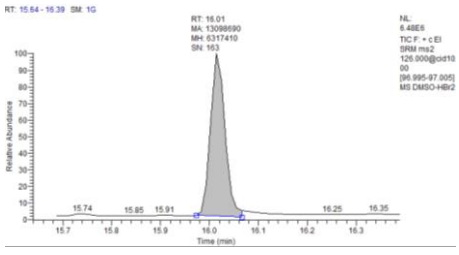

Fig. E1.8: SRM elution profile for 5-(hydroxymethyl)furfural (SAPPI DMSO/HBr product

mixture)

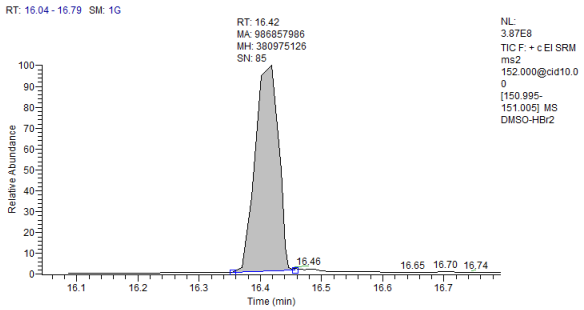

Fig. E1.9: SRM elution profile for vanillin (SAPPI DMSO/HBr product mixture)

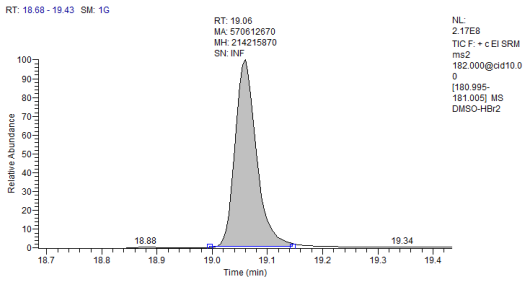

Fig. E1.10: SRM elution profile for syringaldehyde (SAPPI DMSO/HBr product mixture)

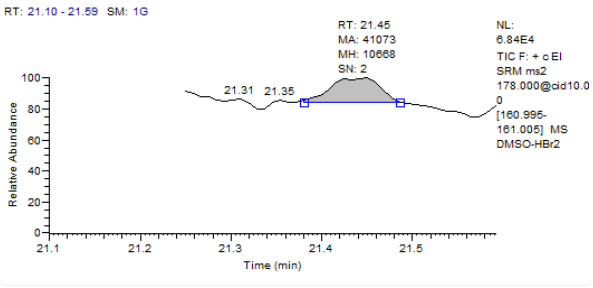

Fig. E1.11: SRM elution profile for coniferaldehyde (SAPPI DMSO/HBr product mixture)

Appendix F

Mass spectra at specified elution volumes for the 160 °C and 180° C fractions

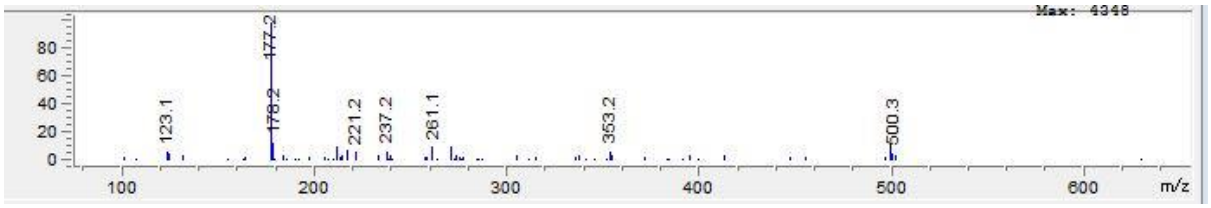

Fig. F1.1: Mass spectrum observed at elution volume of 22.7 Ml of 160°C fraction (phase2)

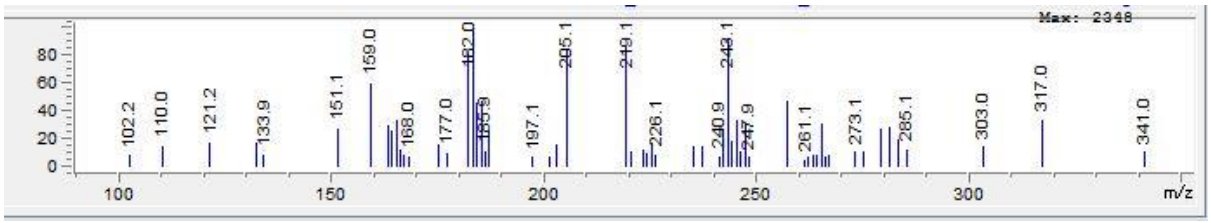

Fig. F1.2: Mass spectrum observed at elution volume of 2.8 mL of 180°C fraction (phase1)

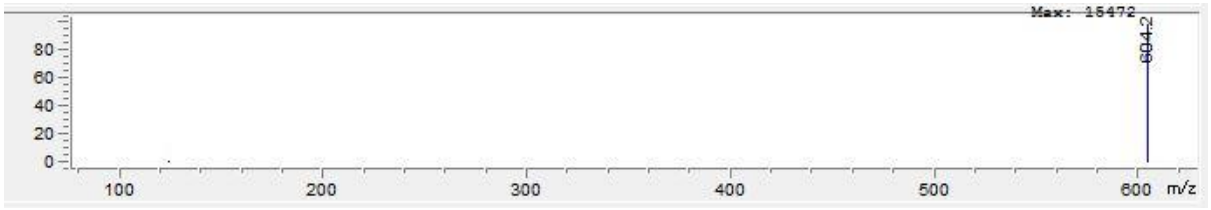

Fig. F1.3: Mass spectrum observed at elution volume of 2.3 mL 180°C fraction (phase1)

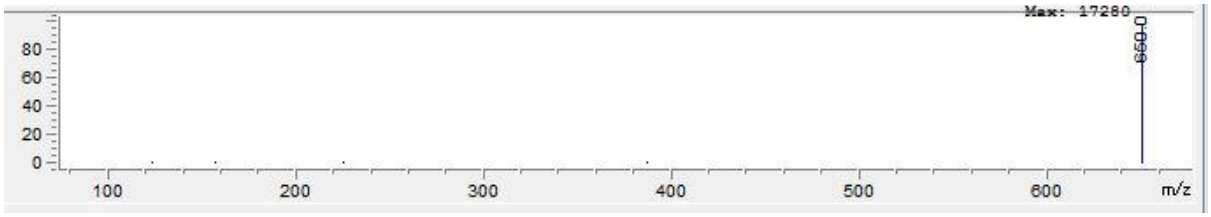

Fig. F1.4: Mass spectrum observed at elution volume of 4.8 mL 180°C fraction (phase1)

Appendix G

DMSO/HBr non-segmented GC-MS full scan

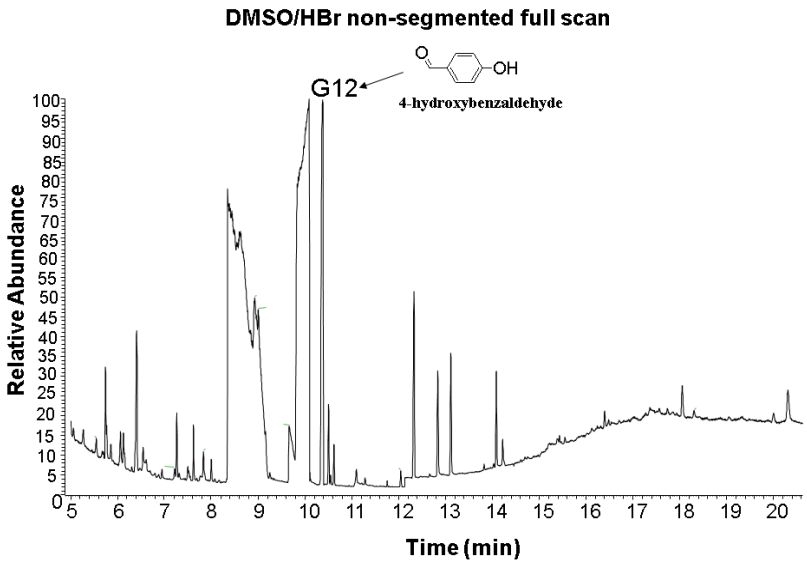

Fig. G1.1: GC-MS non-segmented TIC chromatogram of DMSO/HBr

Appendix H

Analysis of functionalized guaiacol

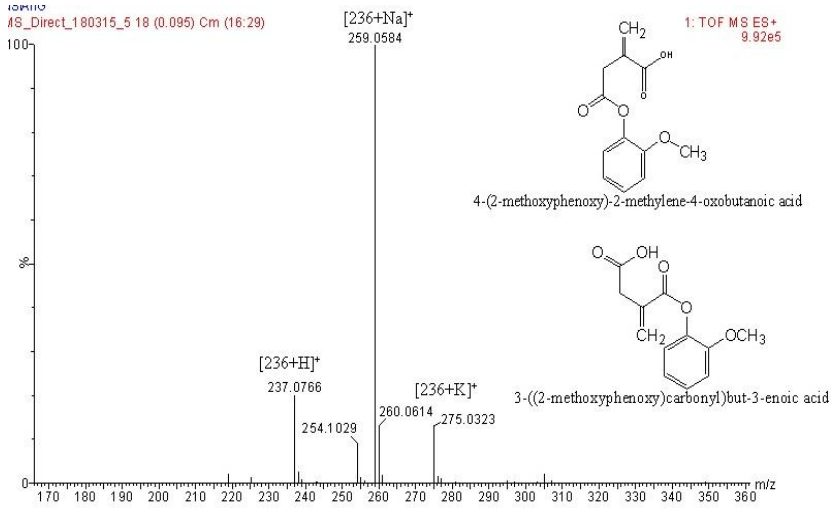

Fig. H1.1: ESI-MS of functionalized guaiacol

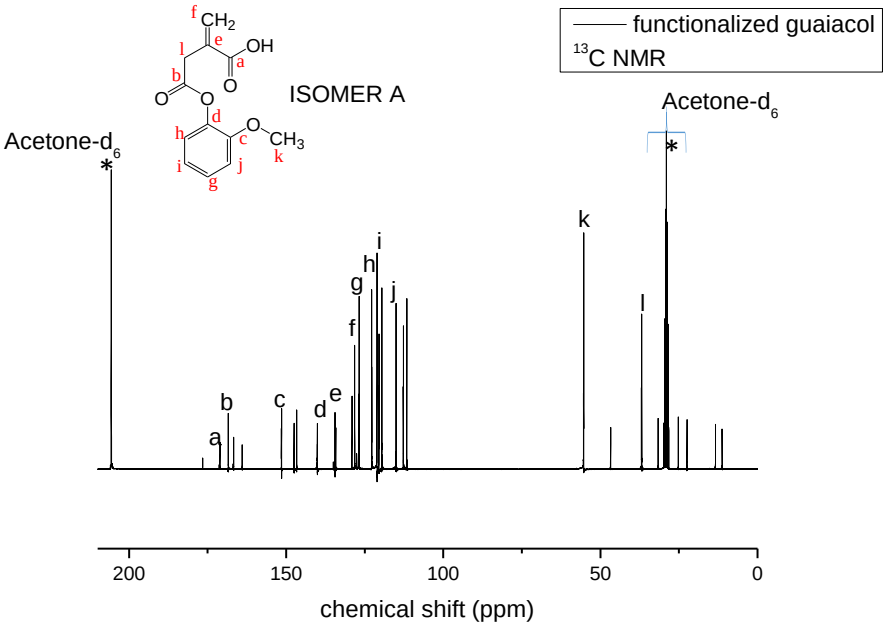

Fig. H1.2: ^{13}C NMR analysis of functionalized guaiacol
(Asterisks represent solvent peaks, other unaccounted peaks in the spectrum are due the tin octoate)

Appendix I

^{1}H NMR analysis of fractions

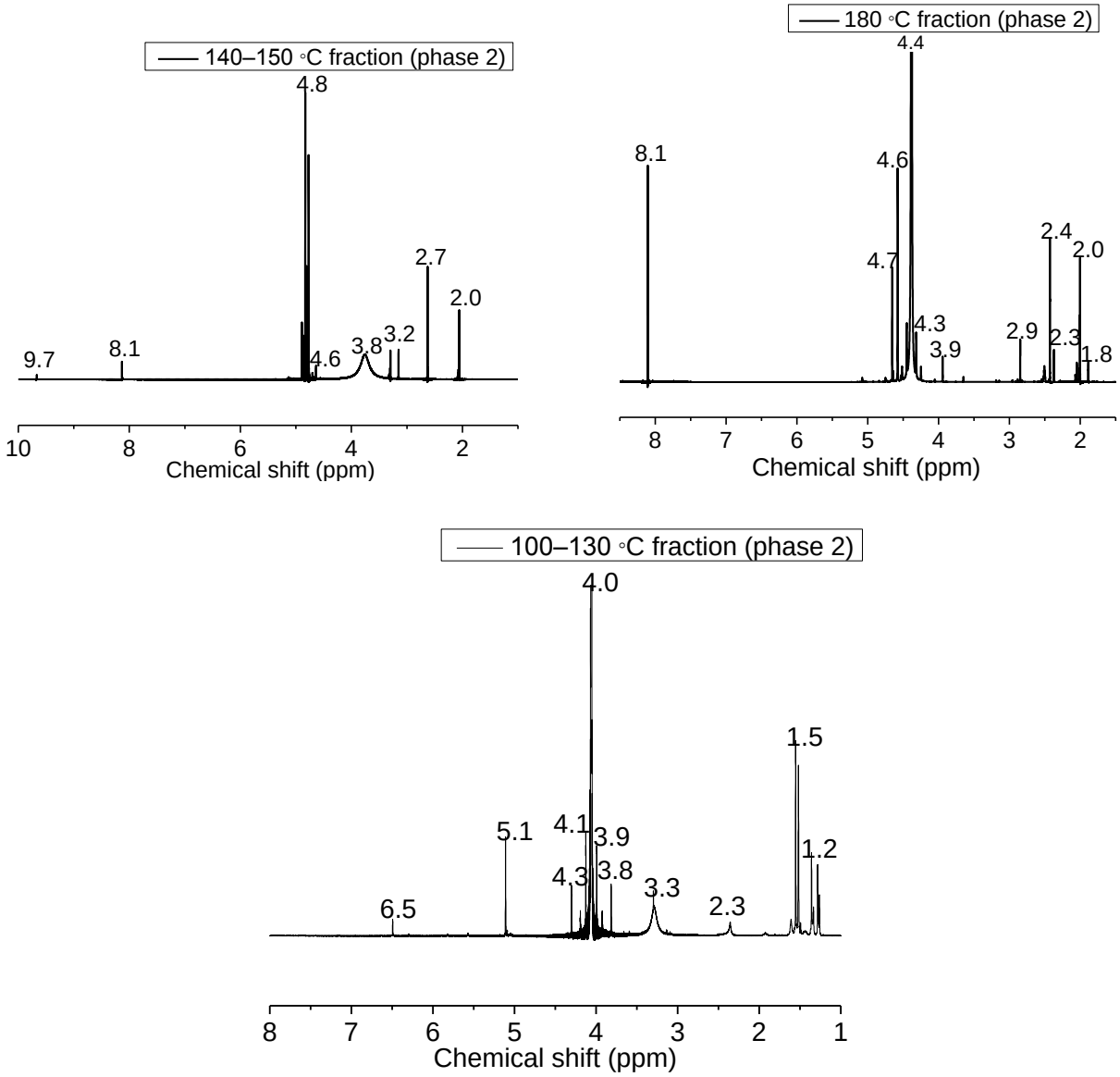

Fig. I.1.1: ^{1} H NMR spectra of fractions

Appendix

Table I1.1: ^{1}H NMR analysis of fractions

Chemical shift (ppm)	Peak assignment
9–10	 (aldehyde protons)
8.1	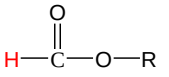 (proton α to the carbonyl group)
4.5–6.5	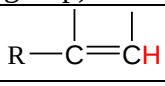 (alkene protons)
3.9–4.4	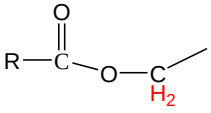 (ester protons)
3.3–3.9	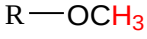 (methoxy protons)
2.7–2.9	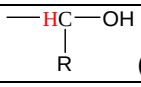 (proton on the α carbon)
2.0–2.4	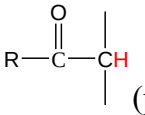 (proton β to the carbonyl group)
1.8–2.0	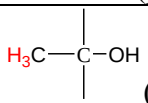 (protons β to –C–OH)
1.5–2.2	Aliphatic protons

(R: Hydrogen, alkyl, alkyloxy, phenyl groups))